

A review of classical aerodynamics and the application of the LMS algorithm to active flutter suppression

A Master's thesis in Mobility Engineering

Hong Hieu Vu

DEPARTMENT OF MECHANICS AND MARITIME SCIENCES

CHALMERS UNIVERSITY OF TECHNOLOGY
Gothenburg, Sweden 2026
www.chalmers.se

Master's Thesis in Mobility Engineering

A review of classical aerodynamics and the application of the LMS algorithm to active flutter suppression

HONG HIEU VU



CHALMERS
UNIVERSITY OF TECHNOLOGY

Department of Mechanical Engineering
Division of Dynamics
Chalmers University of Technology
Gothenburg, Sweden 2026

Negligence in any job is already an immoral sin, but negligence in literature is so despicable!

Nam Cao

Sự cẩu thả trong bất cứ nghề gì đã là một sự bất lương rồi. Nhưng sự cẩu thả trong văn chương thì thật là đê tiện.

Nam Cao

A review of classical aerodynamics and the application of the LMS algorithm to active flutter suppression
HONG HIEU VU

© HONG HIEU VU, 2026.

Supervisor: Petri Piiroinen, Department of Mechanical Engineering
Examiner: Petri Piiroinen, Department of mechanical Engineering

Master's Thesis 2026
Department of Mechanical Engineering
Chalmers University of Technology
SE-412 96 Gothenburg
Sweden
Telephone +46 31 772 1000

Typeset in LaTeX
Gothenburg, Sweden 2026

A review of classical aerodynamics and the application of the LMS algorithm to active flutter suppression

HONG HIEU VU
Department of Mechanics and Maritime Sciences
Division of Division Name
Chalmers University of Technology

Abstract

This work attempts to apply the Least-Mean-Square (LMS) algorithm to estimate the impulse response for an oscillating airfoil in uniform flow. The LMS algorithm is an impulse response estimator and has its traditional application in acoustics. Such as noise cancelling, echo cancelling, etc. Its strength is in its ability to adapt to changing system dynamics, as well as its simplicity. The work also revisits some classical aerodynamics formulations, such as vortices and the use of complex analysis in computing the forces on stationary and oscillating airfoils. It was found that the oscillating airfoil exhibits different system dynamics depending on the speed, as well as past inputs. Additionally, the LMS algorithm could accurately estimate the impulse response of the system at different dynamics corresponding to different air speeds and past inputs, and that it could produce the correct input signal to cancel oscillations before stall flutter develops. However, it was apparent that designing controllers where the LMS' output loops back to its input can cause instabilities. Overall, the result suggests that the LMS has the potential for application in active flutter suppression systems as a component in a controller design.

Keywords: LMS, Least-Mean-Square, aspect ratio, wing, algorithm.

Preface

Hydrodynamics is an old realm of study. Ever since Daniel Bernoulli's publication of *Hydrodynamica, sive de viribus et motibusfluidorum commentarii*[1] in 1738, where the word *Hydrodynamics* was first coined, physicists had been trying to find a general mathematical theory of fluid motion. A breakthrough came in 1755 when Euler published his memoir. It incorporated previous works by Johann Bernoulli and Jean le Rond d'Alembert and Newtonian mechanics to derive a general equation for incompressible inviscid fluid motion [Dar05]. However, Euler considered irrotationality as a condition, which prevented his flow from having vortices, and implies a velocity potential. It took until Helmholtz's work in 1858 to show that vortices can exists in fluids. In the 19th century, Navier-Stokes' equation was derived for a viscid fluid based on knowledge at the time, physicists have been trying to formulate a theory of fluid motion that could explain flow features observed in reality.

But unlike the successes of thermodynamics, which came about due to the need to understand steam driven engines, hydrodynamics got stuck in niche classes of flows that are rarely encountered in reality and of ideal fluids. It got to the point that engineers developed their own field of *Hydraulics* to solve their everyday problems [Dar05]. The main departure between the two were in turbulent flows and boundary layers.

By the 1940s, the theory of hydrodynamics has had significant progress. But classical aerodynamics had taken on substantial mathematical complexity. Aerodynamics, a subclass that concerns mainly with the flow of air around lifting bodies, was also part of the wave. With the advent of more powerful computers in the 80s, and after Launder and Spalding's 1974 paper *Numerical computation of Turbulent Flows*, which some considers as the birth of $k - \epsilon$ model, and the commercialization of CFD codes in the US, CFD became the mainstream in aerodynamics and pushed classical aerodynamics to the sideline.

But it would be a misunderstanding to say that classical aerodynamics had become a relic of antiquity. Before finite-volume CFD was possible (which requires thousands to millions of nodes), computational fluid dynamics relied on the method of panels [2] and discretization of vortex sheets into Helmholtz vortex lines [3]. These discretization methods allowed computers to analytically solve for the flow field around objects of complex geometry, albeit they only account for non-viscid flow. Nonetheless, these were enough for engineers of the day, when wind or water tunnel experimentation and brave men produce measurements to correct for viscid and compressibility effects. Nowadays, these methods of computation are no longer in use commercially in favour of finite-volume methods. By the 1970s, analytical[4] aerodynamics textbooks such as the classic by Anderson [And17] has incorporated the latest in compressible and hypersonic flows, which was the frontier of the era, thus

[1] *Hydrodynamics, a dissertation on the forces and motions of fluids*, title translated according to Darrigol [Dar05]

[2] Still available today in ship design software such as Shipflow and Open VSP.

[3] This method is called Vortex Laticce Method. The VLM and Panel methods could be found in openVSP as VSPAERO.

[4] Here means non-computational.

omitting the complex number method of classical aerodynamics (possibly due to its requirement of knowledge of complex analysis, and making room for advancements in the treatment of the boundary layer). The recent book by Kundu, Cohen, and Dowling [KCD12] gives a treatment of this theory, but in a very contracted form compared to the classics of Thompson [Tho58].

However, CFD is often sensitive on boundary conditions, the "size" of the computational domain required is much larger than classical methods based on vortex lines, and most importantly, the interpretation of CFD results is often an art in itself. On the other hand, classical aerodynamics gives a decomposition of the flow field into constituent elements. Thus, the author believes that knowledge of classical aerodynamics provides valuable insight into the nature of fluid flows, which every engineer should have, and even aids positively in the interpretation of finite-volume CFD results.

On the other hand, when von Kármán wrote his paper on non-steady airfoils in 1938, frequency domain analysis of mechanical system was still in its infancy. It was a classified World War 2 technique. It took until Nichol and Phillip's book *Theory of Servomechanisms* in 1947 for frequency domain analysis to break away from its traditional applications in analogue electronics circuits analysis and found new applications in electro-mechanical system control. Since then, the study of frequency domain analysis has taken long leaps, within which time, electronics signal analysis (be it acoustics or radar) is still the pioneer amongst its applications. This thesis attempts to bring the Least Means Square algorithm - a technique frequently used in system measurement in acoustics - to apply in the measurement of aerofoil response to external disturbance.

Acknowledgements

I hereby take the chance to thank professor Piiroinen for his unwavering support for this work and his tolerance for my sometimes sluggish progress due to my tendency to wander into niche topics in my research, and the inconveniences of our circumstances.

I would like to also extend my gratitude towards my acquaintance Nguyen Thi Van, Khiem Nguyen, Trang Nguyen, and Quynh Nguyen for their support during my time in Sweden. Their help had eased my transition to a life in Sweden. And thanks to my friend Diep Tran who always encouraged me not to give up.

And especially, I would also like to extend my gratitude to my parents Th. N. and H. V. for their emotional and financial support. Without which I would not be able to pursue my study.

Hong Hieu Vu, Gothenburg, 06 2026

List of Acronyms

Below is the list of acronyms that have been used throughout this thesis listed in alphabetical order:

AR	Aspect Ratio
LMS	Least Mean Square

Nomenclature

Below is the nomenclature of indices, sets, parameters, and variables that have been used throughout this thesis.

Nomenclature rules

h	Normal letters are time domain variable
H	Capital letters are frequency domain variable
$\boldsymbol{h}$	Bold letters are vectors
$h[i]$	Indices in square brackets indicates function of a discrete variable
$h(i)$	Indices in round brackets indicates function of a continuous variable
$\hat{\boldsymbol{h}}$	Variables with a hat are unit vectors of the corresponding vector $\boldsymbol{h}$ in geometrical contexts
$\bar{h}$, $\bar{\boldsymbol{h}}$	Variables with a bar are the mean for the corresponding variable h or $\boldsymbol{h}$. If h is a loop or path, then $\bar{h}$ means the path is traversed in the opposite direction to h
$h_{\mathbb{C}}$	Variables with $\mathbb{C}$ as one of its subscript is a complex number variable (in case there is a need to tell apart complex from real variables)

Sets

$\mathbb{C}$	Set of Complex numbers
$\mathbb{N}$	Set of natural numbers
$\mathbb{N}^*$	Set of natural numbers larger than or equal to 0
C	A closed, singly connected contour
C^i	The interior of loop C
C^o	The exterior of loop C
$\bar{C}$	Another closed, singly connected contour traversed in the opposite sense to the contour marked with C

(C)	A circle centred at point C.
(ζ_0, r)	A circle centred at the point with complex coordinate ζ_0 and radius r.

Parameters

c	Chord length
b	Half chord length $b = c/2$
t	time
E	Young's modulus
ν	Poisson's ratio
I_{yy}	Mass moment of inertia around the y axis

Variables

α	Angle of attack
Γ	Circulation, defined as the trace of velocity along a closed contour.
γ	Circulation distribution or sometimes called vorticity distribution. $\gamma(x) = d\Gamma/dx$
ϕ	Velocity potential
ψ	Streamline function
x	Length along the chord, positive towards the trailing edge of the airfoil. $x = 0$ at the middle chord unless otherwise stated.
y	Length along the span of a wing. $y = 0$ at the wing's root.
U	Speed of the freestream
w	Complex velocity potential, $w = \phi + i\psi$
$\boldsymbol{q}$	Velocity

Contents

List of Acronyms **ix**

Nomenclature **xiii**

List of Figures **xix**

List of Tables **xxi**

1 Introduction **1**
1.1 Introduction 1
1.2 Goals 2
1.3 Limitations 3

2 What is the LMS algorithm? **5**

3 Another mathematical framework **9**
3.1 Streamline and Velocity Potential functions 9
3.1.1 Stream function 9
3.1.2 Velocity potential 11
3.1.3 A notable property of ϕ and ψ 12
3.2 Complex Velocity Potential and the Complex Velocity 12
3.2.1 Complex velocity potential 12
3.2.2 The complex velocity 13
3.3 Elementary flows in term of the complex potential 14
3.3.1 Uniform flow 14
3.3.2 Vortex flow 14
3.3.3 Source/Sink 15
3.4 Some useful theorems of Complex Analysis and Hydrodynamics . . . 15
3.4.1 Cauchy's integral theorem 15
3.4.2 Cauchy's residue theorem[5] 15
3.4.3 Blasius' theorem[6] 17
3.4.4 The Circle Theorem[7] 18
3.4.5 Conformal transformations[8] 19

[5]Thompson [Tho58], Sections 3.5, 3.52
[6]Thompson [Tho58], Sections 5.4, 5.41
[7]Thompson [Tho58], Sections 5.1, 5.2
[8]Thompson [Tho58], Section 5.62, 5.70

3.5 Joukowsky transform and Joukowsky airfoil[9] . . . 21
3.5.1 Joukowski's transformation on the domain outside a circle centred at O . . . 22
3.5.2 Joukowski's transformation on the domain outside a circle centred on the x-axis or y-axis . . . 23
3.5.3 Joukowski's airfoil . . . 24
3.6 Matters on flow around Joukowski's airfoil . . . 25
3.6.1 Conformal mapping of a complex field [10] . . . 25
3.6.2 Joukowski's hypothesis . . . 27
3.6.2.1 What about the leading edge? . . . 27
3.6.3 Flow around Joukowski's airfoil[11] . . . 28
3.6.3.1 A property of the general transformation . . . 28
3.6.3.2 Position of stagnation point as a function of circulation strength[12] . . . 29
3.6.3.3 The flow itself . . . 31
3.7 Kutta-Joukowski's theorem[13] . . . 31
3.7.1 Calculating the steady circulation . . . 32
3.7.2 When α approaches $\pi/2$, stalling of aerofoil in inviscid flow . . . 33
3.7.3 Proving the Kutta-Joukowski theorem for aerofoils not derived from the Joukowski transform . . . 34
3.7.4 On the vorticity . . . 36

4 Non-stationary Airfoil Theory 37
4.1 Introduction . . . 37
4.2 Image of a vortex . . . 39
4.3 Induced vorticity distribution as a function of tangential velocity . . . 40
4.4 Circulation, Moment, and Lift on a non-steady airfoil . . . 42
4.4.1 Vorticity distribution caused by a near wake vortex . . . 42
4.4.2 Circulation . . . 44
4.4.3 Momentum stored in the fluid from a vortex pair . . . 45
4.4.4 Lift . . . 45
4.4.5 Angular momentum stored in the fluid from a vortex pair . . . 47
4.4.6 Moment . . . 48
4.4.7 Notes on application . . . 50
4.5 The method to find the wake vortex . . . 50

[9] Thompson [Tho58], sections 6.1, 6.2, 6.3, 6.4

[10] Thompson [Tho58], Section 3.8

[11] Thompson [Tho58], section 5.31, 6.8, 7.01, 7.6

[12] I have seen this formula given many times without proof, such as in Anderson [And17] and even Thompson [Tho58], so I would give it a go.

[13] This section takes a very different approach from Thompson [Tho58], where it is not obvious that this theorem should only be applied to flow around objects that does not generate any more vortices other than the vortex already there, and that the formula of Kutta-Joukowski is only true for an isolated aerofoil. To calculate force and moment on objects that generates singularities as they move, one should fall back to Blasius' theorem. Strangely enough, one of such cases is the airfoil in unsteady motion. But the interested reader could read Thompson's Section 5.5, and Anderson [And17], Chapter. 4

5 Theory of flutter **53**
5.1 What is flutter? . . . 53
5.2 What is its cause? . . . 53
5.3 What has been done in the past? . . . 54
5.3.1 Kussner's formula for flutter speed . . . 54
5.3.2 Mass balancing . . . 54
5.4 Modelling the problem . . . 56
5.4.1 Generate the airfoil . . . 56
5.4.2 Calculate the moment . . . 57
5.4.3 Equations of motion and equilibrium . . . 59
5.5 Equation of motion in case of constant speed . . . 60
5.6 Apply the LMS! . . . 61
5.7 Discretization . . . 61

6 Methods **63**
6.1 Simulation setup . . . 63
6.1.1 Windowing and wait time . . . 65

7 Results **67**
7.1 Angle of attack during transient . . . 67
7.2 Moment components during transient . . . 67
7.3 Impulse response . . . 68
7.4 Validation . . . 70
7.5 Parameter survey . . . 71
7.5.1 Speed U . . . 71
7.5.2 External moment magnitude M . . . 71
7.5.3 Step size parameter μ . . . 71
7.5.4 Window type . . . 72
7.5.5 Time step . . . 73
7.5.6 Active time . . . 73
7.5.7 Settling time . . . 73
7.5.8 Airfoil Camber . . . 74
7.6 A trial case in oscillation suppression . . . 74
7.6.1 method . . . 74
7.6.2 result . . . 77
7.6.3 The effect of LMS length . . . 78
7.6.4 A conceptual understanding of the LMS and a procedure for LMS application . . . 78

8 Conclusion **81**

Bibliography **83**

A Stationary Airfoil Theory **I**
A.1 How does an airfoil generate lift? . . . I
A.2 Lift produced by a small vortex . . . II
A.3 Velocity field generated by a vortex, Circulation . . . III

A.4 How to get the vortex distribution for a given airfoil VII
A.4.1 Solving the fundamental equation of airfoil theory for a general camberline IX
A.4.2 Lift X
A.4.3 Moment X
A.4.4 Moment and lift of a wing with aileron in steady state XI

B Background in Elementary Beam Theory XIII
B.1 Torsion of an I beam XIII
B.2 Torsion when warping is prevented XV

List of Figures

2.1 Implementation of the LMS algorithm 5

3.1 A, P, and Q in an incompressible fluid 9
3.2 Two infinitesimally close streamlines 11
3.3 A domain where $f(z)$ is holomorphic 16
3.4 Forces on an infinitesimal area of surface 17
3.5 ζ and its conformal transformation 20
3.6 $H' : -l + 0i$, $S' : l + 0i$, and $P : \zeta$ in ζ plane, and their transformed points in z plane. 21
3.7 Joukowski's transformation with $l = 1$ for domain outside a circle with center on the x-axis 24
3.8 Joukowski's transformation on a circle on the y-axis 25
3.9 Joukowski's transformation on a circle at an arbitrary position such that H_1 is on it and S_1 is inside it 26
3.10 An arbitrary point P on the circle O_1'. The wind coming in parallel to A_1P. The coordinate centre here is not yet shifted to O_1'. 30

6.1 Thin walled I-beam dimensions, [YB02] 64
6.2 A signal constructed from Equation (6.1) 65
6.3 The input signal after windowing and wait time 66

7.1 Angle of attack during transient for a sinusoidal excitation moment at 1Hz 67
7.2 Close up on aerodynamics moments acting on the airfoil during the active phase of $M(t)$. The horizontal axis shows the instantaneous frequency of the external disturbance moment $M(t)$. Since the frequency varies logarithmically, when it is laid out in a linear scale, the high frequency parts are stretched, allowing us to see the phase lead. 68
7.3 Impulse response when $U = 50\ m/s$ 69
7.4 Actual frequency response (for the case input moment is an impulse) vs estimated frequency response. 70
7.5 Impulse response of Angle of Attack to variation of airspeed, measured at different speeds: (a) 50 m/s, (b) 70 m/s, (c) 110 m/s. Speeds above about 120 m/s leads to divergence. 72
7.6 Impulse response for two different input moments, for the same airspeed: (a) $M0 = 500$ Nm, (b) $M0 = 1000$ Nm 73
7.7 h(t) from LMS for $\mu = 0.05$ (top) and $\mu = 0.9$ (bottom) 74

7.8 No windowing (bottom) vs Hann window (top), frequency contents of the input U. Magnitude has been normalized by input length. . . . 75
7.9 Block diagram for oscillation suppression trial. M_d is the external excitation, M_a is the sum of all aerodynamics moments, and M_c is the controller's moment. The desired signal is $d(t)$. 76
7.10 The LMS' coefficients while the impulse arrive. Vertical axis shows LMS' value for predicted impulse response, horizontal axis shows element count. Note that the LMS in this configuration no longer predicts only the mechanical-fluid system's impulse response, but also partly, of itself, since there is a loop. a) before the impulse arrive, b) 0.25s after the impulse arrive, c) 0.65s after the impulse arrive. 76
7.11 Delayed Impulse. Initial ripple is because initially the airfoil is slightly off equilibrium. It could be seen that before the LMS comes online at $t = 5$ seconds, both cases share the same motion. 77
7.12 Frequency response with and without LMS control. (a) with LMS control according to diagram presented in Figure 7.9. (b) without LMS control. LMS in each subplot refers to how the frequency response was measured. 78
7.13 Controller moment M_c over time. The controller commands a gradual spike ($\approx 4\Delta t$ of rise time, compared to $1\Delta t$ for both rise and fall for the excitation impulse) when it detects the impulse. 79
7.14 Impulse response with control and no control for different LMS filter lengths at $U = 50$ m/s: a) 1 second, b) 5 seconds 80
7.15 Requested M_c for different LMS filter lengths at $U = 50$ m/s: a) 1 second, b) 5 seconds 80

A.1 Wing's disturbance field. Image taken from Raymers' book [Ray18] (fig 4.3) IV
A.2 The angle α VI

B.1 Way to determine the Diameter D of the maximum inscribed circle. Image taken from chapter 5 of Hearn's book [Hea97] XIV
B.2 Dimensions on an I beam. r = fillet radius, D = diameter of largest inscribed circle, t = b if b < d; t = d if d < b; t_1 = b if b > d; t_1 = d if d > b Figure from chapter 10 of [YB02] XIV
B.3 Dimensions for a thin walled I-beam, image from Roak [YB02]. XV

List of Tables

6.1 Airfoil's geometric parameters. (ϵ, τ) is the position of the centre of the circle in ζ plane. 63
6.2 Airfoil's structural parameters 64
6.3 Input parameters to Equation (6.1). 65

1

Introduction

1.1 Introduction

It is common in aerodynamics textbooks of the present day to have a course covering foremost the fundamental principles of hydrodynamics such as Bernoulli's equation, and Laplace's equation for incompressible, inviscid flow. Afterwards, concepts such as the vortex, the (real) velocity potential, the streamline, and the elementary flows are covered. These then lead to an analysis of aerofoil flows, where the vortex around the aerofoil is noticed, which leads to the Kutta-Joukowski equation for its lift. To cover more complex airfoils, Glauert's method of solutions for thin aerofoils are often presented[1]. From there, the lifting line theory, developed by Prandtl in 1918, or the panel methods are often introduced to cover thick aerofoils[2]. These methods reflects the trend in using computers in aerodynamics research at the time.

However, there is another more elegant and beautifully written theory. First conceived by Jean le Rond d'Alembert in 1761[3] and perfected by subsequent theorists. This theory centres around the complex potential: a single function of both the streamline and the velocity potential. The understanding of this theory brings coherent to all material mentioned above, in a manner similar to how Maxwell did to electromagnetism, which, in the words of Arnold Sommerfeld: "*At first, however, electrodynamics was still presented to us in the old manner - in addition to Coulomb and Biot-Savart, Ampère's law [...] the laws of Grassmann, Gauss, Riemann, and Clausius, and as a culmination of the law of Wilhelm Weber, all of which were based on the Newtonian concept of action at a distance. The total picture of electrodynamics thus presented to us was awkward, incoherent, and by no means self-contained*"[4]. Just as when Maxwell and Hertz arrived and give a formulation that matches the underlying world of nature more closely, which as a result explained all of the above-mentioned laws, the complex velocity potential framework explained all of the laws in fundamental aerodynamics for inviscid, incompressible 2D flow. The complex potential framework, as it will be called in this thesis, also lends a hand in the ease of application of the "aeronautical" image method[5]. It allows flows around complex shapes such as an aerofoil to be computed analytically relatively easily, without

[1] This method assumes incoming flow at a shallow angle, and gives an approximate formula for inviscid, non-separating lift that this thesis would then abridge with a more general formula.

[2] The panel method is useful to compute the inviscid, incompressible flow around bluff bodies. OpenVSP has this method in VSPAERO.

[3] Who first pointed out the complex potential. See Darrigol [Dar05]

[4] *Lectures on Theoretical Physics, Vol III.*

[5] Similar to the electrostatics image method, which is also solved using potential.

making use of vortex sheets. It provides a relatively straightforward way to mathematically generate said aerofoils along the way. It is also possible to derive the strength of the circulation around an aerofoil mathematically, as opposed to using the Kutta condition[6]. It also shows that the infinite vorticity at the leading edge happens only on thin aerofoils[7]. Modern textbooks treatment of this method, such as one by Kundu, Cohen, and Dowling [KCD12], is often brief or even omitted entirely, such as in Anderson [And17]. As such, contemporary aeronautical engineers are sometimes unaware of the full potential of this theory.

Thus, the author believes that there are significant gains to be taken when reviewing the old theory.

This thesis sets out to review the classical theory of aerodynamics and to presents it in a way that explains most fundamental characteristics of the aerofoil mathematically and more generally, in a way suitable for pedagogic purposes, and on a seemingly unrelated topic, tries to use a simple algorithm that is used widely in acoustics to predict the oscillatory behaviour of aerofoils. The aerofoil would be simulated based on an experimentally verified, and physically sound, method by Theodore von Kármán and W. R. Sears [KS38] to analytically calculate the lift and moment on a non-steady aerofoil. This thesis also uses the results of the complex potential framework to derive the Kutta-Joukowski equation in a more general way that also mentioned the direction of lift mathematically, to prove mathematically that this theorem is valid for *any* aerofoil, to prove that the Joukowski aerofoils are the approximation of all aerofoils, and re-derives the formula for the lift of an aerofoil in inviscid flow that doesn't require the small incidence angle of Glauert's method, nor the thin aerofoil approximation[8]. These are not novel results, but showing that they are coherent results from the same physical framework could be useful for pedagogical purposes. It also bypasses the use of the vorticity in 2D flow, which some experts such as McLean called a mathematical concept that could mislead engineering judgement [McL13]. This is due to its similarity to the Biot-Savart law[9] which suggests people to believe that vortex flows are caused by vorticity. In reality, experiments with devices intended to cancel vorticity shows that they do not work because of the Kelvin circulation theorem [McL13], while the effect of the supposedly cancelled vorticity is still presence. But more importantly, knowledge of the complex potential framework, which does not make use of the vorticity, makes it easier to avoid these kind of misconception.

1.2 Goals

The goal of this project is two-fold. Firstly, this thesis aims to present the complex potential flow theory and using it to derive all inviscid 2D flow phenomena around the aerofoil in a coherent and logical way. Furthermore, this thesis aims

[6]The Kutta condition could be proven to be a result of this theory.

[7]Some textbooks attributes this anomaly to theory versus reality, but it can be shown that the true cause is the thin aerofoil approximation, where Joukowski's hypothesis is not satisfied.

[8]The result of these approximations is a formula for lift in inviscid flow that is bounded to small angles of attack (less than about 10 degrees, when $\sin(x) \approx x$ holds).

[9]Where a current distribution generates a magnetic field.

to shed light on some fundamental questions of lift generation, namely: why is the Kutta-Joukowski formula true for any kind of aerofoil, and why does it involve only the circulation, what is the significance of the Joukowski aerofoil family? By showing that these results could be coherently derived, the thesis aims to show that this framework is useful for the teaching of aerodynamics for future aeronautical engineers.

Secondly, it is to use the LMS algorithm (or modify it as see fit) to estimate the flutter response of a 2D wing section. This would then be used in a closed loop control circuit to generate a control bending moment to suppress the resultant flutter. The control loop will use the algorithm's estimation of the system's dynamics instead of a linear model.

The variation in the airfoil section's angle of attack could be used as a benchmark for flutter suppression in this work.

1.3 Limitations

The following items have been defined to limit the scope of this work:

- The current work will not investigate the practical setup nor the actuators required to fulfil the algorithm's control signals.
- The work will not investigate the effects of this system on flight performance or manoeuvrer.
- The work will also assume that sufficient controller hardware speed is available.
- The work will not address the case of failure of probing devices which supplies the inputs. Though some discussion of the influence of noise will be provided.
- This work will only consider non-separating flutter.

2

What is the LMS algorithm?

The traditional LMS algorithm is an impulse response estimator widely used in digital acoustic signal processing to estimate the transfer function of signal pathways and has been proven useful in active noise cancellation, echo cancellation, beam forming, etc. It is represented by the following diagram in Figure 2.1:

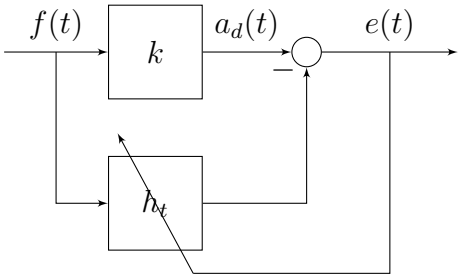


Figure 2.1: Implementation of the LMS algorithm

Where in Figure 2.1, $\boldsymbol{k}$ is a vector consists of I elements and is the impulse response of the system to be estimated, $\boldsymbol{h}_t$ is the predicted impulse response. Note that $\boldsymbol{h}_t$ changes with time, while $\boldsymbol{k}$ is constant. They could be converted into a transfer function via a Fourier transform. $f(t)$ is the input to the system and is called the reference signal.

The output of the LMS' filter is given as a weighted sum of its coefficient and past inputs [NE92][1]:

$$g[t] = \sum_{i=0}^{I-1} h_i f[t - i\Delta t],$$

where $f[t - i\Delta t]$ denotes the reference signal at time $t - i\Delta t$. If we arrange the vector $\boldsymbol{f}$ as:

$$\boldsymbol{f}_t = [f[t], f[t - \Delta t], ..., f[t - (I - 1)\Delta t]]^T, \tag{2.1}$$

Then the output of the LMS is given by:

$$g[t] = \boldsymbol{h}_t.\boldsymbol{f}_t.$$

The algorithm uses the instantaneous error $e = a_d - g[t]$ and a series of present and previous I reference signals $\boldsymbol{f}_t \in M_{I\times 1}(\mathbb{R})$ to update the predicted impulse

[1] Section 4.5 of this book. It was said that this is just one way of implementing a FIR filter.

response in real time [2].

The error will be given by:

$$e(t) = a_d(t) - \boldsymbol{h}_t^T \boldsymbol{f}_t. \tag{2.2}$$

We want to find the vector $\boldsymbol{h}$ that minimize the expectation of the squared error $E(e^2)$.

Notice that at any time t, a_d and $\boldsymbol{f}$ are known. Thus the only variable in $E(e^2)$ is the vector $\boldsymbol{h}$. In order to find the value $\boldsymbol{h} = argmin(E(e^2))$, an iterative approach could be taken where whenever a new value of f arrives, $\boldsymbol{h}$ takes a step in the direction that reduces $E(e^2)$. But since $\boldsymbol{h}$ itself is a vector ($\boldsymbol{h} = [h_0[t], h_1[t], ..., h_I[t]] \in \mathbb{R}^I$), every component is themselves a variable. Thus each one of them has to take a step every iteration. The criteria given above is mathematically expressed as:

$$\begin{aligned} h_i[t + \Delta t] &= h_i[t] - \alpha \frac{\partial E(e^2)}{\partial h_i[t]} \\ &= h_i[t] - \alpha E\left(2e \frac{\partial e}{\partial h_i[t]}\right) \end{aligned} \tag{2.3}$$

Where α is the convergence coefficient, $\frac{\partial E(e^2)}{\partial h_i[t]}$ is the rate of increase of $E(e^2)$ when the i-th component of $\boldsymbol{h}$ is moved by an infinitesimal amount ∂h_i. But since at any time step t we have:

$$\begin{aligned} \frac{\partial e}{\partial h_i} &= \frac{\partial}{\partial h_i}\left(a_d - \boldsymbol{h}^T \boldsymbol{f}\right) \\ &= \frac{\partial}{\partial h_i}\left(a_d - \sum_{j=1}^{I} h_j f_j\right) \\ &= 0 - \sum_{j=1}^{I} \frac{\partial}{\partial h_i} h_j f_j \\ &= -f_i \\ &= -f[t - i\Delta t]. \end{aligned}$$

We thus have:

$$\begin{aligned} h_i[t + \Delta t] &= h_i[t] - \alpha E(2e(-f[t - i\Delta t])) \\ &= h_i[t] + \alpha E(2ef[t - i\Delta t]). \end{aligned} \tag{2.4}$$

It was found that if we update the value of $\boldsymbol{f}$ in real time, then over time, the value of ef_i would be the same as if the expectation was taken, thus:

[2] It is beneficial to restate the nomenclature rule here. Square bracket on a vector means accessing the i-th element $\boldsymbol{f}[i] = f_i$ given that $\boldsymbol{f} = [f_0, f_1, ..., f_N]$, square bracket on a scalar $f[t]$ means a discrete scalar variable, sampled at time t. Subscript i of a scalar (h_i) denotes the i-th element of the corresponding vector $\boldsymbol{h}$, and subscript t of a vector $\boldsymbol{f}_t$ denotes a changing vector visited at time t.

$$h_i[t + \Delta t] = h_i[t] + \alpha.2e(t).f_i \ . \tag{2.5}$$

Note that the i-th element of the impulse response is updated with the i-th preceding reference signal.

The vector $\boldsymbol{h} \in \mathbb{R}^I$ is the estimated impulse response in time domain. When converted to frequency domain by means of a Fourier transform, it will be limited in frequency between 0 and $f_S/2$, where f_S is the sampling frequency of the input $f[t]$, divided equally between I frequency bins, where I is the number of elements in $\hat{\boldsymbol{h}}$. This is the resolution limit of the algorithm.

The convergence coefficient 2α can be replaced by a step size μ in 2 ways. The traditional LMS uses a fixed step size given by:

$$\mu = \frac{\mu_0}{L\sigma_x^2},$$

where L is the length of h and $\sigma_x = \sqrt{\sum_n^N \frac{(\bar{x}-x_n)^2}{N}}$ is the root mean square of the signal. This is proportional to the signal's variance. Thus this step sizing strategy is to take smaller step for a more widely-distributed signals.

The normalized LMS on the other hand takes smaller steps when the energy of the signal is large. Its step size is given by:

$$\mu = \frac{\mu_0}{\boldsymbol{f^T f} + \delta}.$$

The advantage of the LMS algorithm, on the other hand, is that we do not need to have knowledge about the system in advance.

Under static conditions (i.e. invariant systems) and given long enough time, the solution $\hat{\boldsymbol{h}}$ will converge to a Wiener filter [NE92], which minimizes the expectation of the squared error e^2, given that the convergence coefficient is not too large (so that the algorithm does not overshoot).

Under non-static condition (i.e. continuously changing reference system $h(t)$), the algorithm can catch up to the changes if it is updated fast relative to the rate of change, such that the reference system $h(t)$ can be considered constant during the time it takes the algorithm to converge to the new $h(t)$ from $\hat{h}(t) = h(t-1)$.

Its simple update rule and the ability to run in real-time, adapting to changing pathways make it a promising candidate to our application. It could potentially account for changing atmospheric condition (such as density due to height and temperature variations) in real time.

For a wing controlled with an aileron, the reference signal could be the aileron angle. The desired signal a_d would be the angle of attack of the wing.

3

Another mathematical framework

In going from stationary to non-stationary airfoil theory, representing the flow using vector mathematics becomes cumbersome. It has become convention to change to complex number mathematics. Therefore, a detour about relevant mathematical treatments is necessary. The first of which is about the complex representation of flow field, and later a special conformal mapping called Joukowsky transform, which could give the shape of an airfoil naturally, and is one of the first series of aerofoil known and studied. Then we shall prove a useful property of conformal mapping on potential flow. These mathematical treatments (which appears before Section 4.1) follows the steps laid out in Thompson's book [Tho58], though not always in the same order.

3.1 Streamline and Velocity Potential functions

3.1.1 Stream function

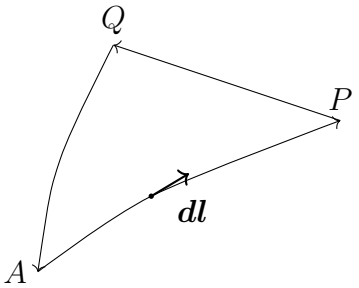


Figure 3.1: A, P, and Q in an incompressible fluid

Consider 3 fixed points A, Q, and P in an *incompressible* fluid ($\rho = const$). The flux is the mass per unit time flowing through a boundary ($\varphi = \int \rho \boldsymbol{v}.\hat{\boldsymbol{n}} dl$) [1]. The orientation of $\hat{\boldsymbol{n}}$ follows the *positive sense rule* with respect to the direction of traverse of the integration variable at any point - represented by the vector $\boldsymbol{dl}$. Mathematically, it is expressed as $\boldsymbol{dl} \times \hat{\boldsymbol{n}} = k\boldsymbol{k}$ and $k \in \mathbb{R}; k > 0$. Positive sense means that $\hat{\boldsymbol{n}}, \boldsymbol{dl}, \boldsymbol{dl} \times \hat{\boldsymbol{n}}$ follows the same right hand rule as $\boldsymbol{i}, \boldsymbol{j}, \boldsymbol{k}$, so that the result of the cross product will be positive if expressed in the same basis vectors $\boldsymbol{i}, \boldsymbol{j}, \boldsymbol{k}$. In this case, if $\boldsymbol{k}$ points out of the page, then $\hat{\boldsymbol{n}}$ points to the *left* of $\boldsymbol{dl}$. But we have

[1] where $\boldsymbol{v}$, $\hat{\boldsymbol{n}}$, dl are the local velocity, local normal unit vector to the curve, and infinitesimal length along the curve. The normal unit vector has 2 possible directions

to resolve to complex number to express this relationship. Let $\hat{n}_{\mathbb{C}}$ be the complex representation of $\hat{\boldsymbol{n}}$, and likewise $dl_{\mathbb{C}}$. The condition is written as a rotation by 90 degrees:

$$\hat{n}_{\mathbb{C}} = i\frac{dl_{\mathbb{C}}}{|dl_{\mathbb{C}}|}.$$

The influx into a closed loop going through A, P, and Q is given by $\oint \rho \boldsymbol{v}.\hat{\boldsymbol{n}} dl = \varphi_{AP} - \varphi_{AQ} + \varphi_{PQ}$ taken over the entire loop [2]. This influx is equal to the accumulation of mass inside the loop over time ($\dot{m} = d(\rho V)/dt$). Due to incompressibility, and because the loop's boundary doesn't move, the mass inside the loop should be a constant, thus:

$$\oint \rho \boldsymbol{v}.\hat{\boldsymbol{n}} dl = \frac{d(\rho V)}{dt} = 0$$
$$\rightarrow \varphi_{AP} - \varphi_{AQ} + \varphi_{PQ} = 0$$
$$\rightarrow \varphi_{AQ} = \varphi_{APQ},$$

but the curve APQ is just any other curve connecting A and Q. So we can conclude that the magnitude of flux between two points in 2D doesn't depend on which curve that we measure it on. In 3D, this principle is the same for flow through a loop. Now we can define a function $\psi(x, y)$ whose value at any point $P(x, y)$ in the fluid equals to the magnitude of flux between the point A and the point $P(x, y)$:

$$\psi_P(x, y) = \varphi_{AP}.$$

This function as defined has a single value at any point in the fluid, as long as the fluid is incompressible.

Interesting properties arise when we consider the case that Q and P lies on a streamline - the path that a fluid particle would have. It could be seen that $\varphi_{PQ} = 0$, thus:

$$\varphi_{AP} = \varphi_{AQ}$$
$$\rightarrow \psi_P = \psi_Q$$

So on a streamline, we have $\psi = const$. This is the most important property. If we take the measurements relative to a different fixed point, then the constant would change.

The streamlines would be useful if we could relate it to the velocities u, v some how. Suppose now P and Q are not on the same streamline, but on 2 streamlines infinitesimally separated. Let $\boldsymbol{dr}$ be the vector from P to Q. We know that $\varphi_{AQ} = \varphi_{AP} + \varphi_{PQ}$, so $\Delta\psi_{PQ} = \psi_Q - \psi_P = \varphi_{PQ}$. Let $\boldsymbol{q} = (u, v)$ be the local velocity vector, we have:

$$d\psi = \varphi_{PQ} = \rho \boldsymbol{q}.\hat{\boldsymbol{n}} dr,$$

where $\hat{\boldsymbol{n}} = (n_x, n_y)$ is the unit vector perpendicular to PQ, pointing in the positive sense relative to $\boldsymbol{dr}$ [3], and PQ is represented as $\boldsymbol{dr} = (dx, dy)$. So:

$$\hat{\boldsymbol{n}}.\boldsymbol{dr} = 0$$

[2] where $\hat{\boldsymbol{n}}$ following the positive sense rule is always pointing into the 2D volume

[3] This means pointing to the left of $\boldsymbol{dr}$. Positive sense with respect to $\boldsymbol{dr}$ means $\boldsymbol{dr} \times \hat{\boldsymbol{n}} = k\boldsymbol{k}$ where $k > 0$. This rule is to ensure that the product of $\boldsymbol{dr}$ and $\hat{\boldsymbol{n}}$ follows the right hand rule

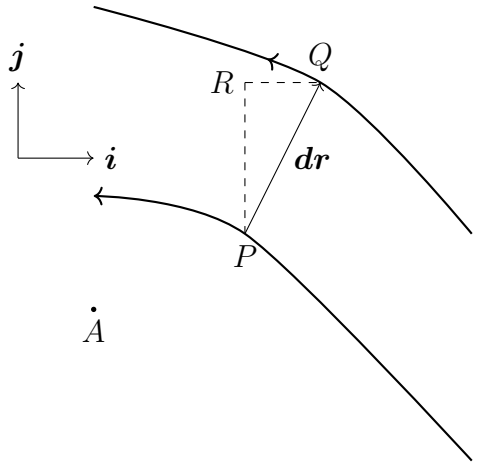


Figure 3.2: Two infinitesimally close streamlines

$$\leftrightarrow n_x dx = -n_y dy,$$

but to ensure the correct orientation ($\hat{\boldsymbol{n}}$ follows the positive sense rule), we need:

$$i(dx + idy) = dr(n_x + in_y) \ ; \ dr = \sqrt{dx^2 + dy^2}$$

$$\leftrightarrow \begin{cases} dx = dr.n_y \\ dy = -dr.n_x \end{cases},$$

thus:

$$\hat{\boldsymbol{n}} = \left(-\frac{dy}{dr}, \frac{dx}{dr} \right),$$

and we have:

$$d\psi = \rho(u\boldsymbol{i} + v\boldsymbol{j}).(n_x\boldsymbol{i} + n_y\boldsymbol{j})dr$$
$$= \rho(u\boldsymbol{i} + v\boldsymbol{j})\left(-\frac{dy}{dr}\boldsymbol{i} + \frac{dx}{dr}\boldsymbol{j} \right)dr$$
$$= \rho(u\boldsymbol{i} + v\boldsymbol{j})(-dy\boldsymbol{i} + dx\boldsymbol{j})$$
$$\rightarrow d\psi = \rho(-u.dy + v.dx)$$

Since:

$$d\psi = \frac{\partial \psi}{\partial x}dx + \frac{\partial \psi}{\partial y}dy$$

we have:

$$\frac{\partial \psi}{\partial x} = \rho v; \frac{\partial \psi}{\partial y} = -\rho u.$$

3.1.2 Velocity potential

Like the gravitational force or the spring force which could be expressed as the gradient of a potential energy, we can think of the velocity as the gradient of some potential field. It is defined as the function ϕ that satisfies:

$$\boldsymbol{q} = -\boldsymbol{\nabla}\phi$$

Where $\boldsymbol{q}$ is the velocity vector. The only thing worth noting is that for vortex flow, ϕ is not a single valued function.

In 2D, the condition for ϕ becomes:

$$-\frac{\partial \phi}{\partial x} = u; -\frac{\partial \phi}{\partial y} = v$$

3.1.3 A notable property of ϕ and ψ

One notable property is seen when we consider $\boldsymbol{\nabla}\phi$ and $\boldsymbol{\nabla}\psi$. These vectors are perpendicular to the equipotential and streamlines respectively:

$$\begin{aligned}
&\boldsymbol{\nabla}\phi.\boldsymbol{\nabla}\boldsymbol{\psi} \\
&= \left(\frac{\partial \phi}{\partial x}, \frac{\partial \phi}{\partial y}\right).\left(\frac{\partial \psi}{\partial x}, \frac{\partial \psi}{\partial y}\right) \\
&= (-u, -v).(-\rho v, \rho u) \\
&= \rho uv - \rho uv = 0,
\end{aligned}$$

meaning that at any point, the equipotential and streamlines are perpendicular.

3.2 Complex Velocity Potential and the Complex Velocity

3.2.1 Complex velocity potential

The complex velocity potential, first coined by Jean le Rond d'Alembert in 1752 [Dar05], is a very useful framework to solve 2D fluid motions. Instead of working with two functions ϕ and ψ, where vector equations eventually have to be projected into x and y, we can work instead with a single complex function [Tho58]. And the *circle theorem* along side with suitable *conformal transformation* also make analysis of flow around aerofoils much easier. From the results above, if instead of mass flux, let ψ be the volumetric flux (with constant density), it could be seen that the functions ψ and ϕ satisfies the Cauchy-Riemann equations:

$$\frac{\partial \phi}{\partial x} = \frac{\partial \psi}{\partial y} = -u,$$

$$\frac{\partial \phi}{\partial y} = -\frac{\partial \psi}{\partial x} = -v.$$

When these conditions are satisfied, and when all the partial derivatives are *continuous*, then we can conclude that the complex function [4]

$$w(z) = \phi(x, y) + i\psi(x, y)$$

is holomorphic, meaning it has the following properties:

[4] where $z = x + iy$

1. It is 1 to 1 within a domain (where said conditions are satisfied) in the complex plane bounded by a curve C
2. It has complex derivative anywhere within the said curve.

This is the complex potential.

The Cauchy-Riemann equation is equivalent to $dw/d\bar{z} = 0$. Meaning w is not a function of $\bar{z}$. The second property is important because the complex velocity is the derivative of w. But in practice, it could be relaxed for a finite or infinite number of points inside C, where the velocity is undefined. Such as at the centre of vortices. This could be done by drawing C in such a way that only enclose the holomorphic region of w.

The fact that w cannot be a function of $\bar{z}$ puts some signs to look for to spot holomorphic functions. If, assuming all reductions has been carried out, w is still a function of stand-alone x or y, then w is not a potential function because then $x = \frac{1}{2}(z + \bar{z})$. w also cannot be a function of $|z|$ because $|z| = \sqrt{z\bar{z}}$.

Geometrically, w gives a vector (in the form of a complex number) at every point on the complex plane, which in turn represents the 2D fluid domain. Thus, w is in essence a representation of a vector field.

3.2.2 The complex velocity

Let $dw(z)$ be the change of $w(z)$ when an observer at z is moved to another point $z + dz$ and take the second measurement $w(z + dz)$. In the spirit of all the other potential quantities, the ratio of these changes is called the complex velocity.

$$\begin{aligned} q_{\mathbb{C}} &= -\frac{dw}{dz} \\ &= -\frac{dw}{dz}\frac{\partial z}{\partial x} \\ &= -\frac{\partial w}{\partial x} \\ &= -\frac{\partial \phi}{\partial x} - i\frac{\partial \psi}{\partial x} \\ &= u - iv. \end{aligned}$$

The speed, however, is indirectly related to the complex velocity as:

$$q = \sqrt{u^2 + v^2} = q_{\mathbb{C}}\bar{q}_{\mathbb{C}}$$

and the complex number representation of the real velocity vector is the conjugate of the complex velocity:

$$\bar{q}_{\mathbb{C}} = u + iv$$

and is computed from the complex potential as:

$$\bar{q}_{\mathbb{C}} = -\frac{d\bar{w}}{d\bar{z}}.$$

3.3 Elementary flows in term of the complex potential

There are many notable elementary flows, namely: uniform, source, sink, doublet, vortex. But in this section, only the uniform, vortex flow, and source/sink will be covered.

3.3.1 Uniform flow

An uniform flow at speed U making an angle α to the x-axis has the following complex potential:

$$w(z) = Ue^{i\alpha}.z$$

We can verify that the streamlines are straight:

$$\psi(x,y) = \Im\Big\{w\Big\}$$

$$= Im\Big\{U(\cos\alpha + i\sin\alpha)(x+iy)\Big\}$$

$$= U(x\cos\alpha - y\sin\alpha)$$

When $\psi = const$, this is the equation of a line.

And the speed can be verified via the complex velocity:

$$q_{\mathbb{C}} = -\frac{dw}{dz}$$

$$= -Ue^{i\alpha},$$

which indeed has constant real and complex parts.

3.3.2 Vortex flow

Let κ be the vortex strength, defined as

$$\kappa = \frac{\Gamma}{2\pi},$$

where the circulation Γ is taken around a closed loop enclosing the center of the vortex. Let the vortex center be at position z_0. The complex potential generated by this vortex would then be:

$$w(z) = i\kappa\ln(z - z_0).$$

Thus $q = -\frac{dw}{dz} = -\frac{i\kappa}{z}$, so that

$$v = \bar{q} = i\frac{\kappa}{\bar{z}}.$$

This velocity implies that the positive vortex direction ($\kappa > 0$) corresponds to the direction of counter clockwise vortices (increasing $\angle z$).

3.3.3 Source/Sink

Their velocity potentials are given by:

$$w(z) = m \ln(z - z_0).$$

This flow satisfies the condition that its flux is constant for any curve encircling the source/sink.

3.4 Some useful theorems of Complex Analysis and Hydrodynamics

With the definition of $q_{\mathbb{C}}$, and having known in advance the importance of integral quantities like Γ, we would encounter integrals of the type

$$\oint f(z)dz$$

taken over a closed and singly connected contour C. With f often being the complex velocity. However, in the case of vortex flow, there exist a singularity at the centre of the vortex. It is therefore required to know about some useful theorems presented in this section to be able to handle these integrals appropriately. Namely, they are Cauchy's integral theorem and Cauchy's residue theorem. There are also some theorem of importance for incompressible inviscid flow, namely Blasius' theorem and the Circle theorem.

3.4.1 Cauchy's integral theorem

Given a complex function such as $f(z)$ and a closed loop (C). If $f(z)$ is holomorphic inside and on (C). We have:

$$\oint_C f(z)dz = 0$$

3.4.2 Cauchy's residue theorem[5]

Consider the following integral taken around a closed loop C, where $z = re^{i\theta}$:

$$\oint (z-a)^n dz$$

$$= \int_0^{2\pi} \left(re^{i\theta}\right)^n (ri.e^{i\theta}d\theta)$$

$$= \frac{r^{n+1}}{n+1} e^{i\theta(n+1)}\Big|_0^{2\pi}$$

$$= \begin{cases} 0 & \text{if } n \neq -1 \\ \oint \frac{dz}{z-a} = \oint \frac{ri.e^{i\theta}d\theta}{re^{i\theta}} = \oint id\theta = 2\pi i & \text{if } n = -1 \end{cases}.$$

[5] Thompson [Tho58], Sections 3.5, 3.52

Suppose there is a holomorphic function $w = f(z)$, but not necessarily holomorphic at a finite number of points a_n ; $n \in [1, N]$. Let the curve C_k enclose a point a_k amongst those singular points. Suppose also that $f(z)$ could be expanded in the vicinity of that singular point $a_n = a$ as follows:

$$f(z) = \sum_{\infty}^{0} A_k(z-a)^k + \sum_{1}^{\infty} \frac{B_k}{(z-a)^k},$$

where $B_1 \neq 0$. Then from the result of the previous integral, we have:

$$\begin{aligned}\oint f(z)dz &= \oint \left(\sum_{\infty}^{0} A_k(z-a)^k + \frac{B_1}{z-a} + \sum_{2}^{\infty} \frac{B_k}{(z-a)^k} \right) dz \\ &= 2\pi B_1 i.\end{aligned}$$

If we now do the same for all other points a_n inside the loop (C), we get a set of values B_n.

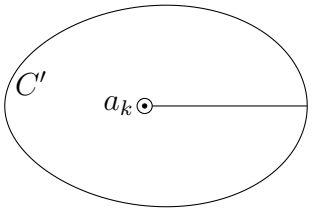


Figure 3.3: A domain where $f(z)$ is holomorphic

Now draw a closed loop C such that it encloses a subset of singular points a_i defined above. $f(z)$ remains holomorphic in between those points and within C. Now for each of those points, draw an infinitesimal circle C_k around them, and connect each circle with C via a path p_k not intersecting any other path (see Figure 3.3). Let C' be the curve consists of C, the infinitesimal circles around singular points, and the path connecting them. By Cauchy's integral theorem, the integral over the curve C' which encloses all the holomorphic part inside C will equate to zero:

$$\oint_{C'} f(z)dx = 0$$

$$\leftrightarrow \oint_C f(z)dz + \sum \left(\int_{p_k} f(z)dz + \int_{\bar{p}_k} f(z)dz + \oint_{\bar{C}_k} f(z)dz \right) = 0,$$

where the circle $\bar{C}_k$ must be traversed in the opposite direction to C if we want to follow C' without crossing any path. Thus:

$$\begin{aligned}\oint_C f(z)dz &= -\sum \oint_{\bar{C}_k} f(z)dz \\ &= \sum \oint_{C_k} f(z)dz \\ &= \sum 2\pi B_k i \\ &= 2\pi i \sum B_k.\end{aligned}$$

This is Cauchy's residue theorem. The values B_i are called residues because they are the only thing contributes to the integral. We can see that only singularities matter in this integral.

3.4.3 Blasius' theorem[6]

Consider an object in a 2D flow with complex potential $w(z)$. Since there is no assumptions about the direction of flow there is no Lift/Drag definition. We will let X and Y be the forces on the object in the x and y directions and let M be the moment of the forces acting on the object with respect to the origin.

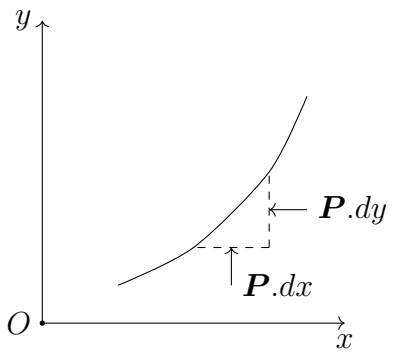


Figure 3.4: Forces on an infinitesimal area of surface

We have:

$$dY = -P.dy$$

$$dX = P.dx$$

$$dM = x.Pdx + y.Pdy.$$

By Bernoulli's principle ($P_0 = P + 1/2\rho q^2 + \rho gh$), by the assumption that ρ is small for air, and by letting $P_0 = 0$ by setting the gauge pressure accordingly, we have:

$$P = -\frac{1}{2}\rho q^2.$$

So that the complex force and real moment are:

$$d(X - iY) = \frac{1}{2}\rho q^2(dy + idx)$$

$$= \frac{1}{2}\rho\left(\frac{dw}{dz}\frac{d\bar{w}}{d\bar{z}}\right)(id\bar{z})$$

$$= \frac{1}{2}\rho i\frac{dw}{dz}d\bar{w}$$

and

$$dM = -\frac{1}{2}\rho\left(\frac{dw}{dz}\frac{d\bar{w}}{d\bar{z}}\right)\Re\{zd\bar{z}\}$$

$$= \Re\left\{-\frac{1}{2}\rho z\frac{dw}{dz}d\bar{w}\right\}.$$

[6] Thompson [Tho58], Sections 5.4, 5.41

On the object's surface, we have $\psi = const \rightarrow d\psi = 0$ so:

$$d\bar{w} = d(\phi - i\psi) = d\phi = d(\phi + i\psi) = dw = \frac{dw}{dz}dz.$$

Thus:

$$d(X - iY) = \frac{1}{2}\rho i\left(\frac{dw}{dz}\right)^2 dz$$

$$dM = \Re\left\{ -\frac{1}{2}\rho z\left(\frac{dw}{dz}\right)^2 dz\right\}.$$

And integrating over the boundary of the object, we found the forces and moments on it:

$$X - iY = \frac{1}{2}\rho i \oint \left(\frac{dw}{dz}\right)^2 dz$$

$$M = \Re\left\{ -\frac{1}{2}\rho z \oint \left(\frac{dw}{dz}\right)^2 dz\right\}.$$

This is Blasius' theorem. However, we can expand it still. By Cauchy's integral theorem, we can expand the boundary by which we take the integral beyond the boundary of the object. This is true as long as the points incorporated into the domain are where $w(z)$ remains holomorphic. Holomorphic means $dw/dz = -q$ exists, so we can expand the boundary into the fluid indefinitely as long as no singular point is incorporated (where q is undefined, such as a vortex centre, source, sink).

3.4.4 The Circle Theorem[7]

Suppose there is an irrotational, inviscid flowing fluid where initially there is no object present in the flow, and its complex potential is $w = f(z)$. Suppose now we insert a rigid circle $|z| = a$ into the flow field. The Circle Theorem says the complex potential becomes:

$$w'(z) = f(z) + \bar{f}\left(\frac{a^2}{z}\right)$$

Where the function $\bar{f}(z)$ is formed from $f(z)$ by replacing all i by $-i$ except those inside z.

When we insert the cylinder, there is only one more condition that the flow field should fulfil and that is there should be no flow penetrating the rigid surface. To prove that this is the potential for the new flow, it is sufficient to prove that the circle becomes a streamline. From what we know about streamline functions, we seek an equation of the form $\psi(z) = Im\{w'\} = const$.

Let $z = re^{i\theta}$, then $a^2/z = a^2/r.e^{-i\theta}$. When the point z is on the circle $|z| = a$:

$$\frac{a^2}{z} = re^{-i\theta} = \bar{z}$$

[7] Thompson [Tho58], Sections 5.1, 5.2

and

$$w'(z) = f(z) + \bar{f}(\bar{z})$$
$$\leftrightarrow \psi(z) = \Im\{w'\} = 0 \ \forall z = ae^{i\theta}.$$

3.4.5 Conformal transformations[8]

Let $z = f(\zeta)$ be holomorphic on and inside a closed loop Γ. On the contour Γ, assume further that $\nexists\, \zeta_1, \zeta_2 \in \Gamma$ such that $f(\zeta_1) = f(\zeta_2)$, and assume that $f'(\zeta) \neq 0$ $\forall \zeta \in \Gamma$. Let C be the contour z traces out when ζ traces Γ.

If we think of z and ζ as coordinates in 2 different 2D planes, then $f(\zeta)$ transforms a contour Γ in the ζ plane into a contour C in the z plane. The fact that $f(\zeta)$ is holomorphic on and inside Γ by definition guarantees that there exist a complex derivative at all points on and within Γ. The complex derivative tells a vector quantity $z = f(\zeta)$ at the point ζ to scale by the module of $f'(\zeta)$ and to rotate by the argument of $f'(\zeta)$. Thus, the transformation in action is to scale and rotate every point on and inside of Γ.

Let ζ, ζ_1, ζ_2 be 3 points very close to each other on the ζ plane. We have:

$$\lim_{\zeta_1 \to \zeta} \frac{z_1 - z}{\zeta_1 - \zeta} = \frac{dz}{d\zeta} = f'(\zeta)$$

$$\lim_{\zeta_2 \to \zeta} \frac{z_2 - z}{\zeta_2 - \zeta} = \frac{dz}{d\zeta} = f'(\zeta).$$

Thus

$$\rightarrow \lim_{\zeta_1 \to \zeta} \frac{z_1 - z}{\zeta_1 - \zeta} = \lim_{\zeta_2 \to \zeta} \frac{z_2 - z}{\zeta_2 - \zeta},$$

and so

$$\arg(f'(\zeta)) = \frac{\arg(z_1 - z)}{\arg(\zeta_1 - \zeta)}\bigg|_{\zeta_1 \to \zeta} = \frac{\arg(z_2 - z)}{\arg(\zeta_2 - \zeta)}\bigg|_{\zeta_2 \to \zeta}$$
$$\leftrightarrow \arg(z_1 - z) - \arg(\zeta_1 - \zeta) = \arg(z_2 - z) - \arg(\zeta_2 - \zeta)$$
$$\leftrightarrow \arg(z_1 - z) - \arg(z_2 - z) = \arg(\zeta_1 - \zeta) - \arg(\zeta_2 - \zeta)$$
$$\leftrightarrow \alpha = \beta.$$

If ζ_1 and ζ_2 are points on 2 contours intersecting at ζ, the limit $\zeta_1 \to \zeta$ means ζ_1 tends to a point on the tangent to its curve at ζ, and likewise for ζ_2. Thus the angle between tangents are preserved. Transformations that preserves tangent angles like this are called *Conformal Transformations* [Nee23].

On the other hand:

$$|f'(\zeta)| = \lim_{\zeta_1 \to \zeta} \frac{|z_1 - z|}{|\zeta_1 - \zeta|} = \lim_{\zeta_2 \to \zeta} \frac{|z_2 - z|}{|\zeta_2 - \zeta|}.$$

So length ratios are also preserved. But again, this is length ratio in the direction of the tangents at ζ, so in general the angle between 3 points far away will not be preserved, so do the lengths between them.

[8] Thompson [Tho58], Section 5.62, 5.70

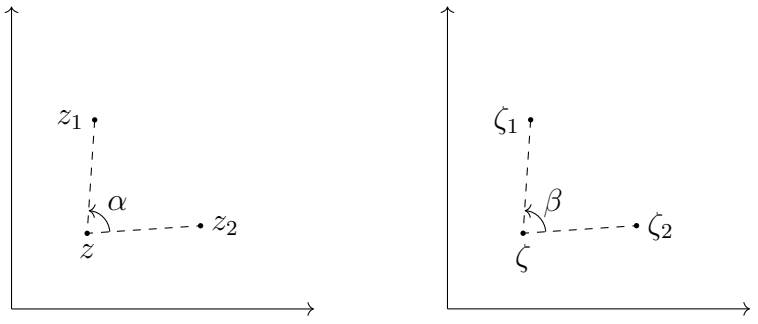


Figure 3.5: ζ and its conformal transformation

Summing the preservation of intersection angles and the preservation of infinitesimal lengths, we can conclude that conformal transformations preserves the shape of infinitesimal objects, and all they do to them is scaling and rotating. However, on the large scale, a conformal transformation could distort shapes. For example, look at the transformation:

$$z(\zeta) = \zeta^2.$$

This transformation rotates the point ζ by $\arg(\zeta)$ and scales up the length from ζ to the origin by $|\zeta|$. Geometrically, we can understand what it does to a shape by looking at what it does to a line. Let $\zeta = x + yi$, $z = u + iv$.

$$z = \zeta^2 = (x + iy)^2 = x^2 - y^2 + 2xyi$$

$$\rightarrow \begin{cases} u = x^2 - y^2, \\ v = 2xy. \end{cases}$$

For horizontal lines in ζ plane, $y = y_0$, thus:

$$x = \frac{v}{2y_0}$$

$$\rightarrow u = \frac{v^2}{4y_0^2} - y_0^2,$$

and for vertical lines $x = x_0$:

$$y = \frac{v}{2x_0}$$

$$\rightarrow u = x_0^2 - \frac{v^2}{4x_0^2}.$$

In the first quadrant, this mapping turns horizontal lines into parabola with foci at the origin and faces right, and turns vertical lines into parabolas facing to the left. Whenever these parabolas intersect, they still do so at 90 degrees as they did in the ζ plane due to the tangential intersection angle preservation property.

3.5 Joukowsky transform and Joukowsky airfoil[9]

Joukowski's transformation is given by:

$$z = \zeta + \frac{l^2}{\zeta},$$

where $l \in \mathbb{R}$. In the ζ plane we define 2 points of importance: H' at $\zeta = -l + 0i$ and S' at $\zeta = l + 0i$. And name their corresponding points in z plane by H at $z = -2l + 0i$ and S at $z = 2l + 0i$ (see figure 3.6).

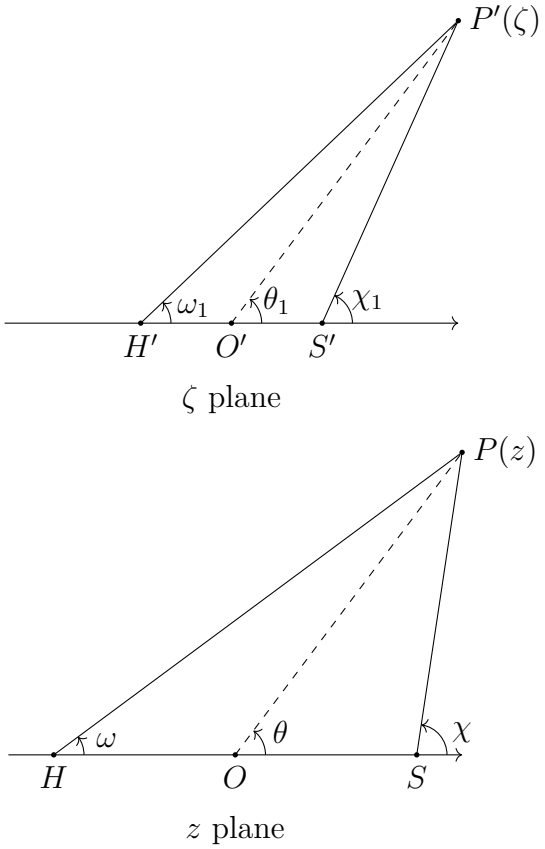


Figure 3.6: $H' : -l + 0i$, $S' : l + 0i$, and $P : \zeta$ in ζ plane, and their transformed points in z plane.

Consider the complex number representing the length from S to P:

$$z_{SP} = z_P - z_S = z - 2l = \frac{(\zeta - l)^2}{\zeta}$$

$$\leftrightarrow \begin{cases} \arg(z - 2l) = 2\arg(\zeta - l) - \arg(\zeta) \\ |z - 2l| = \frac{|\zeta - l|^2}{|\zeta|} \end{cases} \leftrightarrow \begin{cases} \chi = 2\chi_1 - \theta_1 \\ SP.O'P' = (S'P')^2 \end{cases}.$$

[9] Thompson [Tho58], sections 6.1, 6.2, 6.3, 6.4

Consider also the length from H to P:

$$z_{HP} = z_P - z_H = z + 2l = \frac{(\zeta + l)^2}{\zeta}$$

$$\leftrightarrow \begin{cases} \omega = 2\omega_1 - \theta_1 \\ HP.O'P' = (H'P')^2 \end{cases} .$$

From these results, we have:

$$\angle SPH = \chi - \omega = 2(\chi_1 - \omega_1) = 2\angle S'P'H'$$

and

$$SP + HP = \frac{S'P'^2 + H'P'^2}{O'P'}$$

and by Apollonius' theorem, we have:

$$SP + HP = \frac{2O'S'^2 + 2O'P'^2}{O'P'}.$$

Note that at S' and H',

$$\frac{dz}{d\zeta} = 1 - \frac{l^2}{\zeta^2} = 0,$$

thus, the transformation is not holomorphic at these points. Therefore it is not conformal with respect to curves passing through H and P (could be streamlines or equipotential lines). So if we apply this transformation on a flow domain, we must be sure that the domain does not include these 2 points because the intersection angles are not preserved. It is the case because for incompressible flow equations to apply, streamlines and potential lines passing through any point must satisfy the Cauchy-Riemann equations[10] (which dictates that they must intersect at right angles).

To get a sense of Joukowski's transformation, let us apply it to domains having boundary of simple shapes, then how it could naturally give rise to an airfoil will be clear.

3.5.1 Joukowski's transformation on the domain outside a circle centred at O

First we define a domain. Let $(C') : O'_1, a$ be a circle centred at $O'_1(0, 0)$ in ζ plane, having radius $a > l$. The domain will be the potion of space C'^o outside the circle. We are concerned with what shape the boundary of the domain will become. Let $P' \in \zeta$ plane traces the circle C', we have:

$$SP + HP = \frac{2|z_{S'}|^2 + 2|z_{P'}|^2}{|z_{P'}|} = \frac{2(l^2 + a^2)}{a} = const.$$

Thus P traces out an eclipse.

In the special case when $a = l$, $SP + HP = 4l = SH$, then P traces out a line.

[10] See section 3.2.1: Complex Velocity Potential where this is proven. The section about streamlines also state that streamlines only exist in incompressible flows (at least for the kind defined here)

3.5.2 Joukowski's transformation on the domain outside a circle centred on the x-axis or y-axis

Let the centre of (C') be at $O'_1 : b + 0i$. Let $a = b + l$ so that $O'_1H' = b + l = a$ thus H' is on the circle (C').

When $z_{P_1} = z_{H_1} = -l$,

$$SP + HP = \frac{2l^2 + 2(-l)^2}{l} = 4l = HS$$

$$\rightarrow P \equiv H.$$

This is the same equation as the case $a = l$. So the effect of having a focal point on the circle is the transformed curve tends to a flat line, similar to that special case.

Let A' be the other intersection of (C') with the x-axis. When $z_{P'} = z_{A'} = l+2b$:

$$SP + HP = \frac{2l^2 + 2(l + 2b)^2}{l + 2b} = const > HS.$$

This is the same equation as the trivial case. Thus on this end, C looks like part of an eclipse, and S and H are its foci.

The shape is drawn in Figure 3.7. It is sufficient to know the position of H' and S' in order to guess the shape of the final transformation.

On the other hand, if now the centre of (C') is on the y-axis at $0 + \epsilon i$, then for any point P' on the larger $S'H'$ arc, we have

$$\angle SPH = 2\angle S'P'H' = \angle S'O'H'$$

$$\Rightarrow \angle SPH = const.$$

Thus P traces out a partial circle. If P' is on the minor arc, let the line $P'O'$ intersect the circle at R'. By geometry, we have:

$$O'P'.O'R' = l^2$$

$$\rightarrow |\zeta_{R'}| = \frac{l^2}{|\zeta_{P'}|}.$$

Let $\arg(\zeta_{P'}) = \theta'$, and notice that $\zeta_{P'} = i^2\zeta_{R'}$ because they are on the same line on either sides of the coordinate centre, then:

$$z_P = \zeta_{P'} + \frac{l^2}{\zeta_{P'}} = i^2\zeta_{R'} + \frac{l^2}{i^2\zeta_{R'}} = -z_{R'}$$

Since the arc HS is symmetric over the y-axis, $-z_R$ is also on it. Thus the minor arc is also transformed into the same curve. And we can see that the direction of trace on this arc is opposite to the arc traced by the point P' when it travels on the major arc because R' travels in the opposite direction of P'.

The radius of the arc in Figure 3.8 is given by [Tho58]:

$$R = \epsilon + \frac{l^2}{\epsilon}.$$

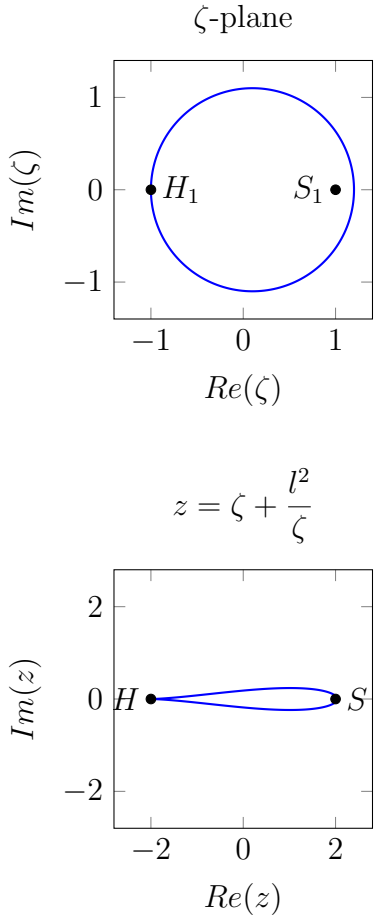


Figure 3.7: Joukowski's transformation with $l = 1$ for domain outside a circle with center on the x-axis

3.5.3 Joukowski's airfoil

Joukowski's airfoil is created by applying Joukowski's transform on a circle whose centre not coincides with the coordinate centre, while having the point H' on the circle. The flow is again happening on the outside of this shape.

Now the centre of (C') is at $b + ci$, and the radius $a = \sqrt{(b+l)^2 + c^2}$ is chosen such that H' stays on the circle and S' is inside the circle. As could be inferred from the cases seen above, the image around H is somewhat close to a line, while the image around S will be close to an eclipse. The real part of the coordinate of the centre of (C') determines how thick the airfoil is, while the imaginary part determines how much camber there is.

An important parameter of Joukowski airfoil is the angle the tail H makes with the real axis.

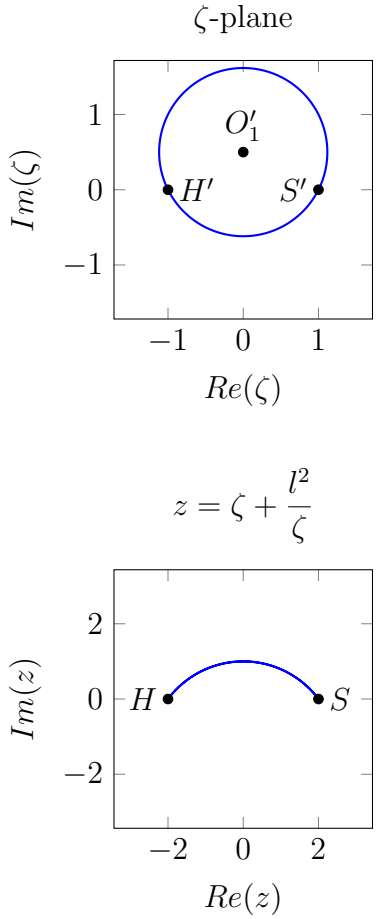


Figure 3.8: Joukowski's transformation on a circle on the y-axis

3.6 Matters on flow around Joukowski's airfoil

3.6.1 Conformal mapping of a complex field [11]

Having known Joukowski's transformation, the idea is to solve for the complex velocity potential around a simple cylinder, then use this transformation *on the domain outside it* to transform this domain into the flow around the corresponding airfoil. Since the transformation is conformal, we know that $\phi = const$ and $\psi = const$ are still perpendicular to each other, thus they would still be valid flow lines. The question remains what is the new form of w.

Given a conformal transformation $z = f(\zeta)$ and a complex field $w(\zeta)$ in ζ plane describing some fluid motion. Since the transformation only change the variable ζ into another variable $f^-1(z)$ and leave the form of w intact, we can see that the corresponding points z_0 and ζ_0 related by $z_0 = f(\zeta_0)$ have the same value of w.[12] Put mathematically, the values of $w(z_0)$ and $w(\zeta_0)$ at $z_0 = f(\zeta_0)$ and ζ_0 are the same, and

[11] Thompson [Tho58], Section 3.8

[12] Another way to think about it, because the mapping is conformal, we can imagine it as twisting the canvas. If each point has a value w attached to it before the twist, then after the twist obviously the same point at its new location still retain the value w.

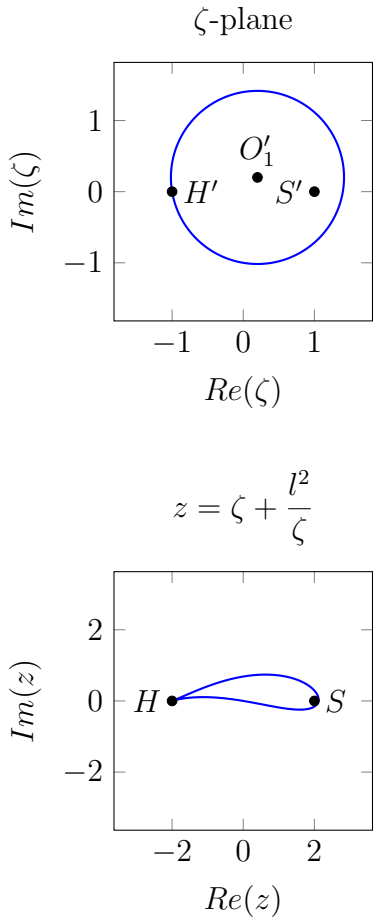


Figure 3.9: Joukowski's transformation on a circle at an arbitrary position such that H_1 is on it and S_1 is inside it

the form of $w(z)$ can be obtained by the substitution: $w(z) = w(f^{-1}(z))$. Thompson [Tho58] remarked that it is often more convenient to not make the substitution but use ζ as an intermediate parameter. Such as when finding the complex velocity, we write:

$$q_z = -\frac{dw}{dz} = -\frac{dw}{d\zeta}\frac{d\zeta}{dz} = -q_\zeta / f'(\zeta).$$

3.6.2 Joukowski's hypothesis

We know that the flow around a spinning cylinder, as long there is no separation, could be obtained by superimposing upon a uniform flow a vortex and a doublet at the centre of the cylinder[And17]. Starting with an uniform flow $f(z) = Ue^{i\alpha}z$, we first use the circle theorem ($w'(z) = f(z) + \bar{f}(a^2/z)$) to get the flow around a cylinder when it is placed into this field. The doublet's potential is easily seen as the part ($\bar{f}(a^2/z)$) added by the circle theorem.

Upon this flow, we add a vortex rotating about the same axis and direction as the cylinder. We can add this vortex because its streamlines are concentric circles, so the cylinder's wall remains a streamline. With this addition, we are trying to capture a viscid flow phenomenon. In an inviscid flow, whether a cylinder is rotating or not should have made no difference. But in a viscid flow, the cylinder grabs the fluid and transfers a rotation into it. But since there is no boundary mechanism to transfer this rotation in inviscid flow[13], the result is that the strength of the vortex is undefined. It is also inappropriate to use the matching tangential velocity condition because the flow is inviscid.

However, we notice that at the trailing edge H, $dz/d\zeta = 0$, meaning the transformation is non-conformal. Thus

$$q_{H'} = -\frac{dw}{d\zeta} = -\frac{dw}{dz}\frac{dz}{d\zeta} = q_H \frac{dz}{d\zeta}$$

$$\rightarrow q_{H'} = 0.$$

So the point H' must be a stagnation point of the flow. This is the Joukowski hypothesis. It is needed because the transformation is not conformal at H'.[14] Since the uniform flow's potential $f(z)$ and doublet's potential $\bar{f}(a/z^2)$ are fixed, the vortex's strength κ will adjust itself such that it cancels out $q_{H'}$. Notice that since $w'(z) = f(z) + \bar{f}(a^2/z)$ already produce a streamline coincides with the wall of the cylinder, the vortex only has to produce a tangential flow $q = \kappa/a = -q_{H'}$

3.6.2.1 What about the leading edge?

For a thin aerofoil, the leading edge is the point S, and is exposed to the flow field since it sits on the circle. This point also has $dz/d\zeta = 0$, thus here the transformation is non-conformal, and the velocity $q_S \rightarrow \infty$. It must be understood that this singularity comes from the transformation, not the physics of the flow. It is more

[13] Hence it doesn't show up in the circle theorem and we added the vortex separately.

[14] In this case, the finite differential condition for holomorphic is violated. We can see that if $q_{H'} \neq 0$ then $q_H \rightarrow \infty$.

intuitive to say that q_S is undefined because the method explained thus far cannot give a value for it.

Unlike the trailing edge, we have no condition for this singularity and let its velocity q_S goes to ∞. And as a result, the vorticity at this point also goes to infinity. This is a peculiar result of the theory. But on the other hand, there is no true thin aerofoil in reality.

For a thick aerofoil, the point S' is enclosed inside the circle, and so this is not an issue.

3.6.3 Flow around Joukowski's airfoil[15]

3.6.3.1 A property of the general transformation

The idea with all of this conformal transformation is that we can solve for flow around an easy shape like the offsetted circle and then get the flow around an airfoil via a clever conformal transformation. We know that if the initial potential is a valid holomorphic function[16] then its transformed image via a conformal transformation will still satisfy the Cauchy-Riemann equations and therefore is also a valid complex velocity potential. However, there is one issue. Given an arbitrary airfoil shape, finding a correct conformal transformation that will give this shape from a circle is non-trivial, and must be done iteratively [Tho58]. With modern computers this task should be solvable as long as an algorithm exists.

Furthermore, far away from the airfoil, the transformation should also map an uniform wind into an *identical* uniform wind. An uniform flow is given by $w(\zeta) = Ue^{i\alpha}\zeta$ for velocity U and angle α relative to the real axis. Far away, it should map to $w(z) = Ue^{i\alpha}f(\zeta) \approx Ue^{i\alpha}(a\zeta + b)$, for $a \in \mathbb{R}, b \in \mathbb{C}$, so we should have

$$f(\zeta) \approx a\zeta + b \quad \forall |\zeta| >> 1.$$

This is satisfied by any transformation $z = f(\zeta)$ that has this property:

$$\lim_{\zeta \to \infty} f(\zeta) = a\zeta + b.$$

Amongst them is the following type of transformation:

$$z = b + a\zeta + \frac{l_1}{\zeta} + \frac{l_2}{\zeta^2} + \frac{l_3}{\zeta^3} + ...$$

where $l_1, l_2, ... \in \mathbb{C}$. An example is Joukowski's transform. Another notable transformation is Karman-Trefftz transform:

$$\frac{z - kl}{z + kl} = \left(\frac{\zeta - l}{\zeta + l}\right)^k$$

where $k < 2$. When $k = 2$, we get Joukowski's transform. The difference between these two is that Karman-Trefftz transform produce an intersection at H instead of a cusp, and therefore it is easier to manufacture.

[15] Thompson [Tho58], section 5.31, 6.8, 7.01, 7.6

[16] Of course except at only a finite number of points.

A consequence of this condition is that these transformations does not change shapes far away from the origin. That means an integration path far away from the centre will be approximately identical. This fact is useful when we want to use Blassius' theorem.

3.6.3.2 Position of stagnation point as a function of circulation strength[17]

Suppose there is an incoming wind at an angle α and strength U. The complex potential is:

$$w(\zeta) = Ue^{i\alpha}\zeta.$$

When a cylinder $|\zeta| = a$ is placed in the flow at the point $O_1' : \zeta_c$, by the Circle Theorem, we know that the complex potential becomes[18]:

$$w(\zeta) = Ue^{i\alpha}(\zeta - \zeta_c) + Ue^{-i\alpha}\frac{a^2}{\zeta - \zeta_c},$$

and we can omit the constant:

$$w(\zeta) = Ue^{i\alpha}\zeta + Ue^{-i\alpha}\frac{a^2}{\zeta - \zeta_c}.$$

Then a circulation $\kappa = \Gamma/2\pi$ is added at the centre of the circle to account for the circulation that would arise in a real airfoil.[19] Its strength is chosen such that Joukowski's hypothesis is satisfied. This circulation adds a complex potential $w_\kappa = i\kappa \ln(\zeta - \zeta_c)$ to the field. The total complex potential is:

$$w(\zeta) = Ue^{i\alpha}\zeta + Ue^{-i\alpha}\frac{a^2}{\zeta - \zeta_c} + i\kappa \ln(\zeta - \zeta_c).$$

By Joukowski's hypothesis, the point H_1 must be a stagnation point. Solving

$$q = -\frac{dw}{d\zeta} = 0,$$

for a general point P' at ζ on the circle, we get:

$$Ue^{i\alpha} - Ue^{-i\alpha}\frac{a^2}{(\zeta - \zeta_0)^2} + i\kappa\frac{1}{\zeta - \zeta_0} = 0.$$

Make a shift of coordinates centre to ζ_0 by letting $\zeta' = \zeta - \zeta_0$ and solve for κ, we get:

$$\kappa = \frac{a^2U - Ue^{i2\alpha}\zeta'^2}{ie^{i\alpha}\zeta'}.$$

[17] I have seen this formula given many times without proof, such as in Anderson [And17] and even Thompson [Tho58], so I would give it a go.

[18] First shift the uniform field to the circle's centre, then apply the theorem

[19] A non-rotating cylinder placed in uniform flow will not generate any circulation, but the asymmetry of an airfoil would.

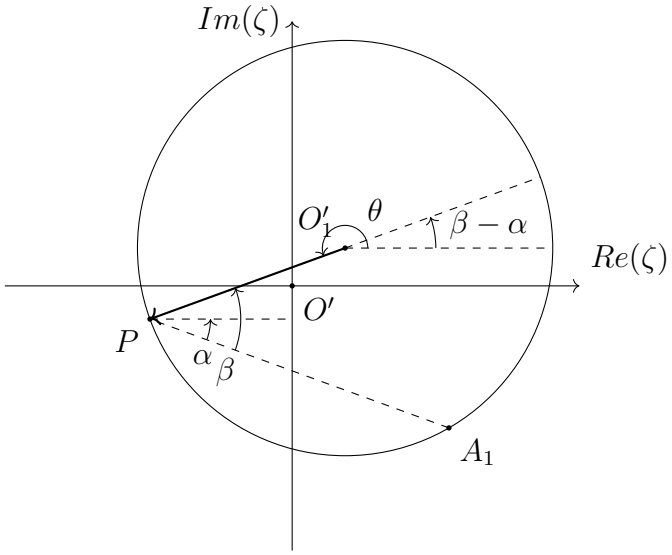


Figure 3.10: An arbitrary point P on the circle O_1'. The wind coming in parallel to A_1P. The coordinate centre here is not yet shifted to O_1'.

The number ζ' refers to the relative position (vector) of P with respect to its centre O_1'. [20] Let $\zeta' = ae^{i\theta}$ (refers to Figure 3.10) and plug into the equation for κ, we get:

$$\kappa = \frac{a^2U - Ue^{i2\alpha}(ae^{i\theta})^2}{ie^{i\alpha}(ae^{i\theta})}.$$

We let β be the angle of the incoming wind relative to the vector $O_1'P$. It could be seen from this figure that $\theta = \pi + \beta - \alpha$, thus $\zeta' = ae^{i\pi}e^{i(\beta-\alpha)} = -ae^{i(\beta-\alpha)}$. Plug into the equation for κ, we get:

$$\kappa = aU\frac{1 - e^{i2\alpha}e^{i2(\beta-\alpha)}}{ie^{i\alpha}(-e^{i(\beta-\alpha)})}$$

$$= aU\frac{1 - e^{i2\beta}}{-ie^{i\beta}}$$

$$= aU\frac{1 - (\cos\beta + i\sin\beta)^2}{-i(\cos\beta + i\sin\beta)}$$

$$= aU\frac{(2\sin^2\beta - 2i\cos\beta\sin\beta)(i\cos\beta + \sin\beta)}{\cos^2\beta + \sin^2\beta}$$

$$= 2aU\sin\beta$$

Therefore we get the following relationship between the radial position of the *trailing side* stagnation point and the strength of the circulation:

$$\kappa = 2aU\sin\beta. \tag{3.1}$$

Now it is by Joukowski's hypothesis that this stagnation point P has to coincide with the trailing edge H'. Thus we can calculate the required strength of the circulation.

[20] In this case, the direction of this complex number becomes important.

3.6.3.3 The flow itself

The flow is given by:

$$u - iv = -Ue^{i\alpha}(\zeta + l - 2ae^{-i\alpha}\cos\beta)\frac{\zeta^2}{(\zeta - \zeta_0)^2(\zeta - l)}$$

using the circle theorem.

3.7 Kutta-Joukowski's theorem[21]

Let there be an airfoil in uniform wind in z domain, a transformation $z = f(\zeta)$ that can map a circle in ζ plane, centred at ζ_c into this airfoil. Let there be a circulation of strength κ around the cylinder in ζ plane that satisfies the Joukowski hypothesis. From Section 3.6.3, we know that the derivative of the velocity potential around the cylinder is:

$$\frac{dw}{d\zeta} = Ue^{i\alpha} + i\frac{\kappa}{\zeta'} - Ue^{-i\alpha}\frac{a^2}{\zeta'^2},$$

where $\zeta' = \zeta - \zeta_c$.

Owning to the fact that the integration path in Blasius' theorem could be extended beyond the object indefinitely as long as no singular point was crossed, we apply it to the airfoil in z plane. Let the path of integration be expanded indefinitely.

By Blasius' theorem, the force on the airfoil is:

$$X - iY = \frac{1}{2}\rho i \oint_C \left(\frac{dw}{dz}\right)^2 dz$$

$$= \frac{1}{2}\rho i \oint_C \left(\frac{dw}{d\zeta}\frac{d\zeta}{dz}\right)^2 dz.$$

By the condition that $\lim_{\zeta\to\infty} f(z) = \zeta$, the path on integration becomes identical in both z and ζ planes, and also $dz \approx d\zeta$ and $d\zeta/dz = 1$. Thus:

$$X - iY = \frac{1}{2}\rho i \oint_C \left(\frac{dw}{d\zeta}\right)^2 d\zeta.$$

Consider:

$$\left(\frac{dw}{d\zeta}\right)^2 = U^2e^{i2\alpha} - \frac{\kappa^2}{\zeta'^2} + \frac{U^2a^4}{e^{i2\alpha}\zeta'^4} - 2Uie^{i\alpha}\frac{\kappa}{\zeta'} - \frac{2Uia^2\kappa}{e^{i\alpha}\zeta'^3} + \frac{U^2a^2}{\zeta'^2}, \tag{3.2}$$

[21] This section takes a very different approach from Thompson [Tho58], where it is not obvious that this theorem should only be applied to flow around objects that does not generate any more vortices other than the vortex already there, and that the formula of Kutta-Joukowski is only true for an isolated aerofoil. To calculate force and moment on objects that generates singularities as they move, one should fall back to Blasius' theorem. Strangely enough, one of such cases is the airfoil in unsteady motion. But the interested reader could read Thompson's Section 5.5, and Anderson [And17], Chapter. 4

by Cauchy's residue theorem, the integral is evaluated and becomes:

$$\oint_C \left(\frac{dw}{d\zeta}\right)^2 d\zeta = 2\pi i \times (-2Uie^{i\alpha}\kappa)$$

$$\rightarrow X - iY = \frac{1}{2}\rho i \times (2\pi i \times (-2Uie^{i\alpha}\kappa))$$
$$= i(2\pi\kappa)\rho U e^{i\alpha}.$$

The lift is:

$$X + iY = -i(2\pi\kappa)\rho U e^{i\alpha}$$

This is the famous Kutta-Joukowski theorem. Written in this complex form, we can also see the direction of the total force. It is

$$-ie^{i\alpha},$$

meaning the total force is rotated by $3\pi/2$ in the positive sense (of the complex number) relative to the incoming wind's vector. Notice that this total force is entirely perpendicular to the incoming flow. It has no drag! This is expected since the flow we concern is inviscid, hence no viscous or pressure drag is observed because the flow follows the body's contour perfectly.[22] Also, this force is calculated with Blasius' theorem, which only accounts for pressure forces in inviscid flow.

The force[23] required to keep a vortex stationary in a moving fluid field is

$$X + iY = i(2\pi\kappa)\rho U e^{i\alpha},$$

which is equal and opposite to the lift. Without it, the vortex will be carried with the flow. The proof is the same, using Blasius' theorem, but the application is onto the opposite side of the volume's boundary because we want to find the force exerted on the fluid. Hence, the lift is the reaction to the force that the wing exerts on the flow to drag its vortex around.

3.7.1 Calculating the steady circulation

Now we have 2 ways to calculate Γ_0. One from the equation of lift in Section A.4.2 and using the Kutta-Joukowski theorem $L_0 = \rho U \Gamma_0$, we get[24]:

$$\Gamma_0 = Uc\left(A_0\pi + A_1\frac{\pi}{2}\right).$$

On the other hand, from equation $\kappa = 2aU\sin\beta$, we can also calculate the quasi-steady circulation as following:

$$\Gamma_0 = 2\pi\kappa$$
$$\leftrightarrow \Gamma_0 = 4\pi aU\sin\beta,$$

[22] It is called D'Alembert paradox.
[23] Exerted on the fluid.
[24] The sign was flipped because the positive vortex convention is different.

where $a = \sqrt{(l+b)^2 + \epsilon^2}$ is the radius of the circle used to generate the airfoil, the centre of that circle is located at $\zeta_0 = b + i\epsilon$, and l comes from Joukowski's transformation. If we realize that $(l+b)^2 >> \epsilon^2$ because $\epsilon, b << 1$, then we can use the approximation: $a \approx l \approx c/4$. The angle β is called the *absolute incidence*. Its construction was shown in Figure 3.10. Plugging in $\beta = \beta_0 + \alpha$, we get

$$\Gamma_0 = 4\pi\frac{c}{4}U\sin(\alpha + \beta_0),$$

where β_0 is the angle β when the angle of attack $\alpha = 0$. Due to camber, this angle is not zero. In Figure 3.10, it happens when P, O', and A_1 are collinear. From geometry, it can be seen that

$$\beta_0 = \arctan\left(\frac{\epsilon}{l+b}\right).$$

We also know from Section 3.5.2 about Joukowski transform that $R = \epsilon + \frac{l^2}{\epsilon} \approx \frac{l^2}{\epsilon}$ is the radius of the camber line. Thus

$$\beta_0 \approx \frac{l^2/R}{l} = \frac{l}{R}.$$

Plugging in, and using $l \approx c/4$, we have:

$$\Gamma_0 = \pi c U \sin\left(\alpha + \frac{c}{4R}\right), \tag{3.3}$$

but there can be only one true for inviscid, incompressible flow. Which one is it?

We can take a guess by noticing that the first formula predicts a lift that infinitely increases with infinitely increasing measure of α. This erratic behaviour exists because we have taken the approximation that $\alpha << 1$ when we derived the first formula in Section A.4. Thus this formula breaks down for large α. Therefore, when $|\alpha| < \pi/2$, we should use Equation (3.3).

3.7.2 When α approaches $\pi/2$, stalling of aerofoil in inviscid flow

From Section 3.6.3.2, we know that the complex potential for flow around a cylinder with circulation κ imposed upon it is:

$$w(\zeta) = Ue^{i\alpha}(\zeta - \zeta_0) + Ue^{-i\alpha}\frac{a^2}{\zeta - \zeta_c} + i\kappa\ln(\zeta - \zeta_c),$$

where ζ_0 is the position of the cylinder's centre.

From the Kutta-Joukowski theorem and the equation for the circulation for a thick aerofoil[25], we get the following formula for lift (as a complex number):

$$L = \pi c\rho U^2 \sin\left(\alpha + \frac{c}{4R}\right)(-ie^{i\alpha}).$$

[25]In which this aerofoil is the result of transforming a circle from ζ plane onto z plane using a conformal transformation $z = f(\zeta)$.

It is apparent that the lift starts to decrease when $\alpha + \frac{c}{4R} > \frac{\pi}{2}$. Thus, the stall angle is

$$\alpha_{stall} = \frac{\pi}{2} - \frac{c}{4R}.$$

3.7.3 Proving the Kutta-Joukowski theorem for aerofoils not derived from the Joukowski transform

One might ask whether this result can be applied to other thick aerofoils - those that are not created from Joukowski's transformation. To which the answer is yes. To prove this, recall that we want to transform the flow outside a cylinder (represented by the circle $|\zeta - \zeta_c| = a$) into the flow outside an aerofoil. In order for the complex fields such as complex velocity to have non-infinity values, the transformation must be holomorphic inside the flow field. *Any* conformal transformation $z = f(\zeta)$ that is holomorphic in an annulus (r, R) can be expanded in a Laurent series centred at the centre ζ_o of the annulus as

$$f(\zeta) = \sum_{n=-\infty}^{\infty} a_n(\zeta - \zeta_o)^n,$$

and $f(\zeta)$ must be holomorphic inside the flow region so that the expansion is valid for the entire flow field.[26]

We can also restrict possible transformations to ones that map uniform flow to uniform flow far away from the aerofoil[27]. Thus the expansion must satisfy $f(\zeta) \approx \zeta$ when $\zeta >> a$. Thus all the high power coefficients must be zero[28].

$$f(\zeta) = a_1(\zeta - \zeta_0) + \sum_{n=-\infty}^{0} a_n(\zeta - \zeta_o)^n.$$

Recall that the Kutta-Joukowski theorem was proven by taking the integral in z-plane

$$\oint_C \left(\frac{dw}{d\zeta}.\frac{d\zeta}{dz}\right)^2 dz$$

[26]In order for this to be true, r must enclose all singular points of the transformation. Those points are where $df/d\zeta = 0$. We have

$$\frac{df}{d\zeta} = \sum_{n=-\infty}^{\infty} a_n n(\zeta - \zeta_o)^{n-1} = 0$$

which is a high degree polynomial. Thus there are potentially many points not coincide with ζ_o that satisfies the condition above. Let r be large enough to touch the furthest of them, although there could be many. The region outside of r up to $R \to \infty$ is the holomorphic region of $f(\zeta)$. The circle $|\zeta - \zeta_c| = a$ could then be drawn enclosing the circle (ζ_o, r), such that it touches the circle (ζ_o, r) at one of the singular points on its circumference. It is proven that on any exposed singular point, the profile will have a cusp or a discontinuity (Thompson [Tho58], Section 7.01). This will be the trailing edge. With this construction, it is guaranteed that the flow field is entirely within the holomorphic region of the transformation.

[27]This means they do not disturb flow far from the cylinder. This is only a preference because it makes analysis easier if the oncoming flow in both z and ζ planes are identical.

[28]There is no need to restrict the 1^{st} order coefficient to 1, as we will see. Any distortion of the uniform flow will cancel because the 1^{st} order term of $dw/d\zeta$ contains a similar distortion of the flow.

on a path far away from the aerofoil. On this path, the negative powers of $f'(\zeta) = \frac{dz}{d\zeta}$ goes to zero, except the 0^{th} power which has coefficient a_1. But also $dz \approx f'(\zeta)d\zeta = a_1 d\zeta$, so the integral becomes:

$$\oint_C \left(\frac{dw}{d\zeta}.\frac{1}{a_1}\right)^2 a_1 d\zeta$$

$$= \oint_C \left(\frac{dw}{d\zeta}\right)^2 \frac{d\zeta}{a_1}.$$

And by Cauchy's residual theorem, the path of integration can be enlarged arbitrarily as long as no singularity was crossed, and that the result only depends on the coefficient a'_{-1} of the Laurent expansion of $w(\zeta)$. Thus we could swap the path C for the corresponding path C' in ζ plane because the only singularity of $w(\zeta)$ is outside the flow domain. The integral becomes:

$$\oint_{C'} \left(\frac{dw}{d\zeta}\right)^2 \frac{d\zeta}{a_1},$$

which is an integral in the ζ plane. Plugging this into Blassius' theorem, we get:

$$L = \frac{1}{2}\rho i \oint_{C'} \left(\frac{dw}{d\zeta}\right)^2 \frac{d\zeta}{a_1},$$

where the a'_{-1} term of $(dw/d\zeta)^2$ is $-2Uie^{i\alpha}\kappa$ in Equation (3.2). However, because this is an integration in ζ-plane, we notice that the uniform flow with magnitude Ua_1 in ζ-plane, at $\zeta >> 1$, given by

$$\begin{aligned} w(\zeta) &= (Ua_1)e^{i\alpha}\zeta \\ &= (Ua_1)e^{i\alpha}\frac{z}{a_1} \\ &= Ue^{i\alpha}z \end{aligned}$$

become a flow with magnitude U in the z-plane. Thus, to produce the correct boundary condition in z-plane, the uniform flow's potential in ζ-plane must be scaled by the transformation $f(\zeta)$'s a_1 coefficient. Replacing U by Ua_1, the a'_{-1} coefficient of the Laurent expansion of $(dw/d\zeta)^2$ is:

$$a'_{-1} = -2(Ua_1)ie^{i\alpha}\kappa.$$

So the integral evaluates to, following Cauchy's integral theorem:

$$\begin{aligned} L &= 2\pi\kappa\rho(Ua_1)\frac{1}{a_1}(-ie^{i\alpha}) \\ &= 2\pi\rho\kappa U(-ie^{i\alpha}). \end{aligned}$$

This is the lift on the aerofoil in z-plane.

This result is independent of the conformal transformation used to create the aerofoil. Thus, any aerofoil shape will tend to look like a Joukowski's aerofoil at a

distance, and thus their lifts are similar (in the inviscid case). We now see that the Joukowski's aerofoil is special in the fact that it is the low-order *approximation of all aerofoils*, so the bulk of the effects of other aerofoil profiles comes down to the equivalent Joukowski aerofoil of the same camber radius, at least in inviscid flow.

This result has one condition that the aerofoil is far away[29] from any other vortex generation device in the field. When there is another vortex near by, an additional force of interaction arises.

3.7.4 On the vorticity

This chapter's derivation differs from the derivation of the lift in Section A.4.1 (which uses Glauert's method) in that no vorticity was used. This difference highlight a property of the vorticity, one which has been voiced before by McLean [McL13], that it is only a mathematical construct. The velocity induced by a vortex filament is given by:

$$d\boldsymbol{w} = \frac{\Gamma}{4\pi r^2} d\boldsymbol{l} \times \hat{\boldsymbol{r}},$$

where Γ is the circulation produced by the vortex filament. This is similar in form to the Biot-Savart law of magnetism. However, unlike with magnetism where the electric current is a real quantity, the vortex filament is not. This is most apparent when we compare the physical causality of the two phenomena [McL13]. Whereas cancelling the electric current will cancel its magnetic field, cancelling a vortex filament is impossible due to Kelvin's principle of conservation of circulation. Thus any device whose job is to cancel the vortex filament in any given volume would only result in the filament taking another path bypassing that volume.

[29] Far away is very relative, but given that the effect of a vortex drops with $1/r$, far away can be relatively close.

4

Non-stationary Airfoil Theory

4.1 Introduction

Non-stationary Airfoil theory is of great importance to flutter analysis. The stationary airfoil theory presented thus far has been dealing with airfoils that do not vibrate in a steady stream of air. Flutter, however, involves vibrating airfoils and in these scenarios, the lift is not a function of the instantaneous parameters such as airspeed U and angle of attack α in the manner presented in steady-state analysis, but lags behind by a phase angle φ as the airfoil undergoes a forced oscillation at angular frequency ω. Historically, eventhough flutter was investigated as early as 1916, real progress in flutter analysis only came about due to the development of non-stationary airfoil theory in the 1920s by pioneers such as Walter Birnbaum [Fun69]. However these theories come with great mathematical complexity. Th. von Kármán and W. R. Sears in 1938 [KS38] established a theory, which, from his view, was to clear the complexity that had taken over the field of airfoil theory. The problem was so bad that to make out the physical essence from the mathematical fog was difficult. This complexity presumably also lead M. A. Biot to come up with a simplified theory of the former in 1942 [Bio42].

The main difference between the two is how the vorticity distribution on the airfoil is found in the case of oscillatory motion. In Biot's more complex theory, though already simplified, it is found by applying boundary conditions on the fluid elements close to the airfoil. In Karman's theory, however, the approach is based on vorticity and is more elegant. By applying Kelvin's circulation theorem ($d\Gamma/dt = 0$ $\forall t$ where Γ is the total circulation in the field), it is seen that when the airfoil deviates from its steady-state such as when it suddenly speeds up or pitch up, additional circulation occurs and to preserve the total circulation additional vortices must be shed in the wake. Kármán then considers what this vortex does to the vortex distribution on the airfoil.

It is also worth noting that in order to design a controller for sytems involving such oscillatory aerodynamics, it is not sufficient to only know steady-state airfoil theory, as we shall see, the steady-state lift/moment is only 1 of 3 components of the force/moment acting on an oscillating airfoil. A controller designed without the knowledge of these additional terms would presumably have narrow working domain and questionable off-design performance.

The following theory derivation for non-stationary airfoil theory is based on the approach laid out in von Karman's work [KS38]. In this work, the lift and moment was derived not form an integration of vortex distributions as stated in previous

sections, but as the consequence of Newton's laws of motion for linear and angular momentums.

The lift and moment in this case is no longer as simple as in the steady state case where it is given by the Kutta-Joukowsky theorem ($L = \rho U \Gamma_0$). Because unlike a steady-state airfoil where $\alpha = const$ and $z = z(x)$, on an unsteady airfoil, $\alpha = \alpha(t)$ and $z = z(x, t)$. We know that the circulation around an airfoil is proportional to its lift (and hence angle of attack α). Thus when the airfoil changes its pitch, the circulation around it also change.

Assume that we have an airfoil in an inviscid fluid. Then by Kelvin's principle of conservation of circulation in such a fluid:

$$\Gamma_{total}(t) = const.$$

Assuming that the airfoil starts in an initially irrotational velocity field and after some time has reached steady state, then:

$$\Gamma_{total} = 0 \ \forall t$$

$$\Leftrightarrow \Gamma_0 + \Gamma_s = 0,$$

where Γ_0 is the steady-state circulation around the airfoil and Γ_s is the starting vortex that the airfoil shreds a long time ago when it starts moving. The condition that some time has passed so that the airfoil is far from its starting vortex has a significance, as we will see shortly, because if there is an obstruction near a vortex, an image of that vortex will form and this equation will have more vortices and circulation terms.

Now if the airfoil changes its pitch or moves up or down, causing the circulation around it to be changed by an amount $\Gamma_1 \neq 0$, then due to Kelvin's vorticity conservation again, another vortex with opposite circulation and strength equal to Γ_1 must be shredded in its wake so that the total in the field is preserved. Theodore von Kármán and Sears [KS38] noticed that in this case the wake vortices are close enough to have an impact on the flow field immediately around the airfoil, unlike in the steady-state case where the starting vortex could be assumed to be far behind.

Before we continue further, it is beneficial to divide the x-axis into 2 parts. Those values within the chord should keep the notation x, while those outside of the chord towards the rear should be called by ξ instead. Mathematically:

$$x \in [-c/2, c/2],$$

$$\xi \in [c/2, \infty],$$

so $\gamma(x)$ is a distribution on the chord, while writing $\gamma(\xi)$ means that this distribution is situated at the wake of the airfoil.

The effect of the wake vortex on the aerofoil is peculiar. Let $\gamma_1(x)$ be such that $\Gamma_1 = \int_{-1}^{1} \gamma_1(x)dx$. Due to the condition that the flow cannot penetrate the airfoil, the system of additional vortices Γ_1 around the aerofoil and $-\Gamma_1$ in the wake must be distributed such that they take the aerofoil as its streamline. If the aerofoil is a circle, then Γ_1 is concentrated at a point on the line connecting the centre and the wake's vortex. However, since the aerofoil is non-circular, it force Γ_1 to spread out

into a vorticity distribution $\gamma_1(x)$ such that the airfoil itself becomes a streamline of the total flow.

Suppose an airfoil undergoes a fluctuation motion producing a fluctuation vortex distribution[1] $\gamma_1(x)$ and its corresponding wake vortex distribution $\gamma_1(\xi)$, satisfying the following condition to preserve the total circulation: $\int_{-1}^{1}\gamma_1(x)dx = -\int_{1}^{\infty}\gamma_1(\xi)d\xi$. As explained above, this small wake vortex shapes a small corresponding portion of the fluctuation vortex $d\gamma(x)$ such that the vortex system comprising of $d\Gamma_1 = \int_{-1}^{1} d\gamma(x)dx$ and $\gamma(\xi)d\xi$ takes the airfoil as a streamline. This phenomena is similar to electrostatic image because they all arise from a redistribution of charge/vortex such that a boundary condition was satisfied on a contour. Thus in this case the redistribution of $d\gamma_1(x)$ was called the vortex image.

By the properties of a conformal representation, streamlines parallel to the airfoil surface will remain parallel in the z' plane. In this plane, a flat airfoil positioned along the x axis, chord spanning from -1 to 1 is transformed into an unit circle centred at the origin.

Before diving into Kármán and Sears' result, I have provided some additional proofs of important results used in that paper.

4.2 Image of a vortex

Suppose that there is a vortex with strength $\kappa = \Gamma/2\pi$ at a point $z_0 = \xi + 0i$, and a circular object of unit radius, centred at $(0, 0)$. It is obvious that the circle's circumference must be a streamline since the flow cannot penetrate it. By experience, we know that pairs of vortices of the same strength and opposite vorticity create circular streamlines, the problem becomes where to put the second vortex such that the circular streamline coincide with the circle at (0,0). This second vortex that arise due to the presence of the object is called the image.

Due to symmetry, the second vortex must be situated on the line connecting the circle's centre and the first vortex. Its strength will be $-\kappa$. Let $z_1 = x + 0i$ be the position of the image.

We know that the complex potential around a vortex is $w = i\kappa\ln(z - z_0)$ where z_0 is the vortex's position. The potential of the system at a point z is then:

$$\begin{aligned} w(z) &= w_\kappa(z) + w_{-\kappa}(z) \\ &= i\kappa\ln\left(\frac{z - z_0}{z - z_1}\right) \end{aligned}$$

now $(z - z_0)/(z - z_1)$ is a complex number, thus:

$$\frac{z - z_0}{z - z_1} = \left|\frac{z - z_0}{z - z_1}\right| e^{i\theta_1},$$

where $\theta_1 = \arg(z - z_0) - \arg(z - z_1)$ is the angle made by 3 points z, z_0, and z_1. So we have:

$$w(z) = i\kappa\left(\ln\left|\frac{z - z_0}{z - z_1}\right| + i\theta_1\right).$$

[1] Which exists on top of the quasi-steady distribution $\gamma_0(x)$.

The streamline's function by definition is the imaginary part of w, thus:

$$\psi(z) = \kappa \ln \left| \frac{z - z_0}{z - z_1} \right|.$$

Streamlines are points on the curve $\psi(z) = const$. The circle with radius r as a streamline is mathematically expressed as:

$$\frac{\partial}{\partial \theta} \psi(r, \theta) \Big|_{r=r_0} = 0$$

$$\leftrightarrow \kappa \left| \frac{z - z_1}{z - z_0} \right| \frac{\partial}{\partial \theta} \left| \frac{z - z_0}{z - z_1} \right| = 0,$$

with z now confined to lie on the circle ($z = re^{i\theta}$, $r = const$). It is obvious that the fraction $\left|\frac{z-z_1}{z-z_0}\right|$ is not equal to 0 unless the points z and z_1 coincides. But then the derivative of ψ can only be 0 at that point. Thus for $\partial\psi/\partial\theta = 0 \ \forall\theta$, we require:

$$\frac{\partial}{\partial \theta} \left| \frac{z - z_0}{z - z_1} \right| = \frac{\partial}{\partial \theta} \left| \frac{r_0 e^{i\theta} - \xi}{r_0 e^{i\theta} - x} \right| = 0$$

$$\leftrightarrow \frac{\partial}{\partial \theta} \left| \frac{r\cos\theta - \xi + ir\sin\theta}{r\cos\theta - x + ir\sin\theta} \right| = 0$$

$$\leftrightarrow \frac{\partial}{\partial \theta} \left(\frac{r^2 - 2r\xi\cos\theta + \xi^2}{r^2 - 2rx\cos\theta + x^2} \right) = 0$$

$$\leftrightarrow \frac{2r\xi\sin\theta(r^2 - 2rx\cos\theta + x^2) - 2rx\sin\theta(r^2 - 2r\xi\cos\theta + \xi^2)}{(r^2 - 2rx\cos\theta + x^2)^2} = 0$$

$$\leftrightarrow 2r\xi\sin\theta(r^2 - 2rx\cos\theta + x^2) - 2rx\sin\theta(r^2 - 2r\xi\cos\theta + \xi^2) = 0$$

$$\leftrightarrow 2r^3\xi\sin\theta - 4r^2\xi x\sin\theta\cos\theta + 2r\xi x^2\sin\theta - 2r^3 x\sin\theta + 4r^2\xi x\sin\theta\cos\theta - 2rx\xi^2\sin\theta = 0$$

$$\leftrightarrow r^2\sin\theta(\xi - x) + x\xi(x - \xi)\sin\theta = 0$$

$$\leftrightarrow -r^2 + x\xi = 0$$

$$\leftrightarrow x = \frac{r^2}{\xi}.$$

4.3 Induced vorticity distribution as a function of tangential velocity

Given the Joukowski transformation $z = \zeta + \frac{a^2}{\zeta} = f(\zeta)$, $z, \zeta \in \mathbb{Z}$, a circle $|\zeta| = a$, and a complex velocity potential w.

On the circle $|\zeta| = a$ in ζ-plane, where we notice that *on this circle*, $\theta = const$ lines are mapped to $x = const$ lines, and $r = const$ line is mapped to $y = const$ line, we have:

$$v_\theta = \left| \frac{dw}{d(a\theta)} \right| = \left| \frac{dw}{dx} \frac{dx}{dz} \frac{dz}{d\theta} \right| \frac{1}{a} = v_x \left| \frac{dz}{d\theta} \right| \frac{1}{a},$$

$$v_r = \left|\frac{dw}{dr}\right| = \left|\frac{dw}{dy}\frac{dy}{dz}\frac{dz}{dr}\right| = v_y(-i)\left|\frac{dz}{dr}\right|.$$

Let $\zeta = re^{i\theta}$, plugging in values for $\frac{dz}{dr} = e^{i\theta} - \frac{a^2}{r^2 e^{i\theta}}$ and $\frac{dz}{d\theta} = ire^{i\theta} - i\frac{a^2}{re^{i\theta}}$, which on the circle $|\zeta| = a$ reduces to:

$$\frac{dz}{dr} = e^{i\theta} - e^{-i\theta} = 2i\sin\theta,$$

$$\frac{dz}{d\theta} = ia(e^{i\theta} - e^{-i\theta}) = -2a\sin\theta,$$

we have:

$$v_\theta = -2v_x\sin\theta,$$

$$v_r = 2v_y\sin\theta.$$

On the other hand, we know that across a vortex sheet, where the vortices rotates clockwise[2], we have, where $\epsilon << 1$:

$$\gamma(x) = v_x(x,\epsilon) - v_x(x,-\epsilon).$$

And since we know that (x,ϵ) and $(x,-\epsilon)$ are mirror over the x-axis, in ζ-plane their tangential velocities would be the same, we have:

$$\gamma(x) = \frac{v_\theta}{-2\sin\theta} - \frac{v_{-\theta}}{-2\sin(-\theta)} = -\frac{v_\theta}{\sin\theta}.$$

This relationship is crucial in Kármán's calculations of the wake vortex's influence on the airfoil. Kelvin's circulation theorem guarantees that any change in airfoil circulation is balanced by a wake vortex of the same strength. The shredding happens in an instance, thus the wake vortex is concentrated at a point $d\xi$. However, the counter vortex on the airfoil is smeared out into a distribution such that the airfoil becomes a streamline[3]. This is the principle of images.

By changing our perspective to the ζ-plane, the airfoil becomes a circle, and by mathematical luck[4], the image is again concentrated into a point vortex. In Kármán and Sears' paper [KS38], they calculate the tangential velocity produced by any pair of wake vortex and the wing's change in vortex strength in ζ-plane. From this tangential velocity, the induced vortex distribution on the wing, which is caused by the wake vortex by the principle of images, is calculated using the formula we arrived at.[5]

And as the reader might have noticed by now, the formula arrived at in this section relates not only tangential velocity to vorticity distribution, but also relate them *across* the Joukowski transformation. If we substitute $z = re^{i\theta} + \frac{a^2}{r^2}e^{-i\theta}$ with $r = a$, we have $z = a(e^{i\theta} + e^{-i\theta}) = 2a\cos\theta$, so that if $z = x + iy$, we have $x = 2a\cos\theta$, and $\sin\theta = \sqrt{1 - (x/2a)^2}$.

[2] And also the x-axis points to the right.

[3] Which is itself an a vortex distribution. And by Kelvin's circulation theorem, their strengths are equal $d\Gamma = \int_{-c/2}^{c/2} d\gamma_1(x)dx = \gamma(\xi)d\xi$, $\xi > c$

[4] Use the *second* circle theorem.

[5] The reason we do not simply transform the image in ζ-plane and instead have to rely on the formula above is because the image lies outside of the domain of the transformation. Recall the awkwardly long titles of the Joukowski transform subsections.

4.4 Circulation, Moment, and Lift on a non-steady airfoil

With the presentation of foundational perspective out of the way, it's now appropriate to present the bulk of Kármán and Sears' non-stationary airfoil theory. The following analysis follows the steps laid out in von Kármán and Sears' 1938 paper [KS38], but was redone for an airfoil of arbitrary chord.

Suppose we have a flat airfoil and due to non-steady movement it shreds a vortex distribution $\gamma(\xi)$ in the wake[6]. Suppose that the airfoil's chord has length $c = 2l$ centred at the origin. By Joukowski's transformation ($2z = \zeta + l^2/\zeta$) this airfoil is the transformation of a circle $r = l$ in ζ-plane, which is also centred at the origin. A factor of 2 was added so that H has coordinate $-l+0i$ instead of $-2l+0i$. Compared with the standard Joukowski transformation, the angle relationships stays the same, and the length relationship becomes $SP + HP = (S'P'^2 + H'P'^2)/2O'P'$, and the whole airfoil is scaled back by a factor of 2.

4.4.1 Vorticity distribution caused by a near wake vortex

Consider a small element of the wake vortex $\gamma(\xi)d\xi$ at position $z_0 = \xi + 0i$ ($\xi > c/2$) in the wake in the physical plane. In the ζ plane, the vortex is situated at $\zeta_0 = \xi + \sqrt{\xi^2 - l^2} = \eta + 0i$. From the result of the section above, we know that in ζ plane the vortex has an image situated at $\zeta_1 = r^2/\eta$. The strength of these two vortices are $d\kappa = \gamma(\xi)d\xi/2\pi$ and $-d\kappa$.

The velocity produced by the set of these 2 vortices on a point ζ on the unit circle is:

$$\begin{aligned} dv(\zeta) &= d\kappa \left| \frac{1}{\zeta - \zeta_0} - \frac{1}{\zeta - \zeta_1} \right| \\ &= d\kappa \left| \frac{1}{\zeta - \eta} - \frac{1}{\zeta - r^2/\eta} \right| \\ &= d\kappa \left| \frac{\eta - r^2/\eta}{\zeta^2 - \zeta(\eta + r^2/\eta) + r^2} \right|. \end{aligned}$$

Because $2z = \zeta + r^2/\zeta$, we have $\eta + r^2/\eta = 2\xi$ and $\eta - r^2/\eta = 2\sqrt{\xi^2 - r^2}$, and let $\zeta = a + ib$, thus:

$$\begin{aligned} dv(\zeta) &= d\kappa \frac{2\sqrt{\xi^2 - r^2}}{|(a+ib)^2 - (a+ib)2\xi + r^2|} \\ &= d\kappa \frac{2\sqrt{\xi^2 - r^2}}{|a^2 + abi - a\xi - b\xi i|2} \end{aligned}$$

[6] We know from Aeroelasticity ([BAL96], chapter 5) that when $u' = u - U << U$, then the airfoil's lift and moment comes from analysing the camber profile, while the thickness profile determines drag. The camber profile can be further decomposed as the sum of a flat moving profile and a stationary cambered profile. Thus a flat airfoil assumption is sufficient because the thickness and camber only shifts the equilibrium position.

$$= d\kappa \frac{\sqrt{\xi^2 - r^2}}{|a + bi||a - \xi|}$$
$$= d\kappa \frac{\sqrt{\xi^2 - r^2}}{r(\xi - a)}$$

because $|\zeta| = r$ and $\xi > r$.

Because the vortices are placed such that they are image of each other, it is guaranteed that this velocity is tangent to the unit circle.

At the trailing edge, we want to apply the Joukowsky condition, meaning that the point H' in ζ plane should be a stagnation point. But since in this two vortex system the circle is already a streamline, we only need to make the tangential velocity go to 0.

We can make this the case by subtracting the tangent velocity at the trailing edge from the general tangent velocity. This velocity is

$$dv(r + 0i) = d\kappa \frac{\sqrt{\xi^2 - r^2}}{(\xi - r)r}.$$

Thus the general velocity on the circle becomes:

$$dv(\zeta) = \frac{d\kappa}{r} \left(\frac{\sqrt{\xi^2 - r^2}}{\xi - a} - \sqrt{\frac{\xi + r}{\xi - r}} \right)$$
$$= \frac{d\kappa}{r} \sqrt{\frac{\xi + r}{\xi - r}} \left(\frac{\xi - r}{\xi - a} - 1 \right)$$
$$= \frac{d\kappa}{r} \sqrt{\frac{\xi + r}{\xi - r}} \frac{a - r}{\xi - a}.$$

According to Kármán and Sears [KS38], the vorticity distribution on the airfoil as a function of tangent velocity is given by[7]:

$$\gamma(x) = -\frac{2v_\theta}{\sin\theta}$$

where $\gamma(x)$ is positive *clockwise*, $a = Re(\zeta)$ and $\theta = \arg(\zeta)$, v_θ is the velocity tangent to the ζ-plane circle. In our case, with the special Joukowski transformation $2z = \zeta + l^2/\zeta$ applied on the circle $r = l$, a point on it will be mapped to $2(x + iy) = e^{i\theta} + e^{-i\theta} = 2\cos\theta$, thus $x = \cos\theta = a$

$$d\gamma(x, \xi) = -\frac{2dv}{\sqrt{r^2 - a^2}}$$
$$= 2\frac{d\kappa}{r} \sqrt{\frac{\xi + r}{\xi - r}} \frac{r - a}{\xi - a} \frac{1}{\sqrt{r^2 - a^2}}$$
$$= 2\frac{d\kappa}{r} \sqrt{\frac{\xi + r}{\xi - r}} \sqrt{\frac{r - a}{r + a}} \frac{1}{\xi - a}$$

[7]The factor 2 comes from the number 2 in Joukowski's transformation used by Karman.

$$= 2\frac{d\kappa}{r}\sqrt{\frac{\xi+r}{\xi-r}}\sqrt{\frac{r-x}{r+x}}\frac{1}{\xi-x}.$$

As we can see, the infinitesimal wake vortex cause a vorticity distribution given by $d\gamma(x,\xi)$.

Plugging in $c = 2r$, we have the formula for any thin, relatively flat airfoil[8]:

$$d\gamma(x,\xi) = 2\frac{d\kappa}{r}\sqrt{\frac{\xi+c/2}{\xi-c/2}}\sqrt{\frac{c/2-x}{c/2+x}}\frac{1}{\xi-x}.$$

This is the additional vorticity distribution on the airfoil produced by an infinitesimal vortex $d\kappa = \gamma(\xi)d\xi/2\pi$ situated at ξ.

4.4.2 Circulation

Now we consider all the vorticities present in the problem. Let $\gamma_0(x)$ be vorticity distribution due to the mean steady motion of the airfoil, $\gamma_1(x)$ be the image of wake vortices - this is also the increase in vorticity due to the unsteady motion of the airfoil, and $\gamma(\xi)$ being the wake vortex distribution. As a reminder: $x \in [-c/2, c/2]$, $\xi \in [c/2, \infty]$.

The circulation around the airfoil due to the image of an infinitesimal wake vortex at ξ is:

$$d\Gamma_1 = \int_{-c/2}^{c/2} d\gamma(x,\xi)dx$$

$$= 2d\kappa\int_{-c/2}^{c/2}\sqrt{\frac{\xi+c/2}{\xi-c/2}}\sqrt{\frac{c/2-x}{c/2+x}}\frac{1}{\xi-x}dx$$

$$= 2\pi d\kappa\left(\sqrt{\frac{\xi+c/2}{\xi-c/2}}-1\right)$$

$$= \gamma(\xi)d\xi\left(\sqrt{\frac{\xi+c/2}{\xi-c/2}}-1\right).$$

Thus the total circulation due to wake vortices is:

$$\Gamma_1 = \int_{c/2}^{\infty}\left(\sqrt{\frac{\xi+c/2}{\xi-c/2}}-1\right)\gamma(\xi)d\xi,$$

and the total circulation around the airfoil is:

$$\Gamma = \Gamma_0 + \Gamma_1$$

$$= \int_{-c/2}^{c/2}(\gamma_0+\gamma_1)dx,$$

and since the total circulation in the flow field must be 0, we have:

$$\Gamma + \int_{c/2}^{\infty}\gamma(\xi)d\xi = 0$$

[8]This is independent of the Joukowski transformation.

$$\leftrightarrow \Gamma_0 + \Gamma_1 + \int_{c/2}^{\infty} \gamma(\xi) d\xi = 0$$

$$\leftrightarrow \Gamma_0 + \int_{c/2}^{\infty} \sqrt{\frac{\xi + c/2}{\xi - c/2}} \gamma(\xi) d\xi = 0. \tag{4.1}$$

4.4.3 Momentum stored in the fluid from a vortex pair

As the title of the section suggests. A single vortex, owning to symmetry, has no net momentum. But a pair of vortices with opposite vorticity, can store some momentum. Kármán and Sears noted that a pair of opposite and equal vortices Γ and $-\Gamma$ has a momentum proportional to their circulation and the distance between the vortices [KS38]:

$$p = \rho \Gamma (x_1 - x_2)$$

For sets of many vortex pairs, each pair having opposite and equal circulation, the formula is generalized:

$$p = \rho \sum \Gamma_i x_i.$$

In the case of our airfoil, the line joining the axis of these vortices is always the x-axis, thus p points in the vertical direction. If the vortices are not on the x-axis then the line joining them will tilt and so does p.

4.4.4 Lift

The momentum of the fluid field is:

$$p = \rho \int_{-\infty}^{\infty} d\Gamma . x$$

$$= \rho \int_{-c/2}^{c/2} (\gamma_0 + \gamma_1) dx . x + \rho \int_{c/2}^{\infty} \gamma(\xi) d\xi . \xi$$

Consider the first term, and for now let $l = c/2$:

$$\int_{-l}^{l} (\gamma_0 + \gamma_1) dx . x = \int_{-l}^{l} \gamma_0(x) dx . x + \int_{-l}^{l} \gamma_1(x) dx . x$$

$$= \int_{-l}^{l} \gamma_0(x) dx . x + \int_{-l}^{l} \left(\int_{\xi=l}^{\infty} d\gamma_1(x, \xi) \right) dx . x$$

$$= \int_{-l}^{l} \gamma_0(x) x dx + \int_{-l}^{l} \int_{l}^{\infty} 2 d\kappa \sqrt{\frac{\xi + l}{\xi - l}} \sqrt{\frac{l - x}{l + x}} \frac{1}{\xi - x} . x dx$$

$$= \int_{-l}^{l} \gamma_0(x) x dx + \int_{l}^{\infty} \frac{\gamma(\xi) d\xi}{\pi} \sqrt{\frac{\xi + l}{\xi - l}} \int_{-l}^{l} \sqrt{\frac{l - x}{l + x}} \frac{1}{\xi - x} x dx.$$

For the second integral, we will integrate with respect to x. Letting $t = \sqrt{\frac{l-x}{l+x}}$, we find $dt = -\frac{1}{4t}(l^2 + t^2)^2 dx$ and then solve the integral, we find that:

$$\int_{-l}^{l} (\gamma_0 + \gamma_1) dx . x = \int_{-l}^{l} \gamma_0(x) x dx + \int_{l}^{\infty} \gamma(\xi) (\sqrt{\xi^2 - l^2} - \xi) d\xi.$$

Thus the momentum is:

$$p = \rho\left(\int_{-l}^{l}\gamma_0(x)xdx + \int_{l}^{\infty}\gamma(\xi)(\sqrt{\xi^2-l^2}-\xi)d\xi\right) + \rho\int_{l}^{\infty}\gamma(\xi)d\xi.\xi$$

$$= \rho\left(\int_{-l}^{l}\gamma_0(x)xdx + \int_{l}^{\infty}\gamma(\xi)\sqrt{\xi^2-l^2}d\xi\right). \tag{4.2}$$

To find the lift, by Newton's 2^{nd} law ($F = dp/dt$), we wish to differentiate p with respect to time. Then we encounter the differentiation of the second term of this equation. We will solve this generally for any function $f(\xi)$ in place of $\sqrt{\xi^2-l^2}$ above. Consider

$$A = \int_{l}^{\infty}\gamma(\xi)f(\xi)d\xi$$

Since a vortex has no net momentum [Tho58], once it was shred into the wake, it is carried away by the flow. From the perspective of the airfoil, the whole wake vortex distribution propagates aft in unison as a travelling static wave. But from the perspective of the flow, the airfoil is moving and the fluid (and thus the vortex) is stationary.

To describe $\gamma(\xi)$ more closely to its nature, it is then reasonable to change the variable ξ which has a moving origin into one with a static origin relative to the fluid. Let X_0 be a static point. Define a new variable X which is the distance to any point of interest measured from X_0. At time t_0, X_0's position is $\xi_X(t_0)$, after some time Δt, its position would be $\xi_X(t+\Delta t) = \xi_X(t_0) + U\Delta t$. Thus:

$$\gamma(\xi) = \gamma(X + U\Delta t) = \gamma(X) + \frac{d\gamma(X)}{dx}U\Delta t + ...$$

$$= \gamma(X),$$

because the distribution is static with respect to the fluid.

The change in A after a small time Δt would be:

$$A + \Delta A = \int_{l-U\Delta t}^{\infty}\gamma(X)f(X+U\Delta t)dX$$

$$\approx \int_{l-U\Delta t}^{\infty}\gamma(X)\Big[f(X) + f'(X).U\Delta t\Big]dX$$

$$= \int_{l-U\Delta t}^{l}\gamma(X)\Big[f(X) + f'(X).U\Delta t\Big]dX + \int_{l}^{\infty}\gamma(X)\Big[f(X) + f'(X).U\Delta t\Big]dX$$

$$\rightarrow \Delta A = \int_{l-U\Delta t}^{l}\gamma(X)\Big[f(X) + f'(X).U\Delta t\Big]dX + \int_{l}^{\infty}\gamma(X)f'(X)U\Delta t dX,$$

so:

$$dA = \lim_{\Delta t\to 0}\Delta A$$

$$= \int_{l}^{\infty}\gamma(X)f'(X)Udt dX$$

$$\rightarrow \frac{dA}{dt} = U\int_{l}^{\infty}\gamma(X)f'(X)dX.$$

A simple change of variable gives the following, keeping in mind that when $\Delta t \to 0$, $X \to \xi$:

$$\frac{dA}{dt} = U \int_l^\infty \gamma(\xi) f'(\xi) d\xi$$

Applying this to find the lift, we have:

$$\begin{aligned}
L &= -\dot{p} \\
&= -\rho \frac{d}{dt}\left(\int_{-l}^{l} \gamma_0(x) x dx + \int_l^\infty \gamma(\xi)\sqrt{\xi^2 - l^2} d\xi \right) \\
&= -\rho \frac{d}{dt}\left(\int_{-l}^{l} \gamma_0(x) x dx \right) - \rho U \int_l^\infty \gamma(\xi) \frac{\xi}{\sqrt{\xi^2 - l^2}} d\xi \\
&= -\rho \frac{d}{dt}\left(\int_{-l}^{l} \gamma_0(x) x dx \right) - \rho U \int_l^\infty \gamma(\xi) \frac{(\xi + l) - l}{\sqrt{\xi^2 - l^2}} d\xi \\
&= -\rho \frac{d}{dt}\left(\int_{-l}^{l} \gamma_0(x) x dx \right) - \rho U \int_l^\infty \gamma(\xi) \sqrt{\frac{\xi + l}{\xi - l}} d\xi + \rho U \int_l^\infty \gamma(\xi) \frac{l}{\sqrt{\xi^2 - l^2}} d\xi \\
&= -\rho \frac{d}{dt}\left(\int_{-l}^{l} \gamma_0(x) x dx \right) + \rho U \Gamma_0 + \rho U \int_l^\infty \gamma(\xi) \frac{l}{\sqrt{\xi^2 - l^2}} d\xi
\end{aligned} \tag{4.3}$$

It could be seen that now the lift is composed of 3 terms. The first term is the contribution of the mass of air displaced due to the airfoil's motion [KS38]. The second term is the steady-state lift of a similar airfoil doing the mean motion. Thus it could be found in the same manner as in steady airfoil theory. The last term is the contribution from the wake vortices.

4.4.5 Angular momentum stored in the fluid from a vortex pair

A vortex pair producing a moment p will have an angular momentum with respect to an observer at the point O. This angular momentum is given by:

$$L_O = |\boldsymbol{r} \times \boldsymbol{p}|,$$

where due to symmetry, $\boldsymbol{r}$ is the vector from O to the midpoint between the vortices. When the vortices are all on the x-axis, we have:

$$\begin{aligned}
L_O &= p \frac{x_1 + x_2}{2} \\
&= \rho\Gamma(x_1 - x_2)\frac{x_1 + x_2}{2} \\
&= \frac{\rho\Gamma}{2}(x_1^2 - x_2^2).
\end{aligned}$$

Once again, generalizing to k pairs of vortices, keeping in mind that each pair have circulations Γ_i and $-\Gamma_i$, we have:

$$L_O = \frac{\rho}{2} \sum \Gamma_i x_i^2.$$

4.4.6 Moment

Let O be an axis not coincide with the origin. If a point's position on the x axis is ξ then let s be the corresponding distance from that point to the O axis. The angular momentum in the fluid field with respect to O is:

$$L_O = \frac{\rho}{2}\left(\int_{-l}^{l} \gamma(x)(x-s)^2 dx + \int_{l}^{\infty} \gamma(\xi)(\xi - s)^2 d\xi \right).$$

If we consider the system consists of the fluid and the airfoil, this moment must be countered by a moment on the airfoi. Thus the moment acting on the airfoil would be:

$$M = -\frac{dL_O}{dt}\bigg|_{s=0}$$

$$\leftrightarrow -\frac{2}{\rho}M = \frac{d}{dt}\left(\int_{-l}^{l} \gamma(x)x^2 dx + \int_{l}^{\infty} \gamma(\xi)\xi^2 d\xi \right)$$

$$+\frac{d}{dt}2s\left(\int_{-l}^{l} \gamma(x)x dx + \int_{l}^{\infty} \gamma(\xi)\xi d\xi \right)$$

$$+\frac{d}{dt}s^2\left(\int_{-l}^{l} \gamma(x) dx + \int_{l}^{\infty} \gamma(\xi) d\xi \right).$$

Here we recognize that the middle term inside the parenthesis is the momentum p/ρ of the fluid. The last term is the total circulation in the field, thus by Kelvin's conservation of circulation, it is 0. We have:

$$-\frac{2}{\rho}M = \frac{d}{dt}\left(\int_{-l}^{l} \gamma(x)x^2 dx + \int_{l}^{\infty} \gamma(\xi)\xi^2 d\xi \right) + 2\frac{d}{dt}(sp/\rho)$$

$$= \frac{d}{dt}\left(\int_{-l}^{l} \gamma(x)x^2 dx + \int_{l}^{\infty} \gamma(\xi)\xi^2 d\xi \right) + 2\dot{s}p/\rho + 2s\dot{p}/\rho.$$

When we let the axis O follows the airfoil, we have $\dot{s} = -U$ because the airfoil moves towards the negative direction and $s = 0$, thus:

$$-2M = \rho\frac{d}{dt}\left(\int_{-l}^{l} \gamma(x)x^2 dx + \int_{l}^{\infty} \gamma(\xi)\xi^2 d\xi \right) - 2Up$$

$$= \rho\frac{d}{dt}\left(\int_{-l}^{l} \gamma_0(x)x^2 dx + \int_{-l}^{l} \gamma_1(x)x^2 dx + \int_{l}^{\infty} \gamma(\xi)\xi^2 d\xi \right) - 2Up$$

$$= \rho\frac{d}{dt}\left(\int_{-l}^{l} \gamma_0(x)x^2 dx + \int_{-l}^{l}\int_{0}^{\kappa} 2d\kappa\sqrt{\frac{\xi+l}{\xi-l}}\sqrt{\frac{l-x}{l+x}}\frac{1}{\xi-x}x^2 dx + \int_{l}^{\infty} \gamma(\xi)\xi^2 d\xi \right) - 2Up.$$

We also let $t = \sqrt{\frac{l-x}{l+x}}$ to solve the integral with respect to x in the middle term. Then make the substitution $2d\kappa = \gamma(\xi)d\xi/\pi$. Doing that, we have:

$$\int_{-l}^{l}\int_{0}^{\kappa} 2d\kappa\sqrt{\frac{\xi+l}{\xi-l}}\sqrt{\frac{l-x}{l+x}}\frac{1}{\xi-x}x^2 dx$$

$$= \int_0^\kappa 2d\kappa \sqrt{\frac{\xi+l}{\xi-l}}\pi\left(\frac{l^2}{2} - l\xi + \xi^2 - \xi^2\sqrt{\frac{\xi-l}{\xi+l}}\right)$$

$$= -\int_l^\infty \gamma(\xi)\xi^2 d\xi + \int_l^\infty \gamma(\xi)\sqrt{\frac{\xi+l}{\xi-l}}\frac{l^2}{2}d\xi + \int_l^\infty \gamma(\xi)\sqrt{\xi^2-l^2}\xi d\xi.$$

Plug in, we get:

$$-2M = \rho\frac{d}{dt}\left(\int_{-l}^{l}\gamma_0(x)x^2dx + \frac{l^2}{2}\int_l^\infty \gamma(\xi)\sqrt{\frac{\xi+l}{\xi-l}}d\xi + \int_l^\infty \gamma(\xi)\xi\sqrt{\xi^2-l^2}d\xi\right) - 2Up.$$

We then realize that the middle integral equates to $-\Gamma_0 = \int_{-l}^{l}(-\gamma_0)dx$ (eq 4.1), and use the A integral defined above to solve the last integral. Then p is expanded by equation (4.2), we have:

$$-\frac{2}{\rho}M = \frac{d}{dt}\left(\int_{-l}^{l}\gamma_0(x)x^2dx + \frac{l^2}{2}\int_{-l}^{l}(-\gamma_0)dx\right) + U\int_l^\infty \gamma(\xi)\left(\sqrt{\xi^2-l^2} + \frac{\xi^2}{\sqrt{\xi^2-l^2}}\right)d\xi$$

$$-2U\left(\int_{-l}^{l}\gamma_0(x)xdx + \int_l^\infty \gamma(\xi)\sqrt{\xi^2-l^2}d\xi\right)$$

$$= \frac{d}{dt}\int_{-l}^{l}\gamma_0(x)\left(x^2 - \frac{l^2}{2}\right)dx - 2U\int_{-l}^{l}\gamma_0(x)xdx - U\int_l^\infty \gamma(\xi)\sqrt{\xi^2-l^2}d\xi + U\int_l^\infty \gamma(\xi)\frac{\xi^2}{\sqrt{\xi^2-l^2}}d\xi$$

$$= \frac{d}{dt}\int_{-l}^{l}\gamma_0(x)\left(x^2 - \frac{l^2}{2}\right)dx - 2U\int_{-l}^{l}\gamma_0(x)xdx + U\int_l^\infty \gamma(\xi)\frac{\xi^2 - (\xi^2-l^2)}{\sqrt{\xi^2-l^2}}d\xi$$

$$\leftrightarrow M = -\frac{\rho}{2}\frac{d}{dt}\int_{-l}^{l}\gamma_0(x)\left(x^2 - \frac{l^2}{2}\right)dx + \rho U\int_{-l}^{l}\gamma_0(x)xdx - \frac{\rho U}{2}\int_l^\infty \gamma(\xi)\frac{l^2}{\sqrt{\xi^2-l^2}}d\xi.$$

Here the moment acting on the airfoil is having 3 terms again. The first term is the contribution of the apparent mass when the airfoil rotates. The second term is the moment of another airfoil in steady state having the same instantaneous angle of attack and speed as this airfoil. Often called the quasi-steady state term. The third term is the contribution from the wake.

One noteworthy thing is that 2 additional terms have opposite direction compared with the quasi-steady state term. This makes the magnitude of the total moment lag behind the quasi-steady state term. Kármán and Sears [KS38] used this fact to produce a simplification in case of sinusoidal oscillation.

Plugging in $l = c/2$, we get:

$$M = -\frac{\rho}{2}\frac{d}{dt}\int_{-c/2}^{c/2}\gamma_0(x)\left(x^2 - \frac{(c/2)^2}{2}\right)dx + \rho U\int_{-c/2}^{c/2}\gamma_0(x)xdx - \frac{\rho U c^2}{8}\int_{c/2}^\infty \gamma(\xi)\frac{1}{\sqrt{\xi^2-(c/2)^2}}d\xi$$

It could be noted that the wake moment is related to the wake lift L_2 as:

$$M_2 = -L_2\frac{c}{4},$$

by comparing the terms. Thus we see that the wake induced lift also sits at the quatre-chord point.

If we plug in the formulas for a thin Joukowski airfoil, it would be found that it is $M_1 = \rho\dot{U}(\frac{c}{2})^4\frac{\pi}{8R}$, where R is the airfoil's radius of curvature. This moment does not depend on the angle of attack!

4.4.7 Notes on application

The positive direction of $\gamma(x)$ used in these sections is clockwise, which is opposite to the positive direction used in Section A.4.1. Thus if equations for $\gamma_0(x)$ from Section A.4.1 is to be used to calculate the $\gamma_0(x)$ terms in the equation for non-steady moment and lift, the sign of $\gamma_0(x)$ shall be flipped.

4.5 The method to find the wake vortex

The following method is also presented in Kármán and Sear's paper [KS38]. Suppose the airfoil has an unit impulse in circulation at $t = 0$, so that $\Gamma_0(0) = 1$. This impulse results in a wake vortex. This vortex will float in the air. After a time t, the vortex is at $\xi = l + Ut$ in the airfoil's coordinate, where again $l = c/2$. Let s be the distance from any point in the wake to the initial position. Let ξ be the coordinate of the same point in airfoil's frame of reference, thus $\xi + s = l + Ut$. Let $\gamma(\xi) = \mu(s) = \mu(l + Ut - \xi)$ where $\mu(s)$ is the wake vortex distribution written with respect to the initial position that is fixed with respect to the air. Thus by Equation (4.1), we have:

$$\Gamma_0 + \int_l^\infty \sqrt{\frac{\xi + l}{\xi - l}}\mu(s)d\xi = 0$$

$$\leftrightarrow 1 + \int_0^{Ut} \sqrt{\frac{2l + Ut - s}{Ut - s}}\mu(s)ds = 0. \tag{4.4}$$

This equation is used to compute $\mu(s)$. The wake's contribution to the lift is then, from the general equation for lift (eq. 4.3):

$$L_2 = \rho U l \int_l^{l+Ut} \gamma(\xi)\frac{d\xi}{\sqrt{\xi^2 - l^2}}$$

$$= \rho U l \int_l^{l+Ut} \mu(l + Ut - \xi)\frac{d\xi}{\sqrt{\xi^2 - l^2}}.$$

At this point we define a new quantity:

$$\Phi(Ut) = -\int_1^{1+Ut} \mu(1 + Ut - \xi)\frac{d\xi}{\sqrt{\xi^2 - 1}}$$

and name it the Lift Deficiency Function. This Φ is true for an airfoil with half chord $l = 1$. To scale it to our problem, we scale our variable Ut by $1/l$ before plugging into Φ, thus:

$$L_2 = -\rho U l.\Phi(Ut/l)$$

In the general case, $\Delta\Gamma_0 = \Delta\Gamma_0(t) \neq 1$ spread out over time, we have:

$$L_2 = -\rho U l \int_0^{\Gamma_0(t)} d\Gamma_0(\tau).\Phi(U(t-\tau)/l),$$

where $d\Gamma_0(\tau)$ is the change in Γ_0 at the time τ, and Ut is the total distance travelled thus far by the airfoil, and thus $U(t-\tau)/l$ is the distance the airfoil travelled since the time instance τ and measured as multiples of half chord l.

In general, computing $\mu(s)$ from Equation (4.4) and thus then calculate $\phi(U(t-\tau)/l)$ is non-trivial. Kármán does not give a derived formula for Φ, but gives two approximations, one of which is more broadly useful (but less accurate within the range $\sigma = U(t-\tau)/l \in (1,2)$). It will be presented here. For $\sigma \in [0;10]$, we have:

$$\Phi(\sigma) = \frac{e^{-\sigma/2}}{4} + (1 + 0.185\sigma)\frac{e^{-0.185\sigma}}{4}.$$

With this formula, the wake's contribution to the lift can be calculated. For $\sigma > 10$, the contribution becomes too small.

It could be seen that $-d\Gamma_0(\tau)$ is the wake vortex generated at time τ when the airfoil's quasi-steady circulation Γ_0 is increased by $d\Gamma_0$. Thus $\phi(U(t-\tau)/l)$ gives the decreasing influence of this wake vortex on the current lift once a time interval equals to $t-\tau$ has elapsed. Fung [Fun69] gives Wagner's full expression for Φ.

And finally the moment could be calculated as

$$M_2 = -L_2\frac{c}{4}$$

$$= \frac{\rho U c^2}{8}\int_0^t \Gamma_0'(\tau).\Phi(U(t-\tau)/l).d\tau,$$

but it is generally easier in computation to have a memory array for changes in Γ_0 over time, which is equal and opposite to wake vortices, and do integration over the wake instead of over time:

$$M_2 = \frac{\rho U c^2}{8}\int_{c/2}^{\infty} d\Gamma_0(\xi).\Phi(\xi/l),$$

where $\xi = U(t-\tau)$ is the position in airfoil coordinate of the wake vortex generated at time τ.

Finally, if the airfoil has a sudden increase in circulation $\Delta\Gamma_0(0) = \Gamma_i$ at $t = 0$, Kármán stated that a term $\Gamma_i\Phi(Ut/l)$ should be added to $-L_2$. Thus, generally the equation becomes:

$$M_2 = \frac{\rho U c^2}{8}\left(\int_{c/2}^{Ut} d\Gamma_0(\xi).\Phi(\xi/l) + \Gamma_i\Phi(Ut/l)\right).$$

5

Theory of flutter

5.1 What is flutter?

Raymers [Ray18] in chapter 8 of his book defined flutter as when "some structural deflection of the aircraft such as wing bending causes an aerodynamic load that tends to amplify the deflection during each oscillation until structural failure is reached." More simply, H. Ashley in his book ([BAL96], chapter 9) defined flutter as "the dynamic instability of an elastic body in an airstream". More specifically, Y. C. Fung in his book [Fun69] defined flutter as when the damping as a function of flow velocity, which normally is sufficiently large to suppress small disturbances, decreases rapidly and thus a small disturbance can cause an instability of great magnitude. He went on to classify flutter as only instability where the primary damping in question is purely aerodynamic in nature.

5.2 What is its cause?

According to Fung [Fun69], flutter is caused when the energy the airstream send into the structure per oscillation period is larger than zero. Since there is no structural or viscid damping involved, there must be two or more degrees of freedom (since a 1 DoF system will always oscillate indefinitely once disturbed). The energy exchange could therefore be written as a function of the phase difference φ between these degrees of freedom in forced oscillation. Depending on the exact form, there will be some values of $\varphi = \varphi(U)$ where the energy into the structure per cycle becomes positive and the oscillation blows up. The speed at which this neutral stability occurs is called the flutter speed U_F.

What these 2 Degrees of Freedom are depends on the exact circumstances and should be understood in a broad sense. A wing that can only bends up and down can still flutter if the lift $L(t)$ is out of phase with its own up-down movement $h(x,t)$ [KS38]. A Wing with both bending and torsion can flutter when the phase difference between these two motions satisfy some condition specific to the problem. A wing that can only move up and down but having an aileron can flutter if these two's motion are a function of one another (thus when one moves, the other also move, leading to them oscillating at the same frequency when one is subjected to forced vibration). Thus, to prevent flutter, it is important to prevent the coupling between various degrees of freedoms in the structure [Fun69].

5.3 What has been done in the past?

Traditionally flutter has been suppressed by either stiffening the wing box, sweeping the wing, or reducing the aspect ratio of the wing. Both stiffening the wing and reducing AR increase the moment of inertia around the y-axis, which make the wing better resists bending torque. Sweeping the wing can increase the divergent velocity (the velocity at which aerodynamic forces equals elastic forces) as has been shown by Diederich and Budiansky [DB48]. Thus sweeping, on the other hand, reduces the aerodynamic forces that acts to bend the wing out of equilibrium. But sweeping only works to an extend until the speed is high enough that the wing can undergo flapping flutter [Fun69].

Active suppression methods are not widely used since failure of such system when the plane is cruising above flutter speed causes flutter to develop fast. The pilot therefore do not have a reaction time fast enough to bring the aircraft's speed down to safe level before flutter fully develops and destroy the wing box ([BAL96], chapter 9).

5.3.1 Kussner's formula for flutter speed

In the past, a clever way to determine the critical speed U_F was devised based on dimensional analysis. Experimental works were performed and it was found that there is a critical reduced frequency k_r that signals the onset of flutter:

$$k_r = \frac{\omega c}{2U} = 0.9 \pm 0.12,$$

where ω is the natural torsional vibration frequency of the wing. The value 0.9 ± 0.12 is specific for aircrafts of the time (1926), thus depending on construction method, materials, wing geometry, etc. and also only valid for wings with mass-unbalanced aileron [Fun69]. Presumably, if this method were to be used with modern construction, more experimental work needs to be done. Furthermore, as explained in [Fun69] and [Wil58], flutter often has many modes of coupling between many aerodynamic features and each of them would have a critical frequency, thus the analyst has to examine all of them to find the lowest U_F. But luckily, experience shows that only the lowest modes exhibits flutter in practice [Wil58]. Presumably still, the numerical value given above would depend also on how particular aircraft are constructed (particularly about the rigidity of each structure). From this critical reduced frequency, the flutter airspeed could be obtained (since this is the only variable) by:

$$U_F = \frac{\omega c}{2k_r}.$$

5.3.2 Mass balancing

A wing often have a well defined torsion axis running from root to tip. For a swept wing, this axis no longer stays stationary under twist but can be assumed, to simplify calculations, as a straight axis passing through points that if vertical loads were to

be applied on those points, no resulting twist would be observed [Wil58]. This axis is assumed to maintain its swept but can move in the vertical plane when under load. If the plane was suddenly given a, for example, upward motion, such as when the aircraft encounters turbulent, its wing would often start twisting due to the unbalanced moment of inertia distribution.

Suppose there is a mass element dm at a perpendicular distance r from the torsional axis. Suppose we take the frame of reference stuck to the aircraft's center of mass. This would be a non-inertial frame. Thus, an inertial force will act on all mass elements of the wing when the aircraft accelerates. An element at a distance x away from the wing's root will have a measurable angular acceleration $\ddot{\theta}$. Suppose the aircraft starts from equilibrium. The instantaneous acceleration on the said element when the aircraft suddenly jolts upward would be:

$$a = x\ddot{\theta}.$$

The inertial moment that this element would exert on the wing with respect to the torsional axis would then be:

$$dM = r.dF = ra.dm = x\ddot{\theta}r.dm.$$

Integrating over all mass elements on the wing, we find the inertial moment with respect to the torsional axis when the aircraft jolt upwards:

$$\begin{aligned} M &= \int_A dM \\ &= \int_A x\ddot{\theta}rdm. \end{aligned}$$

And since at the first instance, the wing is still straight, the angular acceleration with respect to the wing root of every point on it is the same:

$$M = \ddot{\theta}\int_A xrdm.$$

Thus, to make the wing not twist when the aircraft jolts, it is necessary to reduce the quantity

$$J = \int_A xrdm$$

as much as possible. This is called mass-balancing. This balancing could be done with engines, pods, fuel, etc. by consider them as point masses and neglecting aerodynamic forces (since at the first instance, the vertical velocity is low enough that the change in aerodynamic forces in this direction can be neglected). Although in reality, J can rarely be made to go away. A wing with large J will twists more with small aircraft turbulent and more likely to incite flutter. And as explained in the section about the origin of flutter, if the wing twists when the aircraft accelerates vertically, then these two degrees of freedom are coupled, leading to a phase lag φ between them thus make room for energy exchange and flutter. Wilts [Wil58] gives a detailed study on the effects of extra mass on the flutter speed of four types of conventional wings.

5.4 Modelling the problem

In this section, the mathematical treatment of the airfoil flutter simulated in this thesis is carried out.

5.4.1 Generate the airfoil

Since it was found that a flat airfoil exhibits no apparent-mass moment, a cambered airfoil will be used for the simulation for the sake of demonstration. Our airfoil will be generated by using Joukowski transform $z = \zeta + l^2/\zeta$ on a circle centred on the y-axis in ζ-plane, passing through both H' and S' at $-l + 0i$ and $l + 0i$. Suppose the centre is at the location $\zeta_0 = 0 + \epsilon i$. This circle will thus have the radius:

$$a = \sqrt{l^2 + \epsilon^2}.$$

The airfoil will have chord:

$$c = 4l.$$

As we have seen in the section about Joukowski's airfoil, this airfoil will be thin and cambered with the camberline part of a circular arc of radius

$$R = \frac{a^2}{\sqrt{a^2 - l^2}} = \frac{l^2 + \epsilon^2}{\epsilon} = \epsilon + \frac{l^2}{\epsilon}.$$

Thus, the camber profile for this airfoil will be:

$$y(x) = \sqrt{R^2 - x^2} - y_0.$$

When $\epsilon << l$, we have $x < 2l \leq l^2 << R$ as long as $l \geq 1, x \in [-2l, 2l]$. Thus we can approximate the airfoil:

$$y(x) \approx R - \frac{x^2}{2R} - y_0$$

$$\rightarrow \frac{dy}{dx} - \alpha = -\frac{x}{R} - \alpha.$$

Doing the change in coordinate to θ using $x = \frac{c}{2}\cos\theta$, we have:

$$f(\theta) = \frac{dy}{dx} - \alpha = -\frac{2l\cos\theta}{R} - \alpha.$$

Applying the same Fourier transformation as presented earlier in the section on steady-state airfoils:

$$f(\theta) = \frac{dy}{dx} - \alpha$$

$$= A_0 - \sum_{n=1}^{\infty} A_n \cos(n\theta),$$

where the coefficients are:

$$A_0 = \frac{1}{\pi}\int_0^{\pi} f(\theta)d\theta$$

$$A_1 = -\frac{2}{\pi}\int_0^\pi f(\theta)\cos(\theta)d\theta$$
$$A_2 = -\frac{2}{\pi}\int_0^\pi f(\theta)\cos(2\theta)d\theta$$
$$\vdots$$
$$A_n = -\frac{2}{\pi}\int_0^\pi f(\theta)\cos(n\theta)d\theta,$$

we arrive at:

$$A_0 = \frac{1}{\pi}\int_0^\pi \left(-\frac{2l\cos\theta}{R} - \alpha\right)d\theta = -\alpha,$$
$$A_1 = -\frac{2}{\pi}\int_0^\pi \left(-\frac{2l\cos\theta}{R} - \alpha\right)\cos(\theta)d\theta = \frac{2l}{R} = \frac{c}{2R}.$$

And by applying cosine orthogonality property:

$$A_n = -\frac{2}{\pi}\int_0^\pi \left(-\frac{2l\cos\theta}{R} - \alpha\right)\cos(n\theta)d\theta$$
$$= -\frac{2}{\pi}\int_0^\pi \left(-\frac{2l\cos\theta\cos(n\theta)}{R} - \alpha\cos(n\theta)\right)d\theta$$
$$= 0 \ \forall n > 1$$

5.4.2 Calculate the moment

The moment about the leading edge is calculated using Kármán's method, which is, for $l = c/2$:

$$M_O = M_0 + M_1 + M_2,$$

in which:

$$M_1 = -\frac{\rho}{2}\frac{d}{dt}\int_{-c/2}^{c/2}\gamma_0(x)\left(x^2 - \frac{c^2}{8}\right)dx$$

is the apparent-mass contribution, and

$$M_0 = \rho U\int_{-c/2}^{c/2}\gamma_0(x)xdx$$

is the quasi-steady contribution, and

$$M_2 = -\frac{\rho U c^2}{8}\int_{c/2}^{\infty}\gamma(\xi)\frac{1}{\sqrt{\xi^2 - (c/2)^2}}d\xi$$

is the wake's contribution. The quasi-steady vorticity distribution is calculated using the steady airfoil theory presented in Section A.4.1. There we have the steady-state vorticity distribution:

$$\gamma_0(\theta) = -2V_0\left(A_0\frac{1+\cos\theta}{\sin\theta} + \sum_{n=1}^{N}A_n\sin(n\theta)\right),$$

where θ is the result of the change of coordinate $x = \frac{c}{2}\cos\theta$ made earlier in that section.

Substitute back x and the A parameters of our thin cambered airfoil, and changing the sign of γ_0 due to the fact that the positive rotation is clockwise in Karman's paper, we find:

$$\gamma_0(x) = 2U\bigg(-\alpha\sqrt{\frac{c/2-x}{c/2+x}} + \frac{2l}{R}\frac{\sqrt{4l^2-x^2}}{2l}\bigg)$$

$$= 2U\bigg(-\alpha\sqrt{\frac{c/2-x}{c/2+x}} + \frac{\sqrt{4l^2-x^2}}{R}\bigg),$$

We can solve this for a general chord c:

$$M_1 = -\frac{\rho}{2}\frac{d}{dt}\int_{-c/2}^{c/2} 2U\bigg(-\alpha\sqrt{\frac{c/2-x}{c/2+x}} + \frac{\sqrt{(c/2)^2-x^2}}{R}\bigg)\bigg(x^2 - \frac{(c/2)^2}{2}\bigg)dx,$$

and by letting $x = \frac{c}{2}\cos\theta$, we have $\sqrt{\frac{c/2-x}{c/2+x}} = \tan\frac{\theta}{2}$, and by using $\tan\frac{\theta}{2} = \frac{1-\cos\theta}{\sin\theta}$ and the integral $\int_{\pi}^{0}\sin^2\theta d\theta = -\pi/2$, we have:

$$M_1 = -\frac{\rho}{2}\frac{d}{dt}2U\bigg(0 - \frac{\pi}{8R}\bigg(\frac{c}{2}\bigg)^4\bigg)$$

$$= \rho\dot{U}\bigg(\frac{c}{2}\bigg)^4\frac{\pi}{8R}.$$

For the quasi-steady term, it is directly useable after a sign change:

$$M_0 = -\rho\frac{U^2}{2}c^2\bigg(-\alpha\frac{\pi}{2} + \pi\frac{l}{R}\bigg).$$

And finally, the wake moment is:

$$M_2 = \frac{\rho U c^2}{8}\int_{c/2}^{\infty} d\Gamma_0(\xi).\Phi\bigg(\frac{\xi}{c/2}\bigg)$$

In this simulation, the airfoil is assumed to start at equilibrium speed U_0 and initial circulation Γ_i, and an array is maintained of all the wake vortices generated since the first disturbance.

$$M_2 = \frac{\rho U c^2}{8}\sum_{n=1}^{N}\Delta\Gamma_0(n).\Phi\bigg(\frac{U(t-n\Delta t)}{c/2}\bigg),$$

where Δt is the time step of the simulation, N is the current iteration, and Γ_0 is calculated at every time step, given by Equation (3.3), where the sign is changed because the positive direction of vorticity is different:

$$\Gamma_0 = -\pi c U\sin\bigg(\alpha + \frac{c}{4R}\bigg).$$

5.4.3 Equations of motion and equilibrium

Suppose we have an airfoil in freestream, with torsional stiffness k. Its equation of motion along the twist axis is:

$$I_O\ddot{\theta} = -k(\theta + \theta_0) + M_O(\alpha),$$

where M_O is the aerodynamic moment around the leading edge and I_O is the moment of inertia with respect to the leading edge. And θ_0 is the initial twist angle of the airfoil, since any airfoil producing lift will bend.

Suppose that at rest, the wing is at an angle of attack α_0, and the wing is untwisted. At equilibrium at airspeed U, the wing twists an additional angle θ_0. This gives the following balance:

$$k\theta_0 = M_O(\alpha_0 + \theta_0)$$

$$\leftrightarrow k\theta_0 = -\rho\frac{U^2}{2}c^2\left(- (\alpha_0 + \theta_0)\frac{\pi}{2} + \pi\frac{l}{R}\right)$$

$$\leftrightarrow \theta_0 = \frac{\rho\frac{U^2}{2}c^2(\alpha_0\frac{\pi}{2} - \pi\frac{l}{R})}{k - \rho\frac{U^2}{2}c^2\frac{\pi}{2}}, \tag{5.1}$$

is the wing's initial twist at equilibrium.

Expanding the equation of motion, we get:

$$I_O\ddot{\theta} = -k(\theta + \theta_0) + \left(\rho\dot{U}\left(\frac{c}{2}\right)^4\frac{\pi}{8R} - \rho\frac{U^2}{2}c^2\left(- \alpha\frac{\pi}{2} + \pi\frac{l}{R}\right) + \frac{\rho U c^2}{8}\sum_{n=1}^{N}\Delta\Gamma_0(n).\Phi\left(\frac{U(t - n\Delta t)}{c/2}\right)\right),$$

where the angle of attack α is the sum of the equilibrium angle of attack α_0 and the additional twist of the wing θ:

$$\alpha = \theta + \alpha_0.$$

Inserting the equilibrium into this equation of motion, we get:

$$I_O\ddot{\theta} = -k\theta + \left(\rho\dot{U}\left(\frac{c}{2}\right)^4\frac{\pi}{8R} + \rho\frac{U^2}{2}c^2\theta\frac{\pi}{2} + \frac{\rho U c^2}{8}\sum_{n=1}^{N}\Delta\Gamma_0(n).\Phi\left(\frac{U(t - n\Delta t)}{c/2}\right)\right),$$

or rearranging:

$$I_O\ddot{\theta} + \left(k - \rho\frac{U^2}{2}c^2\frac{\pi}{2}\right)\theta = \rho\dot{U}\left(\frac{c}{2}\right)^4\frac{\pi}{8R} + \frac{\rho U c^2}{8}\sum_{n=1}^{N}\Delta\Gamma_0(n).\Phi\left(\frac{U(t - n\Delta t)}{c/2}\right),$$

and this is the primary equation of motion.

5.5 Equation of motion in case of constant speed

To find the transfer function, the form of $\Delta\Gamma_0$ is desired. We know that for any aerofoil in inviscid flow:

$$\Gamma_0 = -\pi c U \sin\left(\alpha + \frac{c}{4R}\right).$$

We have:

$$\Delta\Gamma_0 = \Gamma_0' \Delta t$$
$$= \left[\dot{U} c\pi\left(\alpha - \frac{c}{4R}\right) + Uc\pi\dot{\alpha}\right]\Delta t,$$

and when $U = const$, we have $\Delta\Gamma_0 = Uc\pi\dot{\alpha}\Delta t$. But since $\alpha = \theta + \alpha_0$, we have:

$$\Delta\Gamma_0 = Uc\pi\dot{\theta}\Delta t$$
$$= Uc\pi\Delta\theta.$$

Plugging into the equation of motion along with the condition $U = const$, we get:

$$I_O\ddot{\theta} + \left(k - \rho\frac{U^2}{2}c^2\frac{\pi}{2}\right)\theta = \frac{\rho U c^2}{8}\sum_{n=1}^{N} Uc\pi\Delta\theta.\Phi\left(\frac{U(t - n\Delta t)}{c/2}\right)$$

Let $\tau = n\Delta t$, which implies that $N\Delta t = t$ where t is the current time, and separating the current-time term from the right hand side, we get:

$$I_O\ddot{\theta} + \left(k - \rho\frac{U^2}{2}c^2\frac{\pi}{2}\right)\theta = \frac{\rho U^2 c^3\pi}{8}\sum_{\tau=0}^{t} \Delta\theta(\tau).\Phi\left(\frac{U(t-\tau)}{c/2}\right).$$

Let:

$$\omega_0^2 = \frac{k - \rho\frac{U^2}{2}c^2\frac{\pi}{2}}{I_O},$$
$$\beta = \frac{\rho U^2 c^3\pi}{16 I_O}.$$

Plugging in, and notice that $\Phi(0) = 1/2$, the equation of motion becomes:

$$\ddot{\theta} + \omega_0^2\theta = 2\beta\sum_{\tau=0}^{t}\Delta\theta(\tau).\Phi\left(\frac{U(t-\tau)}{c/2}\right).$$

An immediate and important observation is that this equation is linear! By this fact, we can say that the solution $\theta(t)$ has the form:

$$\theta(t) = \theta_c(t) + \theta_p(t),$$

where $\theta_c(t)$ is the solution to $\ddot{\theta} + \omega_0^2\theta = 0$. For a 2^{nd} order differential equation, $\theta_c(t)$ consists of 2 linearly independent functions. And $\theta_p(t)$ is any other function satisfying the equation of motion while also being linearly independent to all functions in $\theta_c(t)$.

This equation of motion falls into the category of *delayed differential equation* (also called *differential equation with aftereffect*). Φ is referred to as the *kernel* of the equation.

5.6 Apply the LMS!

In this simulation, the LMS will be used to estimate the impulse response or the transfer function between the external moment M (the input/reference signal) and the resultant angle of attack (the desired signal).

Due to the fact that the reference and desired signal now have dimensions, they should be normalized before feeding into the LMS algorithm. In this simulation, the external moment is normalized by a reference moment[1] M_0. The desired signal is normalized by the maximum angle of attack, or the zero-lift angle of attack. Either way doesn't change the result much at all[2].

5.7 Discretization

The equation of motion was discretized using the forward Euler method. The time step $\Delta t = 0.005s$ was selected to minimize artificial energy increase.

[1] Which is a value used to scale the input initially.

[2] In reality, it would be impractical to use the maximum angle of attack since this value is unknown.

6
Methods

6.1 Simulation setup

A simulation in MATLAB using classical flow field method and oscillatory airfoil theory will be used to simulate a wing under load. The wing will be given torsional degree of freedom according to I beam theory. The computed variables with respect to time will be used to test the algorithm's ability to predict the system's frequency response.

The moment is calculated using Karman's unsteady airfoil theory (Section 4.4.6) for a flat Joukowski airfoil with the following geometric parameters generated from the transformation $z = \zeta + l^2/\zeta$:

Parameter	value
l	0.5 m
ϵ	0.01 m
τ	0 m
b	2 m

Table 6.1: Airfoil's geometric parameters. (ϵ, τ) is the position of the centre of the circle in ζ plane.

With these parameters, for the transformation to produce a flat airfoil, the radius of the circle in ζ plane is $a = \sqrt{(l+\tau)^2 + \epsilon^2}$, and the resultant airfoil is a circular arc with radius:

$$R = \epsilon + \frac{l^2}{\epsilon} = 25 \text{ m}$$

and chord

$$c = 4l = 2 \text{ m}.$$

The airfoil is imagined as having an I-beam near the leading edge which bears the structural load for the wing. Thus, the elastic axis of this wing would be near the leading edge. The I-beam has its parameters listed in Table 6.2, where the measurements are defined according to Figure 6.1:

With these parameters, the torsional rigidity is found to be:

$$k = \frac{dM}{d\theta} = 3.93 \times 10^4 \text{ Nm/rad}$$

To ensure that the LMS algorithm can measure the system's response to all frequencies of interest, the input, taken as the speed of incoming flow, will be varied

Parameter	value
b	0.1 m
t	0.005 m
h	0.2 m
t_w	equals to t
E	70×10^9 Ps
ν	0.35
I_{yy}	700 kg/m^2

Table 6.2: Airfoil's structural parameters

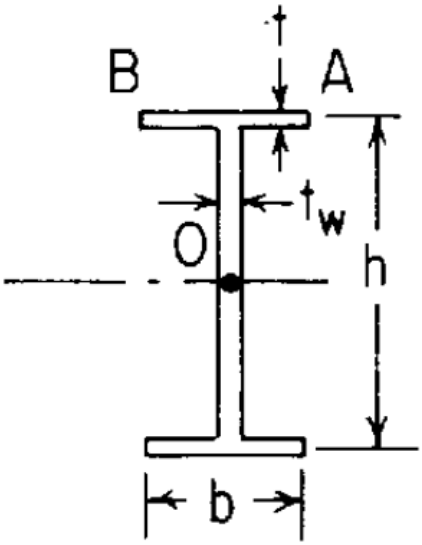


Figure 6.1: Thin walled I-beam dimensions, [YB02]

continuously from one frequency to another. This is because the LMS can only measure the system's response to a frequency if that frequency is present in the input signal. To achieve this varying frequency, a function that generates a pure sinusoidal signal with logarithmically increasing frequency is used. To synthesize this function, first the instantaneous phase angle is given by:

$$\theta(t) = \frac{\omega_1 T}{\ln\left(\frac{\omega_2}{\omega_1}\right)}\left(e^{\frac{t}{T}\ln\left(\frac{\omega_2}{\omega_1}\right)} - 1\right),$$

where $\omega = 2\pi f$. This varying phase angle has an instantaneous frequency given by:

$$f(t) = \frac{\dot{\theta}}{2\pi} = \frac{\omega_1}{2\pi} e^{\frac{t}{T}\ln\left(\frac{\omega_2}{\omega_1}\right)}.$$

It could be verified that $f(0) = \frac{\omega_1}{2\pi} = f_1$ and $f(T) = \frac{\omega_1}{2\pi}\frac{\omega_2}{\omega_1} = \frac{\omega_2}{2\pi} = f_2$. Then the input, which is an external moment M is computed as:

$$M(t) = \frac{M_0}{2}\left(1 + \sin\theta(t)\right). \tag{6.1}$$

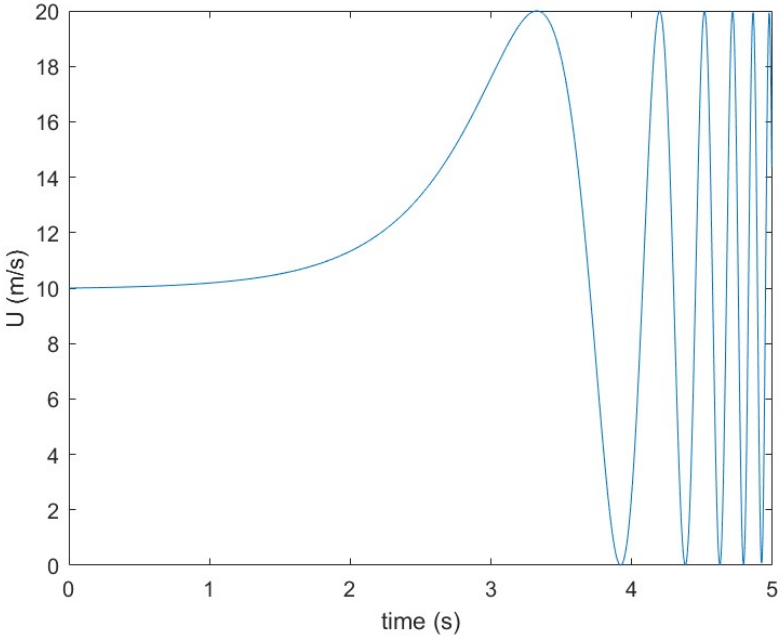


Figure 6.2: A signal constructed from Equation (6.1)

It could be seen that this gives a sinusoidal function with logarithmically increasing frequency from f_1 to f_2 in the time interval $[0, T]$ and mean value $M_0/2$. Values for parameters used to construct the input are listed in Table 6.3, and the input (as described above) is presented in Figure 6.2:

Parameter	value
M_0	500 Nm
f_1	0.01 Hz
f_2	15 Hz
T	20 s
T'	60 s

Table 6.3: Input parameters to Equation (6.1).

As could be seen, the input spent more time in low frequency than in high frequency. This is acceptable if we know that the time domain impulse response of low frequency signals are much longer than high frequency signals. This is true for damped systems where the damping is proportional to the derivative of the system's states (often proportional to a component's velocity). Fung clearly states that the fluttering wing has an artificial damping due to the phase lag between the structural elastic force and the aerodynamic moment [Fun69]. Thus this input signal is appropriate.

6.1.1 Windowing and wait time

However, this input signal is not yet optimal to measure with. Firstly it abruptly ends with high frequency. This does not give enough time for the response of high

frequencies to fully develop and might lead to inaccurate measurement for high frequencies. To remedy, a wait time T' is added whence the input is back to constant M_0.

Secondly, the kink in the signal when it changes from fast varying at frequency f_2 to constant at time T when examined under a discrete Fourier transform reveals many high frequency components. These frequency components are unintended. Thus a window function $\boldsymbol{w}$ is applied to the sweeping portion of the input. The window chosen is the Hanning window. This is a shifted cosine that starts at 0 and returns to 0 only at the end. The application is a vector dot product:

$$M_i \leftarrow M_i.w_i,$$

where each value of M is replaced. The signal after this transformation is presented in Figure 6.3.

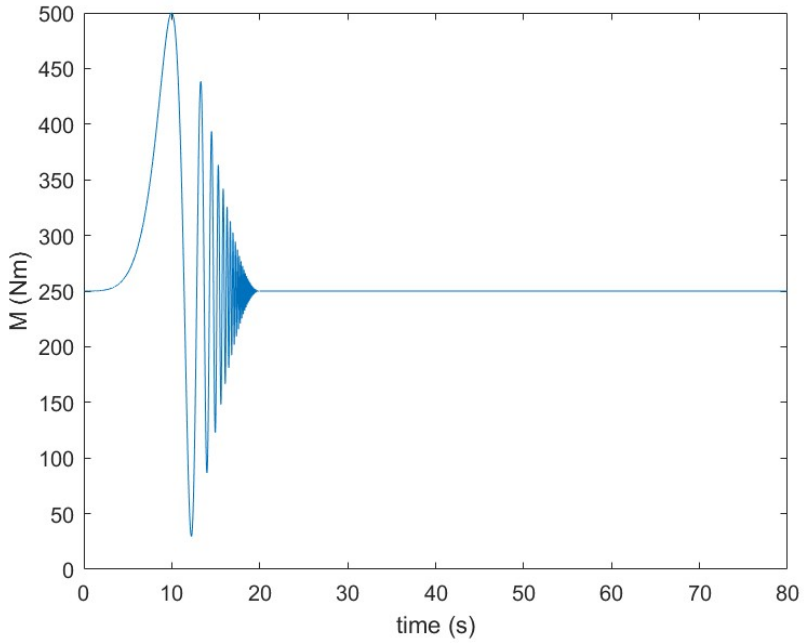


Figure 6.3: The input signal after windowing and wait time

7

Results

7.1 Angle of attack during transient

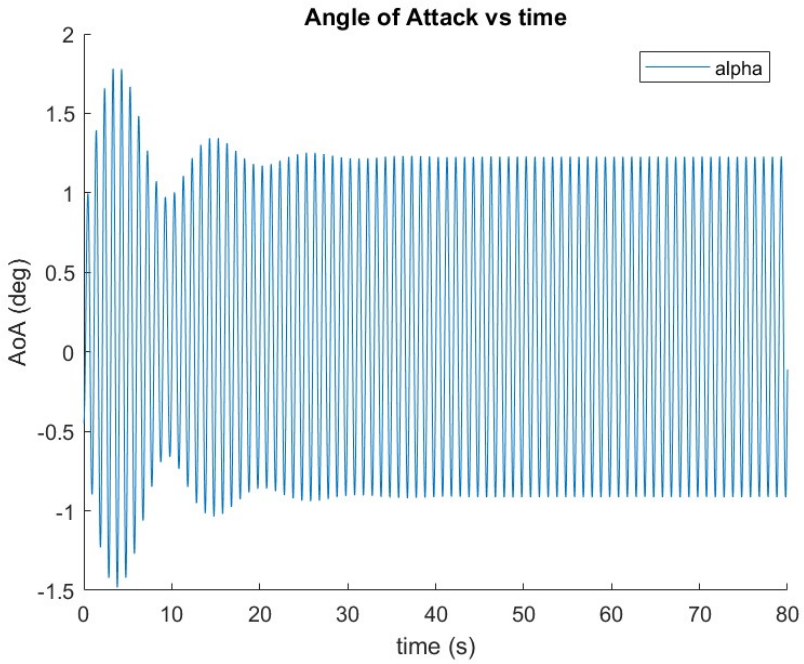


Figure 7.1: Angle of attack during transient for a sinusoidal excitation moment at 1Hz

For this simulation, an airfoil is subjected to a sinusoidal excitation moment. It could be seen from Figure 7.1 that there is a transient response. This transient response's envelope appears to have a phase shift of about $-\pi$ at $t = 0$.

7.2 Moment components during transient

The aerodynamics moment is presented in Figure 7.2. It shows the wake induced moment has a phase leading by 90 degrees compared to the phase of the quasi-steady moment.

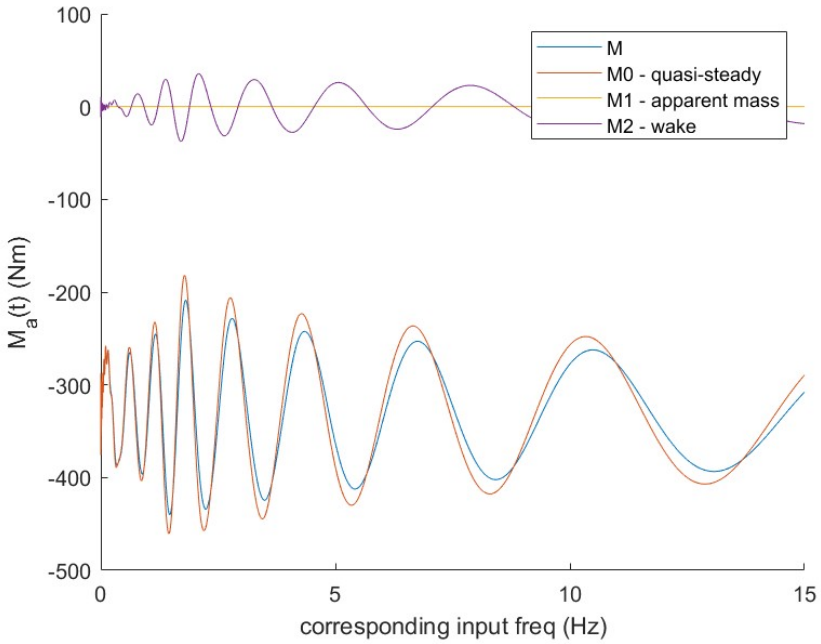


Figure 7.2: Close up on aerodynamics moments acting on the airfoil during the active phase of $M(t)$. The horizontal axis shows the instantaneous frequency of the external disturbance moment $M(t)$. Since the frequency varies logarithmically, when it is laid out in a linear scale, the high frequency parts are stretched, allowing us to see the phase lead.

7.3 Impulse response

The impulse response estimated in Figure 7.3 was estimated using the LMS algorithm with $M_0 = 500Nm$ and $U = 50\ m/s$, and a varying input frequency between $0.01 - 10Hz$.

From this result, it could be seen that the overall dynamics of the system is like an exponentially damped oscillator. However, more useful insights could be gained by doing a parameter survey. Of those parameters, M_0/k and U are the ones having the most impact on the impulse response.

From this observation, it is appropriate to postulate some things about the solution to the equation of motion *for this particular input moment* $M(t)$. Let θ_c be the complementary solution[1] of the equation of motion. Let θ_p be the particular solution. These postulates are:

1. θ_p has the same form as θ_c because the first complementary solution becomes the particular solution in the next time step.
2. θ_p contains $\int f(t)dt$ because the RHS of equation of motion contains an integral.
3. twice differentiation of $f(t)$ mentioned above gives the same function, differs by a constant, and potentially some other parts that is cancelled out by $\dot{f}(t)$. This is because the equation of motion has a 2nd order differential.

[1] Sometimes called homogenous solution.

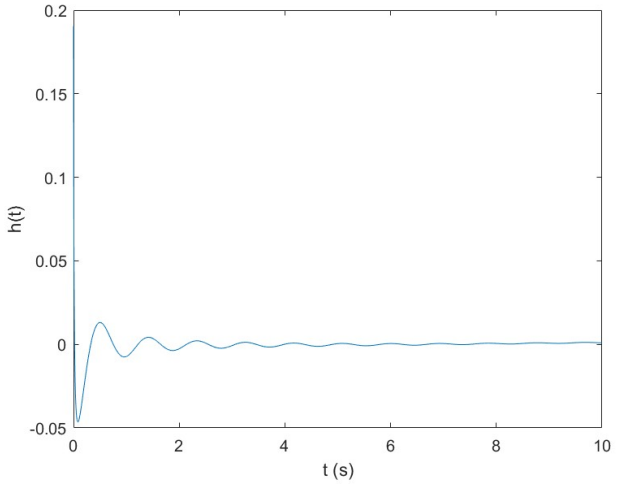


Figure 7.3: Impulse response when $U = 50\ m/s$

4. $\lim_{t\to\infty}(\angle\theta_p) = -\lim_{t\to\infty}(\angle\theta_c)$ because the complementary solution to the equation of motion: $\theta_c(t) = \theta_0/2(e^{i\omega_0 t} + e^{-i\omega_0 t})$ is an infinite oscillation, so the only way for θ_p to cancel out this equation as $t \to \infty$ is by having the opposite phase, and the same magnitude.
5. $\lim_{t\to\infty} |\theta_p(t)| = \lim_{t\to\infty} |\theta_c(t)|$
6. $|\theta_p|$ has the form $1 - \sum e^{-\alpha_i t}$, where $\alpha \in \mathbb{R}, \alpha > 0$ because by having this form, $|\theta_c(t) + \theta_p(t)|$ will become an exponential decay.

It was also observed that the impulse response changes for different kinds of input! This is because part of the dynamics of the system contain past states, which are in turn functions of the input. For inputs that are not impulse, and for systems that couldn't be solved analytically like this one, the impulse response is unavailable to measure directly. Thus the LMS algorithm provides a practical way to estimate an instantaneous impulse response.

If this algorithm is ran at a fast enough rate, the parameters of the system could be said to remain constant within a time step. The system during which will behaves like a Linear Time Invariant system, which exhibits an impulse response and corresponding transfer function. The LMS could then estimate the this instantaneous transfer function and control logic could be designed appropriately based on this estimated plant.

The strength of the LMS comes in the fact that it can continuously update its transfer function estimate as new data[2] comes in.

[2]Required data are the measured output state d and error $e = d - (h_e * u)[n]$ between the measured and estimated output state, h_e is the estimated impulse response array, n denotes the last element of an array, u is an array of past inputs.

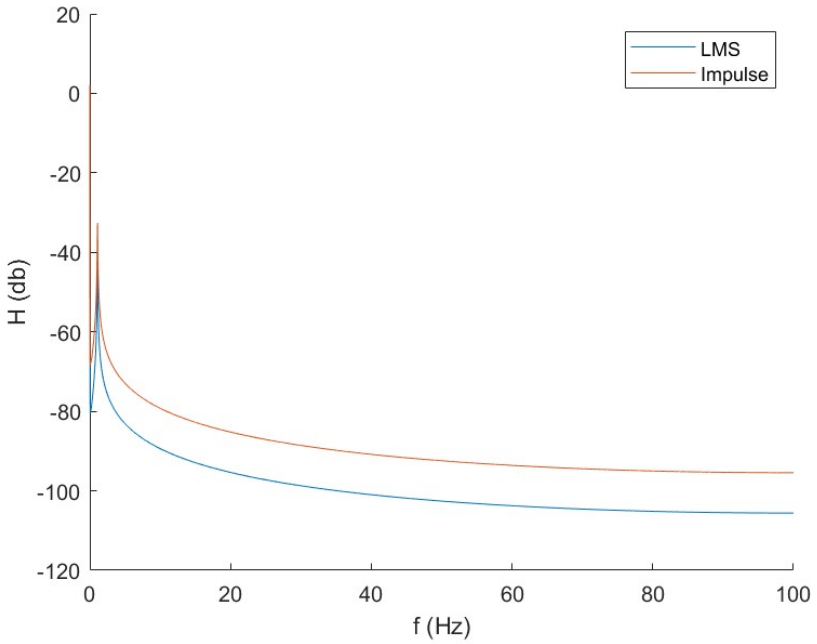


Figure 7.4: Actual frequency response (for the case input moment is an impulse) vs estimated frequency response.

7.4 Validation

Despite the fact that the impulse response changes when the input moment takes different forms, it is still possible to simulate the system when the input is an impulse, and measure the impulse response for this case and compare with the LMS's result.

For an aerofoil travelling at $U = 50$ m/s and an input moment $M = M_0\delta(0)$, the impulse response and estimated impulse response (at the end of a time of 80 seconds) is shown in Figure 7.4. The LMS' vector length was set to capture 10 seconds of the impulse response. At a simulation frequency of 200 Hz, that is 2000 elements. The impulse response was converted to frequency domain by a Fourier transform for ease of comparison.

As could be seen, they agree quite well. There is a constant multiplication factor difference between the two methods. Thus the gain with respect to each frequency is different. This is potentially because of the difference in units of the measured impulse response (rad) vs the estimated impulse response (rad/Nm). However due to time limitation, it was not possible to go to the root of the problem. It is also not guaranteed that the scaling factor is the same for other input moments.

This discrepancy in the gain could be solved at the control system design level. Namely a higher gain is applied in the control loop if the plant and the estimated states are always differs by a constant scalar multiplication. However, as said in the section previously, this system has different transfer function/impulse response for different types[3] of the input M. Thus if the gains are different for each case, and the aerofoil encounters different types of M over time, then this simple gain would

[3]By types I mean different function forms

not work.

7.5 Parameter survey

For these simulations, a sweep excitation moment from $0.01 - 10$ Hz was used, and a mean external moment value of $M_0 = 500$ Nm. Wait time is set to 10 seconds, active time 10 seconds.

These aerofoils were all initially set at their respective equilibrium angles[4] so that they don't initially have energy. This angle is given by:

$$\alpha(0) = \alpha_0 + \theta_0,$$

where α_0 is the angle of attack of the wing with respect to the fuselage (mounting angle), and θ_0 is the twist of the wing at equilibrium, given by Equation(5.1). These are the default parameters, unless otherwise specified.

7.5.1 Speed U

A comparison of the estimated impulse response between 3 different speeds were carried out and result is shown in Figure 7.5. These plots were obtained using the same external moment.

It could be seen that the higher the speed, the more damping there is in the system. Thus, looking at the equation of motion, we can conclude that this damping comes from the wake moment term M_2.

As U gets larger than about 120 m/s for this particular airfoil, the angle of attack increase indefinitely until stall. Thus in this case, a bifurcation happens.

7.5.2 External moment magnitude M

Similarly, a comparison of the impulse response between 2 different values of M is given in Figure 7.6 for the same airspeed $U = 50$ m/s.

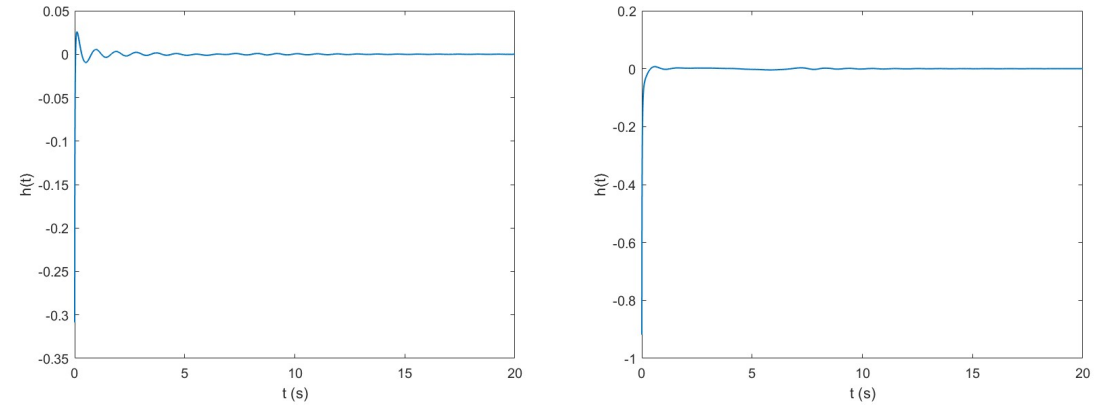
It could be seen that the larger the external moment, the larger the impulse response. This is because even though the signal M varies, it has non-zero mean, thus the amount of energy transferred into the system is higher if the mean of M is higher. Thus the stronger impulse response.

7.5.3 Step size parameter μ

It was found that the LMS algorithm struggles to find the minimum of $E(e^2)$ when the step size parameter is set too high. When this happens, the estimated impulse response $h(t)$ shows artificial ripples.

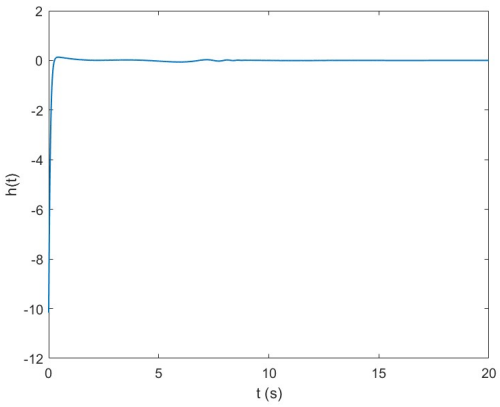
The effect could be seen on Figure 7.7. The LMS algorithm is unable to find the minimum because the distance to minimum is shorter than the smallest step it could make. Thus it couldn't do anything but jump back and forth. And since the

[4] Recall that it depends on the speed.



(a)

(b)



(c)

Figure 7.5: Impulse response of Angle of Attack to variation of airspeed, measured at different speeds: (a) 50 m/s, (b) 70 m/s, (c) 110 m/s. Speeds above about 120 m/s leads to divergence.

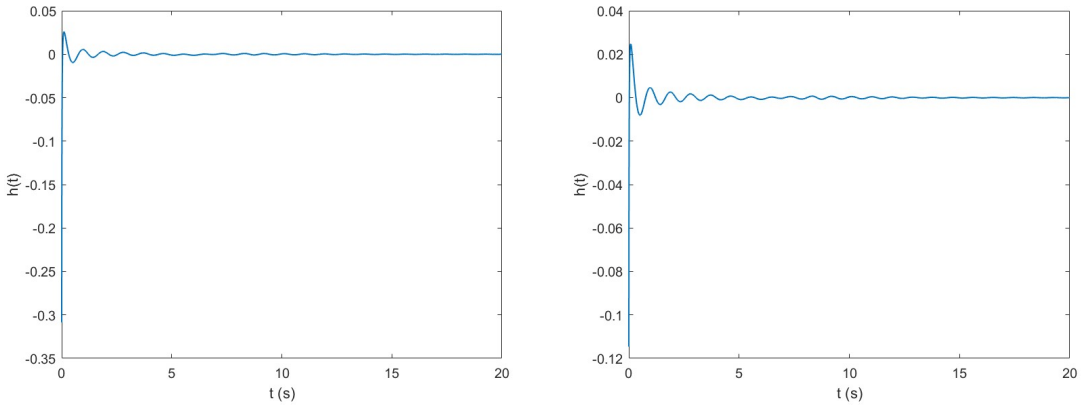
LMS algorithm does not find the minimum at every step it takes[5], this jumping is shown over time. This setting affects the traditional LMS method more than the normalized-LMS method.

7.5.4 Window type

The effect of window type could be seen most clearly at Figure 7.8 for an input sweep from $0.001Hz$ to $10Hz$. Without window, the frequencies outside the desired range has magnitude in the range of 10^{-3}, while with the Hann window, their magnitude is in the range 10^{-8}.

It is also clear that the function form of the window significantly reduces the

[5]The LMS uses a fact that the error times past input $e.f_i$ goes towards the Expectation $E(e.f_i)$ over time. Thus when a new signal arrives, the LMS doesn't immediately step in the direction of minimal error $E(e^2)$, but it goes towards the direction of minimizing the product $e.f_i$, knowing that $e.f_i \to E(e.f_i)$ over time.



(a) **(b)**

Figure 7.6: Impulse response for two different input moments, for the same airspeed: (a) $M0 = 500$ Nm, (b) $M0 = 1000$ Nm

strength of the

7.5.5 Time step

The time step Δt determines the sampling frequency f_S of the simulation. Therefore, it is limited by the higher input frequency f_2. It is mandatory that $f_S > 2f_2$ by Nyquist sampling theorem.

And also by the same reason, windowing must be used because otherwise high frequency contents (those higher than f_S) gets an alias at frequencies lower than f_S and poisons the signal.

7.5.6 Active time

The active time is the amount of time that the input $M(t)$ spent sweeping. Due to the fact that the input sweep generator function described in the previous section already spread the frequencies over time, the active time has little effect on the input's frequency content.

However, the system has a natural frequency of oscillation. If the total time (active plus settling time) is too short such that the system's response to the latest frequencies in the input doesn't manage to complete a meaningful number of cycle then the LMS might produce an incorrect estimate for those frequencies.

7.5.7 Settling time

The settling time, however, is important. Due to the fact that our input is logarithmically changing its tone, the bulk of the input frequencies are concentrated at the later portion of the input's active time. Therefore, a certain wait time is required so that the system fully show its response to these late frequencies.

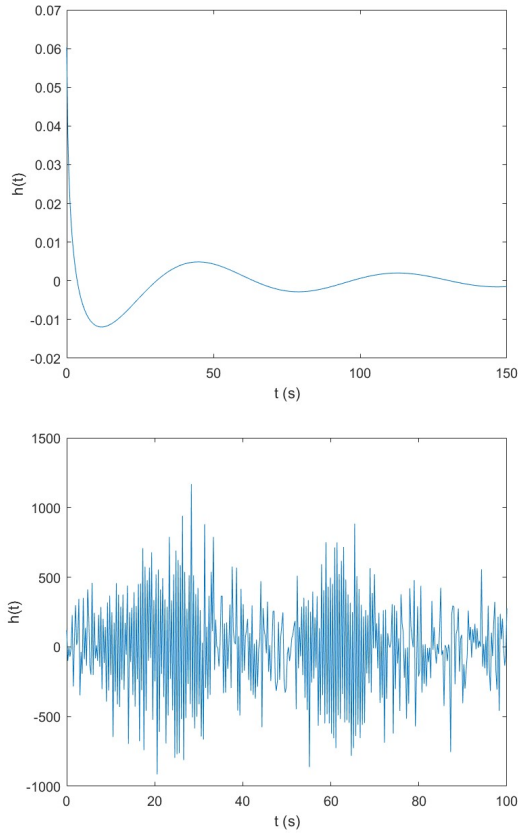


Figure 7.7: h(t) from LMS for $\mu = 0.05$ (top) and $\mu = 0.9$ (bottom)

7.5.8 Airfoil Camber

The effect of airfoil's camber is to change the angle of zero moment.

7.6 A trial case in oscillation suppression

7.6.1 method

In this trial, an airfoil is placed in uniform flow at $U = 100$ m/s. An impulse is exerted on the airfoil at $t = 10$ seconds. The impulse's strength is 50 Nm.s, applied within the time interval $\Delta t = 0.005$ s.

The oscillation suppression trial's block diagram presented in Figure 7.9. k is the torsional stiffness coefficient, measured in Nm/rad. The plant comprises of H and H_a. $M_a(t)$ is the aerodynamics moment, and M_d is the disturbance (impulse in this case). H_a is the aerodynamics moment transfer function, which internally is an infinite delayed sum filter. H is the structural component's transfer function.

The LMS is configured to produce an output moment cancelling M_a and M_d. The input to the LMS is the angle of attack α. The error signal is $e(t) = \alpha(t) - d(t)$, where $d(t)$ is the desired AoA. In this trial, at every time step, the LMS starts out uninitialized, and it learned the dynamics of the system using a number of past inputs equivalent to $t_{reRun} = 5$ seconds. This time value is also set to be equal to the

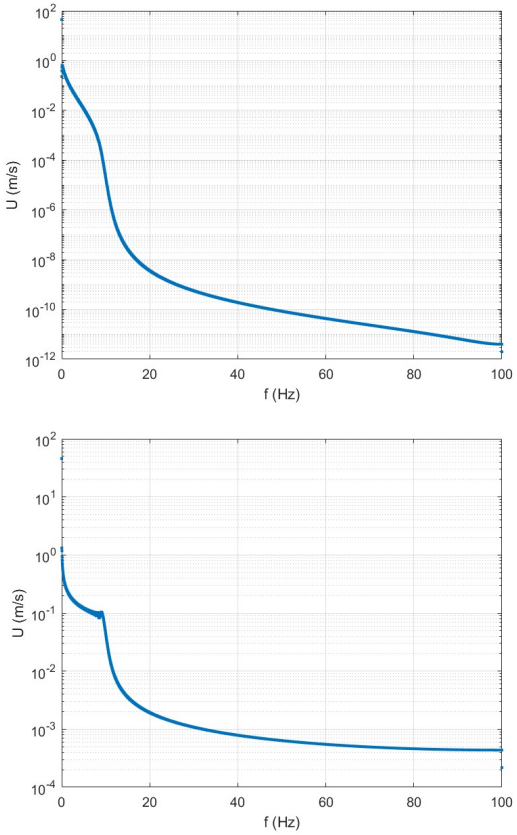


Figure 7.8: No windowing (bottom) vs Hann window (top), frequency contents of the input U. Magnitude has been normalized by input length.

length of the LMS filter, where the number of elements of this filter is $N = t_{LMS}/\Delta t$. During the first t_{LMS} seconds, there is not enough information to initialize the LMS, so the control moment M_c is set to zero.

In the usual implementation, one would need access to both the input and output signals, at least during the forming phase of the LMS. However, in our case, we have no access to the value of aerodynamic moment. And even if we do have access to it during some static measurement, the fact that the system's impulse response depends on its past inputs (which includes the unknown disturbance moment M_d) makes the initial estimation wrong rather quickly. As a result, it was decided to use past AoA values as the input to the LMS, and the difference between the current AoA and a reference value α_0 as the desired signal. The error is thus:

$$\boldsymbol{e}(t) = \boldsymbol{d}(t) - \boldsymbol{f}(t)\boldsymbol{C}(t),$$

where N is the length of the LMS and the desired signal, $\boldsymbol{C}$ is the LMS' estimated impulse response, $\boldsymbol{d}$ are past desired signals, $\boldsymbol{f}$ is the vector of past α arranged in reversed order.

As another note, the usual implementation of a digital filter would be to let the output of the LMS filter be the sum of the product of filter coefficients and past input values [NE92][6]. However, it was found that if the LMS is implemented in that

[6]Section 4.5

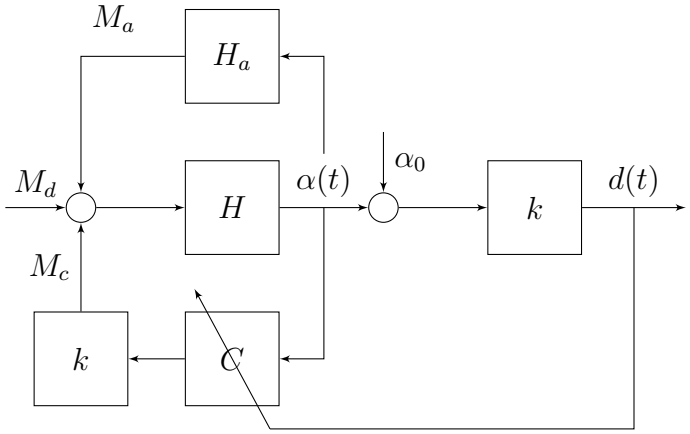
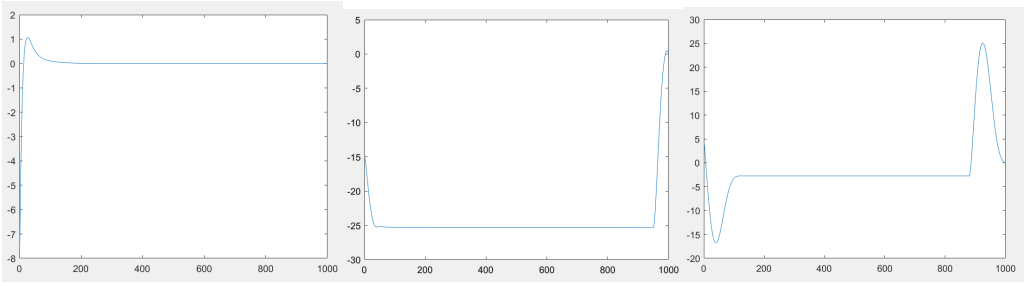


Figure 7.9: Block diagram for oscillation suppression trial. M_d is the external excitation, M_a is the sum of all aerodynamics moments, and M_c is the controller's moment. The desired signal is $d(t)$.



(a) **(b)** **(c)**

Figure 7.10: The LMS' coefficients while the impulse arrive. Vertical axis shows LMS' value for predicted impulse response, horizontal axis shows element count. Note that the LMS in this configuration no longer predicts only the mechanical-fluid system's impulse response, but also partly, of itself, since there is a loop. a) before the impulse arrive, b) 0.25s after the impulse arrive, c) 0.65s after the impulse arrive.

way, for this control circuit, the result is an infinite oscillation with 2 modes. Thus, the controller C is modified. It computes the error for the LMS in the usual way as $\boldsymbol{e}(t) = \boldsymbol{d}(t) - \boldsymbol{f}(t)\boldsymbol{C}(t)$. It also runs the LMS as defined in Chapter 2 without modification. However, when it's time to compute the output, it takes only the second to last value of past input vector multiply with the second to last coefficient of the LMS filter. Since the LMS is a digital filter, this is within the engineer's design choice.

$$M_c = h_{N-1} f_2 k,$$

where f_2 is the input at time $t - (N-1)\Delta t$ [7], and k is the stiffness coefficient.

To understand the motivation for this implementation, it is useful to have a look at the LMS filter's coefficients while the impulse is arriving (Figure 7.10). It could

[7] It takes position 2 in the vector $\boldsymbol{f}$ because this vector is arranged in reverse order, as described in Chapter 2.

be seen that when the impulse arrives, the system's peak reverses polarity, becoming negative. Thus the author hypothesizes that this is an unstable feedback[8]. This is possibly the effect of the loop in the control diagram design (Figure 7.9) where the output of the LMS makes it way back as an input after some time[9]. Thus, it is the most easy, in a digital implementation perspective, to discard all elements belonging to the inverted peak and its tail. It was found that the easiest way is to use the simple multiplication above.

7.6.2 result

The result of this trial is presented in Figure 7.11. It was found that the LMS can produce the correct signal to suppress the oscillation caused by this impulse. This is also evident looking at the frequency response, presented in Figure 7.12. It could be seen that the peek at 0.5 Hz has disappeared when the LMS control is active. This is the response peak of the plant.

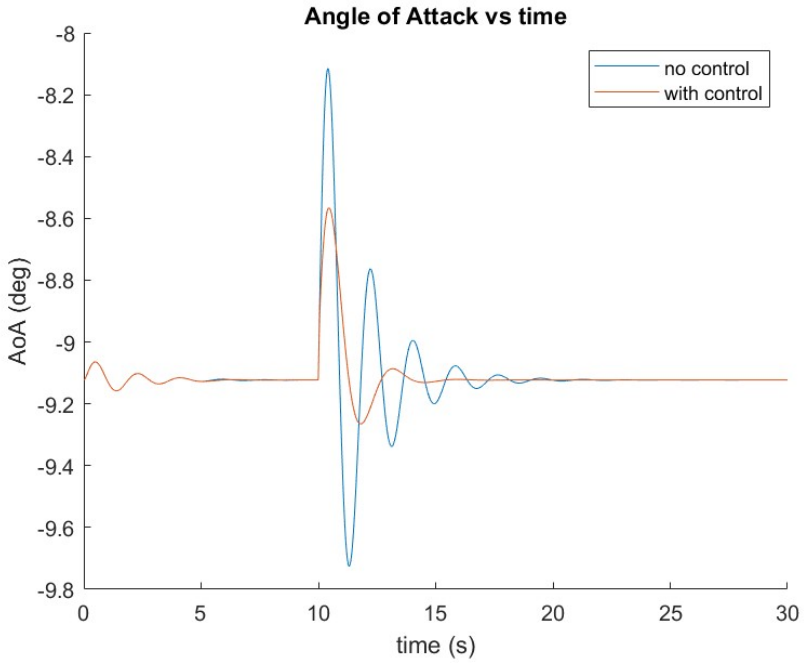
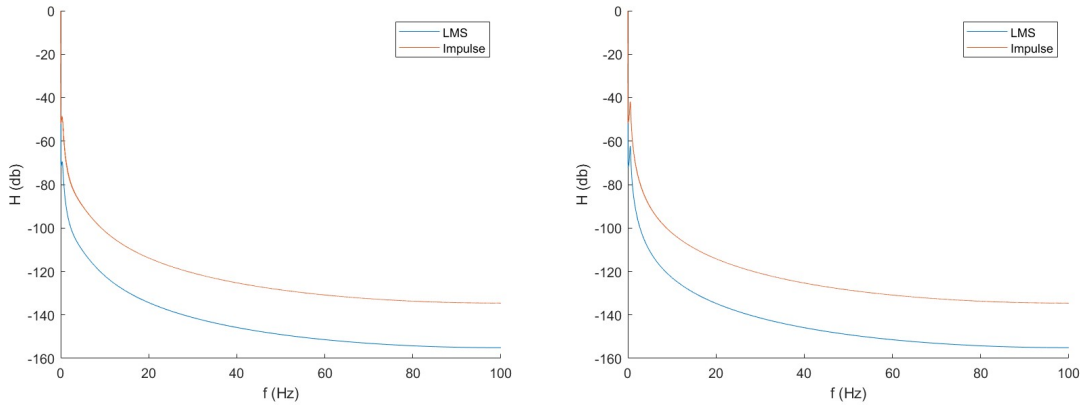


Figure 7.11: Delayed Impulse. Initial ripple is because initially the airfoil is slightly off equilibrium. It could be seen that before the LMS comes online at $t = 5$ seconds, both cases share the same motion.

The requested input moment is presented in Figure 7.13. The strength of the LMS is that the requested control moment's strength is much less than the excitation moment (400 Nm vs 10000 Nm). In real application, this kind of impulse moment could be achieved, hypothetically, with pulsed compressed air mounted on advantageous lever arms.

[8]Because before the impulse arrive, the system is stable and the peak has positive polarity.
[9]Depends on the delay inherent in H, and also in H_a



(a) **(b)**

Figure 7.12: Frequency response with and without LMS control. (a) with LMS control according to diagram presented in Figure 7.9. (b) without LMS control. LMS in each subplot refers to how the frequency response was measured.

7.6.3 The effect of LMS length

The length of the LMS filter N has a positive impact on the performance of the controller. It was found that a longer filter allows the LMS to come up with an M_c that has lower magnitude, more gradual, and less ripple (Figure 7.15). On the other hand, a longer filter results in an $\alpha(t)$ response that is less damped (Figure 7.14). However, the choice of the filter length is a careful balance between how bursty of an M_c that the actuator could follow[10], and how much oscillation there is that the designer can tolerate.

The observations above could be expressed as the following equation:

$$\frac{M_c \tau_c}{\Delta t_c \tau_\alpha} = \beta \frac{1}{t_{LMS}}, \tag{7.1}$$

where τ_c is the characteristic time of the controller moment, τ_α is the characteristic time of the impulse response $\alpha(t)$. These values are the envelopes of $M_c(t)$ and $\alpha(t)$, which are assumed to take the exponential decay form $e^{-t/\tau}$. Δt_c is the width of the first peak of the requested moment M_c, and β is a coefficient of proportionality.

7.6.4 A conceptual understanding of the LMS and a procedure for LMS application

The LMS could be thought of as being similar to an operational amplifier. While the OpAmp does its best to make the voltage at its input terminals equal, the LMS does its best to make 2 signals contained in the error $e(t)$ equal.

Thus, the essence in applying the LMS is to determine that when the desired phenomenon happens, what *needs* to be equal.

[10]Here we have assumed that the actuator is instantaneous and could produce any requested M_c

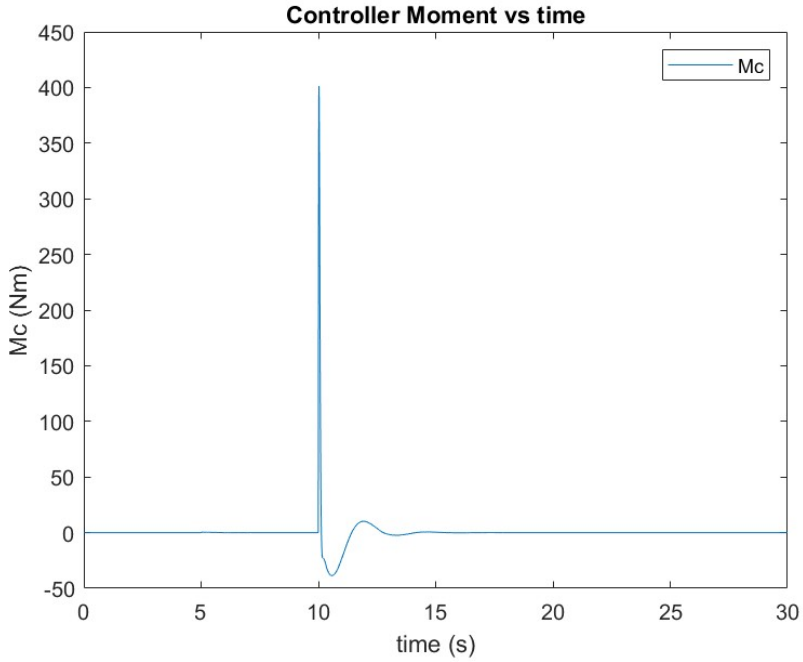


Figure 7.13: Controller moment M_c over time. The controller commands a gradual spike ($\approx 4\Delta t$ of rise time, compared to $1\Delta t$ for both rise and fall for the excitation impulse) when it detects the impulse.

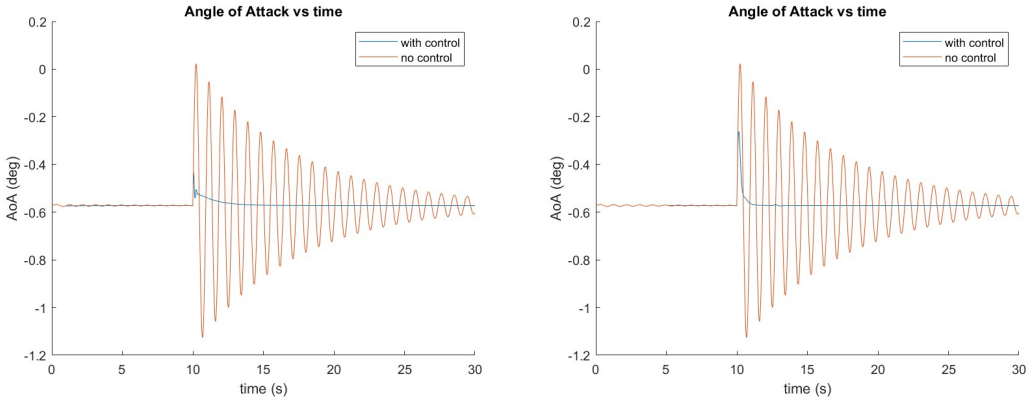
With that being said, the LMS does not concern with what its inputs are, but in order to have meaningful outputs, it is advised to have them in the same dimensions (units). Converting units is the task of 2 k blocks in the control diagram in Figure 7.9. It is found, to the surprise of the author, that the LMS couldn't convert units. It requires the input (α) and the output be of the same units[11]. Thus the need to convert α (in radians) to moment before feeding it into the LMS[12].

It was also found that in order to use the LMS as a controller, it is **mandatory** to let the LMS fully converge before applying its output. Otherwise, if the disturbance arrives before the LMS has converged, divergence is guaranteed. Due to time limitations, this was observed but not proven. A safe implementation is to just turn off M_c while the LMS is forming.

In the application of the LMS, this algorithm could be run just once for each new data point (or sample). However, it was found that for this case of a system having a delayed differential equation as equation of motion, and thus a continuously changing impulse response, running the LMS just on the new data is not sufficient. Thus at each time step, the LMS is re-run on a number of past input samples equivalent to t_{reRun} seconds. It was found that for stability, $t_{reRun} = t_{LMS}$ must be satisfied. For either smaller or larger number of samples all lead to divergence.

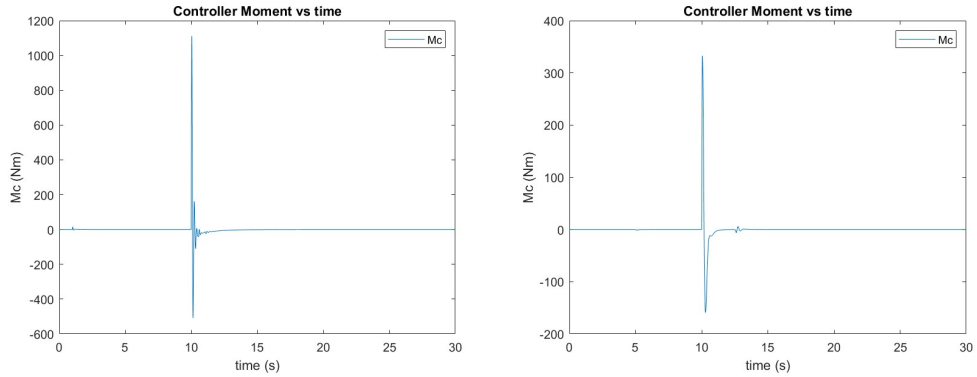
[11] In this case, if this condition is unsatisfied, the LMS' output is artificially small.

[12] And since in a block diagram of linear operators, multiplying before or after is the same, the k block is drawn after the control block.



(a) **(b)**

Figure 7.14: Impulse response with control and no control for different LMS filter lengths at $U = 50$ m/s: a) 1 second, b) 5 seconds



(a) **(b)**

Figure 7.15: Requested M_c for different LMS filter lengths at $U = 50$ m/s: a) 1 second, b) 5 seconds

8

Conclusion

It was found that the LMS is suitable to use as a controller for oscillation suppression. The signal it produce to cancel oscillations could be tuned, in both magnitude and its erratic-ness. However, care must be taken to ensure no looping occurs as it could cause instability. At the same time, the LMS requires knowing both he input and output of the system being estimated, thus difficulties arise in designing the control diagram for aerodynamics systems where the inputs are difficult to measure, or when measurement couldn't be done at the same time as application while the system changes its dynamics due to delayed aftereffect. Therefore, the LMS as a controller is worth further investigation to refine the technique in the realm of aerodynamics control.

Via a review of the classical theory of aerodynamics, important results of aerodynamics pertaining to the aerofoil in inviscid flow was also derived, thus showing that this framework is useful for pedagogical purposes as it provides clarity and coherence to otherwise separate theorems. Furthermore, it also shows that there are other mathematical frameworks that does not make use of the vorticity nor small angle approximations when dealing with cambered, thick aerofoils. Thus, the author suggests bringing back the framework to the centre of the treatment of inviscid flow in aerodynamics courses.

Bibliography

[And17] John D. Anderson. *Fundamentals of Aerodynamics*. Mc GrawHill, 2017.

[BAL96] R. L. Bisplinghoff, H. Ashley, and R. L.Halfman. *Aeroelasticity*. Dover, 1996.

[Bio42] M. A. Biot. "Some simplified methods in airfoil theory". In: *Journal of the Aeronautical Sciences* (1942).

[Dar05] Oliver Darrigol. *A history of Hydrodynamics from the Bernoullis to Prandtl*. Oxford University Press, 2005.

[DB48] F. W. Diederich and B. Budiansky. "Divergence of swept wings". In: *NACA* (1948).

[Fun69] Y. C. Fung. *An introduction to Aeroelasticity*. Dover, 1969.

[Hea97] E. J. Hearn. *Mechanics of Material, volume 2*. Butterworth Heinemann, 1997.

[KCD12] Pijush K. Kundu, Ira M. Cohen, and David R. Dowling. *Fluid Mechanics 5th Edition*. Elsevier, 2012.

[KS38] Th. von Karman and W. R. Sears. "Airfoil Theory for non-uniform motion". In: *Journal of the Aeronautical Sciences* (1938).

[McL13] Doug McLean. *Common Misconceptions in Aerodynamics*. Lecture at the University of Michigan department of Aerospace Engineering. 2013. URL: `https://youtu.be/QKCK4lJLQHU`.

[NE92] P. A. Nelson and S. J. Elliot. *Active Control of Sound*. Academic Press, 1992.

[Nee23] Tristan Needham. *Visual Complex Analysis, 25th Aniversary Edition*. Oxford University Press, 2023.

[Ray18] Daniel P. Raymer. *Aircraft Design: A Conceptual Approach*. AIAA, 2018.

[Tho58] L. M. M. Thompson. *Theoretical Aerodynamics*. Macmillan and Company, 1958.

[VR17] B. Villone and C. Rampf. "Hermann Hankel's On the general theory of motion of fluids, an essay including an English translation of the complete Preisschrift from 1861". In: *European Physical Journal H* (2017).

[Wil58] C. H. Wilts. "Incompressible flutter characteristics of representative aircraft wings". In: *NACA* (1958).

[YB02] Warren C. Young and Richard G. Budynads. *Roark's Formulas for Stress and Strain*. McGraw-Hill, 2002.

A

Stationary Airfoil Theory

Stationary airfoils are those undergoing motion at constant speed and angle of attack.

A.1 How does an airfoil generate lift?

For simplicity, take the x-axis such that it is parallel to the incoming freestream, which has a speed of V_0.

Firstly, the lift and pitch moments of an airfoil will be derived.

Let u, v be the disturbance velocity, given by:

$$\begin{aligned} V_x &= V_{0x} + u, \\ V_y &= V_{0y} + v, \end{aligned} \tag{A.1}$$

where V_x, V_y are the x and y components of velocity measured at a point (x, y) in the domain and V_{0x}, V_{0y} be the x and y components of the freestream flow. From our choice of coordinate, it is obvious that $V_{0x} = V_0$ and $V_{0y} = 0$.

The velocity field around the airfoil (except for near the stagnation points) have the property that they differs from the freestream velocity (V_0) by very little. Meaning $V_x >> u$. Thus:

$$\begin{aligned} V^2 = V_x^2 + V_y^2 = (V_0 + u)^2 + v^2 \approx V_0^2 + 2V_0 u \\ => V^2 - V_0^2 = 2V_0 u. \end{aligned}$$

On the other hand, for a non-turbulent flow, and neglecting gravity's effect on the pressure (ρgh) since ρ is too small, Bernoulli's principle gives:

$$V^2/2 + P/\rho = const. \tag{A.2}$$

Since it holds between a point on the surface of the airfoil and a point at infinity (on the same streamline, but since all points at infinity have the same flow numerically, which point is on the streamline leading to our point of interest on the airfoil doesn't really matter), we have:

$$\begin{aligned} V^2/2 + P/\rho = V_0^2/2 + P_0/\rho_0 \\ => P - P_0 = \rho_0(V_0^2/2 - V^2/2) \\ => P - P_0 = \rho_0(-V_0 u). \end{aligned} \tag{A.3}$$

Now, if we assume that the disturbance velocity is the gradient of a velocity field ϕ:

$$u = \frac{\partial \phi}{\partial x}; v = \frac{\partial \phi}{\partial y} \tag{A.4}$$

$$=> P - P_0 = -\rho_0 V_0 \frac{\partial \phi}{\partial x}. \tag{A.5}$$

The assumption that the disturbance field is a gradient has a consequence. It is that the disturbance field has zero rota everywhere. In mathematical form, if $\boldsymbol{w} = (u, v)$, and $\boldsymbol{w} = \boldsymbol{\nabla}\phi$, then:

$$\boldsymbol{\nabla} \times \boldsymbol{w} = 0.$$

The lift is then given as the force resultant of pressure difference between the upper and lower wing surfaces (P_u and P_b). Let dL be the lift per unit span:

$$dL = (P_b - P_u)dx = (P_b - P_0 - (P_u - P_0))dx$$

$$= -\rho_0 V_0 \left(\frac{\partial \phi_b}{\partial x} - \frac{\partial \phi_u}{\partial x} \right) dx.$$

Now it is tempting to integrate in terms of the velocity potential ϕ and find the lift. However, a question remain: how to deduce the velocity potential's function from a given airfoil shape? Without this information, integration is impossible. To solve it, notice that when we plot only the (u, v) field from experiment, i.e. when we subtract the freestream from the local velocity, what remains is a vortex circulating around the airfoil (figure A.1). Thus, the airfoil drags around a vortex with it.

A.2 Lift produced by a small vortex

Suppose we have a flat airfoil at an arbitrary point in space. This airfoil would generate a vortex centered around it, as seen in figure A.1. Let u, v defined as

$$u(x, y) = (\boldsymbol{V} - \boldsymbol{V}_0)\hat{\boldsymbol{i}},$$

$$v(x, y) = (\boldsymbol{V} - \boldsymbol{V}_0)\hat{\boldsymbol{j}}$$

be the disturbance velocity field generated by such a vortex.

A circular flow resulting from this vortex would leave a trace along a closed loop. Let $d\Gamma$ be the circulation per unit span, defined as the trace of the velocity along a closed loop that bounds the vortex. For simplicity, let the loop be an infinitesimal rectangular box bounding the vortex's center. We then have:

$$d\Gamma = \oint \boldsymbol{V}.\boldsymbol{dl} \tag{A.6}$$

$$= \left(V_0 + \frac{\partial \phi_u}{\partial x} \right) dx + \left(-\frac{\partial \phi_r}{\partial y} \right) dy - \left(V_0 + \frac{\partial \phi_b}{\partial x} \right) dx + \frac{\partial \phi_l}{\partial y} dy.$$

Let $\gamma(x)$ be the intensity of circulation, defined as:

$$\gamma(x) = \frac{d\Gamma}{dx} \tag{A.7}$$

$$= \left(\frac{\partial \phi_u}{\partial x} - \frac{\partial \phi_b}{\partial x}\right) + \left(\frac{\partial \phi_l}{\partial y} - \frac{\partial \phi_r}{\partial y}\right) dy/dx.$$

In the case of an airfoil, its chord is much larger than its thickness (T). On the other hand, the loop must enclose the airfoil entirely since the path of integration cannot leave the flow domain. Assuming a flat airfoil, then we have $\lim_{T\to 0} dy/dx = 0$ from the above reasoning. Thus:

$$\lim_{T\to 0} \gamma(x) = \frac{\partial \phi_u}{\partial x} - \frac{\partial \phi_b}{\partial x}. \tag{A.8}$$

Thus, for a thin airfoil, the lift from the pressure distribution now becomes:

$$dL = \rho_0 V_0 \gamma(x) dx. \tag{A.9}$$

This equation tells us that the lift is contributed from a distribution of vortices ($\gamma(x)$). What's left is to find a way to relate the airfoil geometry to its equivalent vortex distribution.

However, there is a small note before we could proceed: an isolated vortex is impossible in reality. Kelvin's Circulation theorem, which states that for the same set of fluid particles over time, we have the following:

$$\frac{d\Gamma}{dt} = 0 \tag{A.10}$$

under the condition that all forces acting on these particles are conservative forces [VR17]. Thus, if we neglect viscous forces, the total circulation in a flow field is always constant. Since all airfoil have to start from rest (the field around having no net circulation), the total circulation in the flow field around them should remain zero even when they start moving.

Therefore, for an airfoil to produce a circulation Γ around it, it must leave behind another circulation $-\Gamma$ in the wake [KS38]. This second circulation doesn't necessarily move with the wing. Initially when the airfoil was starting to move forward, two vortices of equal and opposite strength were born. One of them circulates around the airfoil and another one next to it, circulating around itself. If the airfoil speeds up, its own vortex gets stronger while a new vortex is immediately formed in its wake to counter. As the airfoil accelerates in space, it leaves behind a distribution of vortices $-\gamma_1(x)$ which together counters the strength of the airfoil's vortex Γ.

A.3 Velocity field generated by a vortex, Circulation

Having seen the role of vortices, it is time to study them mathematically. First we have to define the vortex flow. Suppose we can grab an infinitesimal fluid element

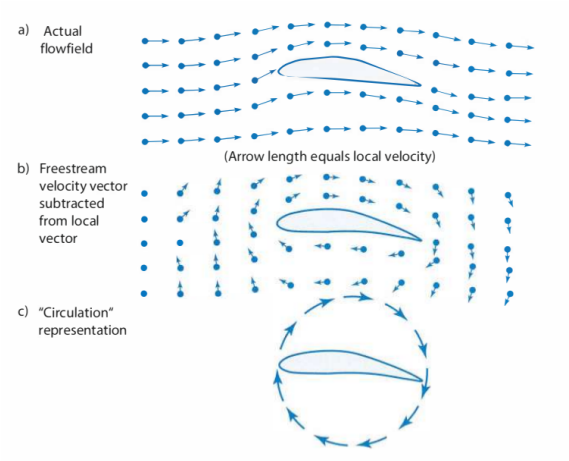


Figure A.1: Wing's disturbance field. Image taken from Raymers' book [Ray18] (fig 4.3)

and twist it at the rate ω radians per second. Due to the intermolecular interaction in the fluid, this fluid element will not be rotating alone but would drag its neighbouring elements into circular motion. Albeit with one crucial difference: in this field, only the element that we grabbed is rotating around itself, while all other elements are only rotating around the first element while keeping a constant orientation. This might come as unintuitive since we would expect the other elements to also start rotating, but keep in mind that we are considering inviscid fluids. Thus, the rota of any other element, except from the one we spin, will be zero.

From the influential 1861 essay "On the general theory of motion of fluids", Hermann Henkel while attampting to put forward a theory of fluid motion based on the Lagrangian approach to fluid mechanics, which as a side note went on to win him the prize from the philosophical faculty of Georgia Augusta in the University of Götingen [VR17], derived the following law for the velocity a rotating fluid element (whose volume is dV) would impart on another element at a distance r away:

$$dw = \frac{dV}{2\pi r^2}\omega \sin\alpha,$$

where α is the angle between $\boldsymbol{r}$ and the element's angular momentum vector $\boldsymbol{\omega}$. When rewritten into vector form, we have:

$$\begin{aligned} d\boldsymbol{w} &= \frac{dV}{2\pi r^2}\boldsymbol{\omega} \times \hat{\boldsymbol{r}} \\ &= \frac{dA.dl}{2\pi r^2}\boldsymbol{\omega} \times \hat{\boldsymbol{r}} \\ &= \frac{dA.\omega}{2\pi r^2} d\boldsymbol{l} \times \hat{\boldsymbol{r}}. \end{aligned}$$

In 2D, we could imagine an infinitely long *straight* rotating filament cutting through our plane at 1 point. Performing the integral of all $d\boldsymbol{w}$ from the filament to find the velocity at an arbitrary point on the 2D plane, at a distance d_0 from the filament, we have:

$$d\boldsymbol{w}_{dA} = 2\int_0^\infty \frac{dA.\omega}{2\pi r^2} d\boldsymbol{l} \times \hat{\boldsymbol{r}}.$$

The reason we still get a differential form of $\boldsymbol{w}$ is that we still have to integrate over space. Also, note that we have that $\omega = ((\boldsymbol{\nabla} \times \boldsymbol{V})/2)\hat{\boldsymbol{\omega}}$. Performing the remaining integral, we have:

$$\begin{aligned}
\boldsymbol{w} &= \iint_S d\boldsymbol{w}_{dA} \\
&= 2\int_0^\infty \iint_S \frac{dA.\omega}{2\pi r^2} d\boldsymbol{l} \times \hat{\boldsymbol{r}} \\
&= 2\int_0^\infty \iint_S \frac{((\boldsymbol{\nabla} \times \boldsymbol{V})/2)\hat{\boldsymbol{\omega}} dA}{2\pi r^2} d\boldsymbol{l} \times \hat{\boldsymbol{r}} \\
&= 2\int_0^\infty \iint_S \frac{((\boldsymbol{\nabla} \times \boldsymbol{V})/2).d\boldsymbol{A}}{2\pi r^2} d\boldsymbol{l} \times \hat{\boldsymbol{r}} \\
&= 2\int_0^\infty \oint_C \frac{(\boldsymbol{V}.d\boldsymbol{C})/2}{2\pi r^2} d\boldsymbol{l} \times \hat{\boldsymbol{r}},
\end{aligned}$$

where S is a surface in 3D that contain the filament's cross-section dA, and C is S's circumference.

There is no other condition on S other than it is singly-connected because Stoke's theorem is going to be used. The bounds of S doesn't matter for the double integral because only the element dA contains rotation and at all other points in S we have $\omega = 0$ thus $\boldsymbol{\nabla} \times \boldsymbol{V} = 0$ and so their integral would vanish in Stokes' theorem. As a result we can define a term Γ which will be a constant for all surfaces S as long as the filament passes through S only once:

$$\Gamma = \oint_C (\boldsymbol{V}.d\boldsymbol{C}),$$

where C is S's circumference.

Since the filament passes through S once, it imples that the surface S is open, and the filament exits through that opening. Thus the curve C encloses the filament. And since S is arbitrary as long as the filament passes through its opening, the curce C as the consequence can be any curve that encloses the filament. Rearranging:

$$\begin{aligned}
\boldsymbol{w} &= 2\int_0^\infty \frac{1}{4\pi r^2} \oint_C (\boldsymbol{V}.d\boldsymbol{C}) d\boldsymbol{l} \times \hat{\boldsymbol{r}} \\
&= 2\int_0^\infty \frac{\Gamma}{4\pi r^2} d\boldsymbol{l} \times \hat{\boldsymbol{r}}.
\end{aligned}$$

Continue with the outer integration, we find, where α (Figure A.2) is the angle between the perpendicular projection of the point where $\boldsymbol{w}$ is living to the vortex filament and the vector $\boldsymbol{r}$:

$$\begin{aligned}
\boldsymbol{w} &= 2\int_0^{\pi/2} \frac{\Gamma}{4\pi r^2} dl \cos\alpha.\hat{\boldsymbol{\theta}} \\
&= 2\int_0^{\pi/2} \frac{\Gamma}{4\pi r^2} \frac{r d\alpha}{\cos\alpha} \cos\alpha.\hat{\boldsymbol{\theta}}
\end{aligned}$$

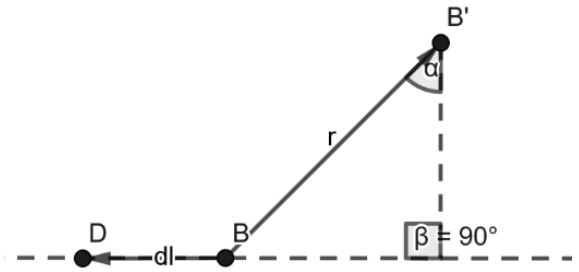


Figure A.2: The angle α

$$
\begin{aligned}
&= 2\int_0^{\pi/2} \frac{\Gamma}{4\pi(d/cos\alpha)} d\alpha.\hat{\boldsymbol{\theta}} \\
&= 2\int_0^{\pi/2} \frac{\Gamma}{4\pi d}\cos\alpha d\alpha.\hat{\boldsymbol{\theta}} \\
&= \frac{\Gamma}{2\pi d}\sin\alpha\Big|_0^{\pi/2}\hat{\boldsymbol{\theta}} \\
&\rightarrow \boldsymbol{w} = \frac{\Gamma}{2\pi d}\hat{\boldsymbol{\theta}}. \qquad \text{(A.11)}
\end{aligned}
$$

In 3D, we only have to relax the condition that the filament is straight. Since $dV = dA.dl$, we need 2 integrals to get $\boldsymbol{w}$ from Henkel's equation. Let's first integrate over a surface to eliminate dA and afterwards integrate over the filament to eliminate dl.

The chosen surface S must include dA, but other than that it only need to be singly-connected (since Stokes' theorem will be used) and the filament should only passes through the surface S once. Performing integration over the surface S and note that we have that $\omega = ((\boldsymbol{\nabla}\times\boldsymbol{V})/2)\hat{\boldsymbol{\omega}}$:

$$
\begin{aligned}
d\boldsymbol{w} &= \iint_S \frac{dA.\omega}{2\pi r^2} d\boldsymbol{l}\times\hat{\boldsymbol{r}} \\
&= \iint_S \frac{((\boldsymbol{\nabla}\times\boldsymbol{V})/2)\hat{\boldsymbol{\omega}}dA}{2\pi r^2} d\boldsymbol{l}\times\hat{\boldsymbol{r}} \\
&= \iint_S \frac{((\boldsymbol{\nabla}\times\boldsymbol{V})/2)d\boldsymbol{A}}{2\pi r^2} d\boldsymbol{l}\times\hat{\boldsymbol{r}}.
\end{aligned}
$$

Applying Stokes' theorem:

$$
\begin{aligned}
d\boldsymbol{w} &= \oint_C \frac{(\boldsymbol{V}.d\boldsymbol{C})/2}{2\pi r^2} d\boldsymbol{l}\times\hat{\boldsymbol{r}} \\
&= \oint_C \frac{(\boldsymbol{V}.d\boldsymbol{C})}{4\pi r^2} d\boldsymbol{l}\times\hat{\boldsymbol{r}}
\end{aligned}
$$

$$d\boldsymbol{w} = \frac{\Gamma}{4\pi r^2} d\boldsymbol{l} \times \hat{\boldsymbol{r}}.$$

This is similar in form to Biot-Savart's law in Electromagnetics. The velocity produced by a rotating fluid element is similar to the force produced by a current element, where its strength and direction are similar to $\Gamma d\boldsymbol{l}$.

[BAL96] complains, within potential flow framework, that this flow would require an infinite angular momentum and energy. This happens at the center where the velocity tends to infinity (i.e. a singularity). However, Anderson [And17] accepts it as a fundamental flow field (besides Uniform flow, Source flow, and Doublet flow) by excluding the singularity point at the center of the vortex from the domain. Note that among the other three fundamental flows, Source and Doublet flow also have singularities of their own, but for Vortex flow, the singularity must be excluded because potential flow framework requires that $\boldsymbol{u} = \nabla\phi$, thus $\nabla \times \boldsymbol{u} = \nabla \times (\nabla\phi) = 0$. But when we plug in the vector (u_ϕ, u_r) we find that its curl is not 0 at the center.

A.4 How to get the vortex distribution for a given airfoil

An airfoil's drag and lift, as long as the flow is still attached, according to Aeroelasticity [BAL96], can be regarded as the superposition of the drag coming from the thickness profile vs chord, the lift/moment of the airfoil's camberline at 0 degree angle of attack, and a flat camberline placed at the original airfoil's angle of attack. Thus, if only the lift and moment are of concern, the properties of a cambered airfoil in motion (in which the angle of attack changes with time) is the same as a flat airfoil doing the same motion. The camberline's effect is to displace the equilibrium state by a certain amount and could be compensated by translating the α coordinates. [1]

Anderson [And17] presents in his book a way to get a vortex distribution for a thin airfoil[2]. This is called Glauert's method. We first replace the airfoil with a distribution of vortices[3] $\gamma(x) = d\Gamma/dx$ placed on the projection of the camberline to the x-axis and find a function for this distribution ($\gamma(x)$) such that the camberline becomes a streamline. To satisfy this, the field's velocity on the camberline must be tangent to it.

Define a plane where the x-axis points to the right, the z-axis points up. An airfoil spanning the interval $[-c/2, c/2]$ is placed on the x-axis. Suppose that the camberline is given by $z(x)$ and $\boldsymbol{n}(x)$ is the vector perpendicular to the camberline, the condition above is mathematically given by the following, $\forall x_0 \in [-c/2, c/2]$:

$$\boldsymbol{V}(x_0, 0).\boldsymbol{n}(x_0) = 0$$

[1] Note that this is true only for small motions where the disturbance velocity u is much smaller than freestream velocity U [BAL96].

[2] In his book, the airfoil is placed entirely on the positive x-axis, but this introduced a shift in the transformation of coordinate (which will be presented soon) that seems unnatural.

[3] These are infinitely long vortices penetrating the page.

$$\leftrightarrow \boldsymbol{V}(x_0, 0).\left(-\left.\frac{dz}{dx}\right|_{x_0} \boldsymbol{i} + \boldsymbol{k}\right) = 0. \tag{A.12}$$

Another condition to satisfy is the total circulation must equal to the airfoil's:

$$\int_0^c \gamma(x)dx = \oint_C \boldsymbol{V}\boldsymbol{dl},$$

where C is a closed curve surrounding the airfoil.

Suppose that the incoming flow V_0 comes at a narrow angle α. We have:

$$\begin{aligned}\boldsymbol{V_0} &= V_0(\cos\alpha.\boldsymbol{i} + \sin\alpha.\boldsymbol{k}) \\ &\approx V_0(\boldsymbol{i} + \alpha\boldsymbol{k}).\end{aligned}$$

On the other hand, suppose the vortices in the sheet has their vortex line direction align with the negative $\boldsymbol{j}$ axis[4]. Since the sheet of vortex is on the x axis, according to the Biot-Savart law, its resulting field at a point $(x_0, 0)$ on the x axis would point solely in the z direction.

$$\begin{aligned}\boldsymbol{w}(x_0, 0) &= \int_0^c \frac{\gamma(x)}{2\pi(x_0 - x)}dx.\boldsymbol{k} \\ &= w(x_0, 0)\boldsymbol{k}.\end{aligned}$$

Thus, the total velocity field at any point $(x, 0) : x \in [-c/2, c/2]$ on the x axis with the presence of a vortex distribution on this axis is:

$$\begin{aligned}\boldsymbol{V}(x, 0) &= \boldsymbol{V_0} + \boldsymbol{w}(x, 0) \\ &\approx V_0(\boldsymbol{i} + \alpha\boldsymbol{k}) + \int_0^c \frac{\gamma(\epsilon)}{2\pi(x - \epsilon)}d\epsilon.\boldsymbol{k} \\ &= V_0\boldsymbol{i} + \left(V_0\alpha + \int_0^c \frac{\gamma(\epsilon)}{2\pi(x - \epsilon)}d\epsilon\right)\boldsymbol{k}.\end{aligned}$$

Plugging the above into Anderson's vortex distribution equation (A.12) above yields the fundamental equation of aerodynamics:

$$V_0\left(-\frac{dz}{dx}\right) + V_0\alpha + \int_0^c \frac{\gamma(\epsilon)}{2\pi(x - \epsilon)}d\epsilon = 0. \tag{A.13}$$

It is via this equation that we can find a family of distributions $\gamma(x)$ that gives a correct flow distribution for a given camberline $z(x)$. Turns out that to specify a specific function for $\gamma(x)$, we need the Kutta condition, which states:

$$\gamma(c) = 0.$$

Meaning the vortex distribution's strength falls to zero at the trailing edge. This law was obtained from experiment.

[4]This is out of the page, for the x-axis points to the right and the z axis points up.

A.4.1 Solving the fundamental equation of airfoil theory for a general camberline

According to Anderson [And17], it is easier to solve this equation if we change the coordinate system to one based on ϕ, which is as follows:

$$\epsilon = \frac{c}{2}\cos\phi$$
$$\rightarrow d\epsilon = -\frac{c}{2}\sin\phi d\phi.$$

And the fundamental equation (A.13) becomes, for all position θ, (which is the transformation of the position variable x):

$$\frac{1}{2\pi}\int_0^\pi \frac{\gamma(\phi)\sin\phi}{\cos\phi - \cos\theta}d\phi = V_0\left(\frac{dz}{dx} - \alpha\right). \tag{A.14}$$

The following procedure to solve this equation is presented in Anderson's book [And17] (Glauert's method). First we use Fourier series to decompose the general airfoil shape into sine and cosine functional bases. Let:

$$f(\theta) = \frac{dz}{dx} - \alpha$$
$$= A_0 - \sum_{n=1}^{\infty} A_n\cos(n\theta),$$

where the coefficients are:

$$A_0 = \frac{1}{\pi}\int_0^\pi f(\theta)d\theta$$
$$A_1 = -\frac{2}{\pi}\int_0^\pi f(\theta)\cos(\theta)d\theta$$
$$A_2 = -\frac{2}{\pi}\int_0^\pi f(\theta)\cos(2\theta)d\theta$$
$$\vdots$$
$$A_n = -\frac{2}{\pi}\int_0^\pi f(\theta)\cos(n\theta)d\theta$$

Plug it into the fundamental equation of airfoil theory (equation A.14) we have:

$$\frac{1}{2\pi}\int_0^\pi \frac{\gamma(\phi)\sin\phi}{\cos\phi - \cos\theta}d\phi = V_0\left(A_0 - \sum_{n=1}^{\infty} A_n\cos(n\theta)\right).$$

Solving this equation is not trivial so the solution given in Anderson's book is[5]:

$$\gamma(\theta) = -2V_0\left(A_0\frac{1+\cos\theta}{\sin\theta} + \sum_{n=1}^{N} A_n\sin(n\theta)\right).$$

[5]In this result, $\gamma(x)$ takes the opposite sign to Anderson's because we placed the vortex lines pointing in the $-\boldsymbol{j}$ direction, which is out of the page, resulting in counter-clockwise vortices receive positive strength.

A.4.2 Lift

The lift in this case can be found using the Kutta-Joukowsky theorem:

$$\begin{aligned} L &= \rho V_0 \Gamma \\ &= \rho V_0 \int_0^c \gamma(x) dx \\ &= \rho V_0 \int_0^\pi \gamma(\theta) \frac{c}{2} \sin\theta . d\theta \ . \end{aligned}$$

When the general solution for $\gamma(\theta)$ is plugged in, we have:

$$L = -\rho V_0^2 c \left(\int_0^\pi A_0 (1 + \cos\theta) d\theta + \int_0^\pi \sum_{n=1}^{N} A_n \sin(n\theta_0) \sin\theta d\theta \right)$$

$$= -\rho V_0^2 c \left(A_0 \pi + \int_0^\pi \sum_{n=1}^{N} A_n \sin(n\theta_0) \sin\theta d\theta \right).$$

The second term could be solved using the orthorgonality property of sine functions:

$$\int_0^\pi \sin(n\theta) \sin(m\theta) d\theta = \begin{cases} \pi/2 & \text{if } m = n \\ 0 & \text{if } m \neq n \end{cases}$$

Thus all terms of the sum equates to zero except the first. The lift is then:

$$L = -\rho V_0^2 c \left(A_0 \pi + A_1 \frac{\pi}{2} \right).$$

A.4.3 Moment

The moment about the leading edge is given as, assuming moment bending towards positive θ (pitching down) is positive:

$$\begin{aligned} M_O &= \int_0^c d_{x,O} . dL \\ &= \int_0^c d_{x,O} . \rho V_0 \gamma(x) dx \\ &= \rho V_0 \int_0^\pi \frac{c}{2} (1 - \cos\theta) . \gamma(\theta) . \frac{c}{2} \sin\theta d\theta \\ &= -\rho \frac{V_0^2}{2} c^2 \int_0^\pi (1 - \cos\theta) \left(A_0 (1 + \cos\theta) + \sum_{n=1}^{N} A_n \sin(n\theta_0) \sin(\theta) \right) d\theta \\ &= -\rho \frac{V_0^2}{2} c^2 \left(\int_0^\pi (1 - \cos^2\theta) A_0 d\theta + \sum_{n=1}^{N} \int_0^\pi (1 - \cos\theta) A_n \sin(n\theta_0) \sin(\theta) d\theta \right) \\ &= -\rho \frac{V_0^2}{2} c^2 \left(A_0 \frac{\pi}{2} + \sum_{n=1}^{N} \int_0^\pi A_n \sin(n\theta_0) \sin(\theta) d\theta + \sum_{n=1}^{N} \int_0^\pi A_n (-\cos\theta) \sin(n\theta_0) \sin(\theta) d\theta \right) \end{aligned}$$

Applying the same sine's orthogonality property:

$$M_O = -\rho\frac{V_0^2}{2}c^2\left(A_0\frac{\pi}{2} + A_1\frac{\pi}{2} - \sum_{n=1}^{N}\int_0^\pi \frac{A_n}{2}\sin(n\theta_0)\sin(2\theta)d\theta\right)$$

$$= -\rho\frac{V_0^2}{2}c^2\left(A_0\frac{\pi}{2} + A_1\frac{\pi}{2} - A_2\frac{\pi}{4}\right).$$

A.4.4 Moment and lift of a wing with aileron in steady state

Suppose the aileron's hinge line is at position x_a from the tip and its deflection angle is δ, positive downward. Without loss of generality as explained in section A.4, we can add the aileron to the flat term of the camberline superposition. The equation of this camberline is:

$$z(x) = \begin{cases} 0, & (0 < x < x_a) \\ -\tan\delta(x - x_a), & (x_a < x < c) \end{cases}$$

$$\Rightarrow \frac{dz}{dx} = \begin{cases} 0, & (0 < x < x_a) \\ -\tan\delta, & (x_a < x < c) \end{cases}$$

$$\Rightarrow f(x) = \frac{dz}{dx} - \alpha = \begin{cases} -\alpha, \\ -\tan\delta - \alpha, \end{cases}$$

In θ coordinate:

$$f(\theta) = \begin{cases} -\alpha, \\ -\tan\delta - \alpha, \end{cases}$$

The coefficients becomes:

$$A_0 = \frac{1}{\pi}\int_0^\pi f(\theta)d\theta = \begin{cases} -\alpha, \\ -\tan\delta - \alpha, \end{cases}$$

$$A_1 = -\frac{2}{\pi}\int_0^\pi f(\theta)\cos(\theta)d\theta = \begin{cases} 0, \\ 0, \end{cases}$$

$$\vdots$$

Thus the vortex distribution is:

$$\gamma(\theta) = \begin{cases} -2V_0(-\alpha)\left(\frac{1+\cos\theta}{\sin\theta}\right), & (0 < \theta < \theta_a) \\ -2V_0(-\tan\delta - \alpha)\left(\frac{1+\cos\theta}{\sin\theta}\right), & (\theta_a < \theta < \pi) \end{cases}$$

where $\theta_a = \arccos\left(1 - \frac{2x_a}{c}\right)$ is the position of the aileron hinge line in the theta coordinate. The moment about a pivot O at the leading edge is:

$$M_O = \int_0^c d_{O,x}dL$$

$$= \int_0^c d_{O,x}\rho V_0\gamma(x)dx.$$

Unfortunately, the integral has to be broken up at the hinge-line x_a so the sin function's orthogonality property no longer apply because the bounds of the integral is no longer a multiple of π, thus this integral has to be solved again.

$$M_O = \int_0^\pi \frac{c}{2}(1-\cos\theta).\rho V_0\gamma(\theta).\frac{c}{2}\sin\theta d\theta$$

$$= \frac{c^2}{4}\rho V_0\left(\int_0^{\theta_a}(1-\cos\theta)\sin\theta.2V_0\alpha\frac{1+\cos\theta}{\sin\theta}d\theta + \int_{\theta_a}^{\pi}(1+\cos\theta)\sin\theta.2V_0(\tan\delta+\alpha)\frac{1+\cos\theta}{\sin\theta}d\theta\right)$$

$$= -c^2\rho\frac{V_0^2}{2}\alpha\int_0^{\theta_a}(1-\cos^2\theta)d\theta + c^2\rho\frac{V_0^2}{2}(\tan\delta+\alpha)\int_{\theta_a}^{\pi}(1-\cos^2\theta)d\theta$$

$$= -c^2\rho\frac{V_0^2}{2}\alpha\left(\int_0^{\theta_a}d\theta - \int_0^{\theta_a}\cos 2\theta\frac{d2\theta}{2}\right)\frac{1}{2} + c^2\rho\frac{V_0^2}{2}(\tan\delta+\alpha)\left(\int_{\theta_a}^{\pi}d\theta - \int_{\theta_a}^{\pi}\cos 2\theta\frac{d2\theta}{2}\right)\frac{1}{2}$$

$$= -c^2\rho\frac{V_0^2}{2}\alpha\left(\theta_a - \frac{\sin 2\theta_a}{2}\right)\frac{1}{2} + c^2\rho\frac{V_0^2}{2}(\tan\delta+\alpha)\left(\pi-\theta_a+\frac{\sin 2\theta_a}{2}\right)\frac{1}{2}$$

$$= -c^2\rho\frac{V_0^2}{2}\alpha\pi\frac{1}{2} + c^2\rho\frac{V_0^2}{2}\tan\delta\left(\pi-\theta_a+\frac{\sin 2\theta_a}{2}\right)\frac{1}{2}$$

$$= -c^2\rho\frac{V_0^2}{2}\left(\frac{\pi}{2}\alpha + \left(\pi-\theta_a+\frac{\sin 2\theta_a}{2}\right)\frac{1}{2}\tan\delta\right). \tag{A.15}$$

A few things are worth of note. The calculations above applies to an airfoil where the aileron has been kept constant for a while. In retrospect they are more similar to flaps than to ailerons. When the aileron moves (that is $\delta = \delta(t)$), they increase the circulation on the wing, and by Kelvin's conservation of circulation, a small and opposite vortex is shredded in the wake. This vortex, while still near the airfoil, would produce an additional moment. Further, when the airfoil's circulation increase, an apparent-mass moment would also appear, that is proportional to $d\Gamma/dt$, thus this term is out of phase with the main moment.[6] The total moment, therefore, is also out of phase with whatever change that caused the change in circulation.

[6]The one calculated with Γ

B

Background in Elementary Beam Theory

B.1 Torsion of an I beam

Suppose there is a member in torsion where one end is fixed but its cross section still allowed to warp. An external torque $M = M(x)$ is distributed along the length of the member. Assume the cross sections are all circular, and that its cross section as a function of length is non-uniform, thus the beam's cross section's polar moment of inertia $J = \int r^2 dA$ about the geometric centre (centroid) is non-uniform given by $J = J(x)$, with the condition that the centroids are aligned in a straight line, then the infinitesimal deflection angle contributed by a segment dx as a function of distance from a fixed end is:

$$d\varphi(x) = \frac{M(x)}{G.J(x)}dx, \tag{B.1}$$

where $G = \frac{E}{2(1+\nu)}$ is the modulus of rigidity, E is Young's modulus, ν is Poisson's ratio (both of which are specific to the material), $M(x)$ is the external torque applied on the infinitesimal slice at x, and $J(x)$ is the polar moment of inertia of the cross section at x, calculated about the centroid.

For a wing, both $J(x)$ and $M(x)$ would both indeed be functions of x if the wing has any shape other than a rectangle. Most commercial airlines that are capable of reaching a meaningful flutter speed employ some form of trapezoidal/slanted trapezoidal wing.

Luckily, A common structural stiffener of wings is to rely on a large I beam that runs along the span, passing through the fuselage. This I beam would bear most of the structural load. Thus we could ignore the rest of the wing in this calculation. For this beam, however, derivation of φ is not straightforward since for a non-circular cross section, the beam's cross sections also deform out of plane as torque is applied. Young [YB02] provides a formula to calculate the angle of twist for an I beam fixed at one end and subjected to a torque M at its free end as follows, given that the cross section at this fixed end is still allowed to warp:

$$\varphi = \frac{M}{KG}L, \tag{B.2}$$

where $K = 2K_1 + K_2 + 2\alpha D^4$, in which $K_1 = ab^3\left(1/3 - 0.21\frac{b}{a}(1 - \frac{b^4}{12a^4})\right)$, $K_2 = \frac{1}{3}cd^3$, $\alpha = \frac{t}{t_1}\left(0.15 + 0.1\frac{r}{b}\right)$, D is the diameter of the maximum inscribed circle given by

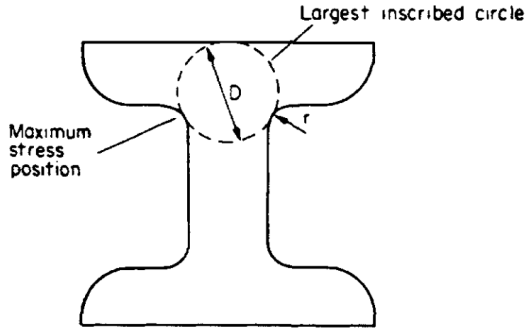


Figure B.1: Way to determine the Diameter D of the maximum inscribed circle. Image taken from chapter 5 of Hearn's book [Hea97]

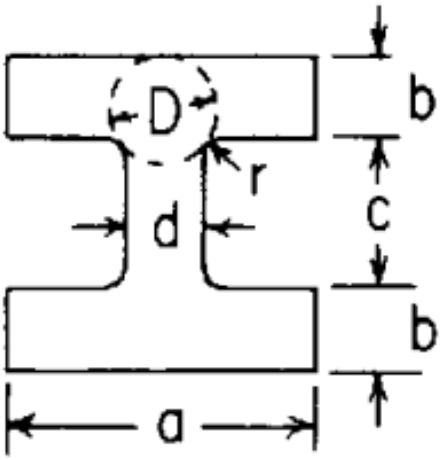


Figure B.2: Dimensions on an I beam. r = fillet radius, D = diameter of largest inscribed circle, t = b if b < d; t = d if d < b; t_1 = b if b > d; t_1 = d if d > b Figure from chapter 10 of [YB02]

$D = \frac{(b+r)^2+rd+d^2/4}{2r+b}$ for this specific shape. a, b, c, d, t_1 are dimensions of the I beam defined in figure B.2. L is the beam's length.

In general, $K < J$ and only equals for a circular cross section ([YB02], Section 10.2).

From equation (B.1) and even (B.2) above, it could be seen that the more moment there are applied on the wing at any spanwise location, the more angle of attack is added by a quantity φ. Thus increasing $\gamma(x)$, and the cycle repeats.

As the speed increase, so does the moment on the wing, given with respect to a point on the wing tip by:

$$M_y = \int_0^b x.dL = \int_0^b x.\rho_0 V_0 \gamma(x) dx \tag{B.3}$$
$$= \rho_0 V_0 \int_0^b x.\gamma(x) dx,$$

where $\gamma(x) = d\Gamma/dx$ is the intensity of circulation.

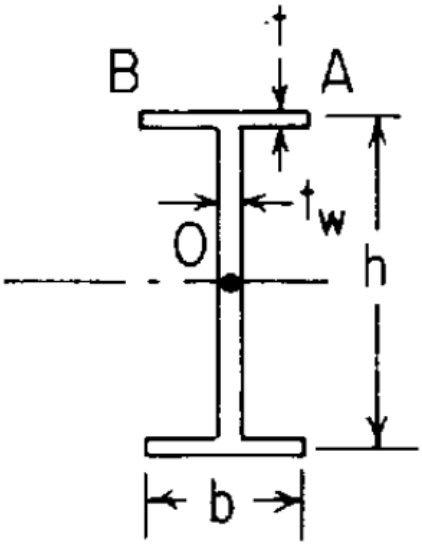


Figure B.3: Dimensions for a thin walled I-beam, image from Roak [YB02].

This moment is a positive one that tends to pitch up the wing. As is shown above, when the angle of attack increase, so does $\gamma(x)$ and thus the moment M_y increases. This in turn twists the wing even more causing additional AoA.

B.2 Torsion when warping is prevented

When the fixed end is also supported in a way that to prevent warping, there are extra normal stresses applied. These stresses increase the stiffness of the beam. For a box-cross section beam, the effect is minimal. But for an I-beam, the flanges provides significant additional restraint to torsion [YB02].

Suppose there is a beam fixed on one end by wielding to a base, such that no warping is possible. Apply a torque T to the other end. In this case, the twist is given by ([YB02], Table 10.3 and 10.2):

$$\varphi(x) = \frac{T}{C_w E \beta^3}\left(\beta(l-x) - \tanh\beta l + \frac{\sinh(\beta x)}{\cosh(\beta l)}\right),$$

where

$$\beta = \sqrt{\frac{KG}{C_w E}},$$

and where $K = \frac{1}{3}(2t^3 b + t_w^3 h)$ and $C_w = h^2 t b^3/24$, refers to Figure B.3, and where x is measured from the end torque was applied.

DEPARTMENT OF MECHANICS AND MARITIME SCIENCES
CHALMERS UNIVERSITY OF TECHNOLOGY
Gothenburg, Sweden 2026
www.chalmers.se



CHALMERS
UNIVERSITY OF TECHNOLOGY